

Multiple animals modelling with the sharing of behavioural features

Gianluca Mastrantonio

Polytechnic of Turin, Department of Mathematical Science, Turin, Italy.

Summary.

In the late years, many models to analyze animal tracking data have been proposed. Among these, the most popular ones are mixture-type models, where the latent classification is used to infer the behaviour exhibited by the animal in the observed time-window. Although data on multiple animals are often available, they are typically analysed assuming independence between animals, and any inference regarding the group is performed post-hoc.

Motivated by a real data problem, where the GPS coordinates of six Maremma Sheepdogs are observed, we propose a hidden Markov model, based on the hierarchical Dirichlet process, that can model multiple animals at the same time. As in the standard mixture-type models, the behaviour is described by the parameters of the emission distribution, in our case the recently proposed STAP. We introduce dependence between animals, allowing behaviours to share parameters, which let us able to investigate similarities and differences between animals. The results show that most behaviours shared features, such as a common attractive point, or step-length and turning-angle distributions. On the other hand, we are also able to detect animal-specific behavioural features.

Keywords: Maremma Sheepdog, Ornstein-Uhlenbeck, STAP, Step-Length

1. Introduction

The statistical models to analyze animal movement data have become increasingly popular and, since the first paper of [Dunn and Gipson \(1977\)](#), very flexible and complex approaches have been proposed. These are used to understand different aspects of the movement, ranging from the habitat selection ([Hebblewhite and Merrill, 2008](#)) to behaviour analysis ([Merrill and David Mech, 2000](#); [Anderson and Lindzey, 2003](#); [Maruotti et al., 2016](#); [Mastrantonio, 2018](#)); for a detailed review, the reader may refer to [Hooten et al. \(2017\)](#). Movement data often take the form of time series of 2-dimensional spatial coordinates, which are recorded using GPS devices attached to animals, and the time-intervals between consecutive observations (called also *fixes*), are set by the researcher.

The majority of the models can be grouped into two categories: the continuous-time dynamic models (CTM) ([Blackwell, 1997](#); [Johnson et al., 2008](#); [Fleming et al., 2014](#)) and the discrete-time dynamic models (DTM) ([Morales et al., 2004](#); [Jonsen et al., 2005](#); [McClintock et al., 2012](#); [Mastrantonio et al., 2019](#)). Both are often used in mixture-type models, as the hidden Markov models (HMMs), where the latent discrete variables are used to identify the different behaviours. The Ornstein-Uhlenbeck (OU) process ([Dunn and Gipson, 1977](#); [Blackwell, 1997](#)) and the step-and-turn (ST) approach ([Michelot et al., 2016](#)) are the most commonly used emission distribution of HMMs under, respectively, the CTM

and DTM. The HMM is used due to the easiness of implementation and interpretation (see for example [Langrock et al., 2012](#); [Michelot et al., 2016](#)).

The OU assumes a biased movement toward a *center-of-attraction*, which is generally used to define the home range ([Christ et al., 2008](#)) or a general tendency to stay on a patch of space ([McClintock et al., 2012](#)). On the other hand, in the ST, instead of the coordinates, is customary to work with the *movement-metrics*, called *step-length* and *turning-angle*, which are, respectively, proxies of the movement speed and the change of direction. The movement-metrics can be used to introduce directional persistence in the movement ([Jonsen et al., 2005](#)). Recently [Mastrantonio \(2020\)](#) proposed a new distribution, called step-and-turn with an attractive point (STAP) distribution, that has the defining characteristics of the OU and ST, i.e., center-of-attraction and directional persistence.

Although often coordinates of different animals are recorded, the literature on multiple animals modelling is not as extensive as the one on single individuals, but, recently, the interest is increasing, see for example [Westley et al. \(2018\)](#). Following the classification given by [Scharf and Buderman \(2020\)](#), two categories of models can be used when multiple animals are observed. In the first, called *indirect*, the parameters that govern the behaviour are seen as random effects across animals, i.e., they come from a common distribution whose parameters must be estimated, and the animals are then conditionally independent (see for example [McClintock et al., 2013](#); [Buderman et al., 2018](#)). On the other hand, in the *direct* approach, the dependence between animals is described by an unobserved graph or social network, see (see [Calabrese et al., 2018](#); [Hooten et al., 2018](#)).

In this work, we propose a model to describe multiple animals movement, based on the hierarchical Dirichlet process (DP) ([Teh et al., 2006](#)), that can be seen as a generalization of the sticky hierarchical Dirichlet process HMM (sHDP-HMM) of [Fox et al. \(2011\)](#). In our proposal, given the latent classification and likelihood parameters, the movement of each animal is supposed to be independent from the others, and the behaviour, for any time-point and animal, is completely described by the 5 parameters of the STAP distribution, which is the emission-distribution of our model. The dependence between animals, as in the indirect approach, is modelled at a lower level of the model hierarchy. For each of the 5 parameters we introduce a draw from a DP, and their atoms and weights are then combined to define a discrete distribution. This distribution allows the sharing of parameters between animals ensuring that two behaviours cannot have the same set of 5 parameters, but it is possible to share a subset, e.g., two animals can have the same spatial attractive point, but the attraction strength can be different. This feature allows us to investigate the differences and similarities between behaviours/animals. The model is estimated under the Bayesian framework.

Our proposal is used to model the trajectories of 6 Maremma Sheepdogs, that are our motivating data, observed in Australia, with fixes every 30 minutes. These dogs are used all over Europe and Asia to protect livestock from possible predators and, in recent years, also in Australia, see for example ([van Bommel and Johnson, 2016](#); [Gehring et al., 2017](#)). Maremma Sheepdogs are able to work in synergy with the shepherd, to keep the stock together but, when the extension of the property is too large, as in Australia, this is not always possible. For this reason, the dogs are often left alone in keeping the livestock safe, and are visited by the shepherd rarely. The owner has no supervision over the dogs, and

(Jammalamadaka and Kozubowski, 2004), and

$$\mathbf{R}(x) = \begin{pmatrix} \cos(x) & -\sin(x) \\ \sin(x) & \cos(x) \end{pmatrix}$$

is the 2-dimensional rotation matrix.

Owing to ϕ_{t_i} (see equation (2)), the conditional distribution of $\mathbf{s}_{t_{i+1}}$ depends on \mathbf{s}_{t_i} and $\mathbf{s}_{t_{i-1}}$, and then the STAP is Markovian of the second order, unless $\rho = 0$, since in this case $\mathbf{R}(\rho\phi_{t_i})$ reduces to the identity matrix and then $\mathbf{s}_{t_{i+1}}$ depends only on \mathbf{s}_{t_i} . Coordinate \mathbf{s}_{t_1} is considered fixed while \mathbf{s}_{t_0} is a further parameter that must be estimated in the model fitting, defining an appropriate prior, e.g., $\mathbf{s}_{t_0} \sim U(\mathcal{D})$. If (1) holds, we write

$$\mathbf{s}_{t_{i+1}} | \mathbf{s}_{t_i}, \mathbf{s}_{t_{i-1}}, \boldsymbol{\theta} \sim \text{STAP}(\boldsymbol{\theta}).$$

The reasoning behind the STAP formalisation can be understood considering the three cases: $\rho = 0$; $\rho = 1$, and $\rho \in (0, 1)$.

If we assume $\rho = 0$, equation (1) reduces to

$$\mathbf{s}_{t_{i+1}} = \mathbf{s}_{t_i} + \nu(\boldsymbol{\mu} - \mathbf{s}_{t_i}) + \boldsymbol{\epsilon}_{t_i}, \quad (3)$$

that is a parametrisation of the OU model, often used in the context of animal movement modelling (see for example Blackwell, 2003). In (3), the movement path is attracted (or biased) to a point in space, called center-of-attraction, identified by $\boldsymbol{\mu}$ in equation (3). The drift toward $\boldsymbol{\mu}$ depends only on the spatial distance $\|\mathbf{s}_{t_i} - \boldsymbol{\mu}\|$ (Iglehart, 1968) and its strength is ruled by ν , such that the closer is ν to 1 and the stronger is the attraction to $\boldsymbol{\mu}$. If $\nu = 0$ the movement is a random walk with independent increments. Matrix $\boldsymbol{\Sigma}$ represents the variability of the 2-dimensional increments.

On the other hand, if $\rho = 1$ equation (1) is equal to

$$\mathbf{s}_{t_{i+1}} = \mathbf{s}_{t_i} + \mathbf{R}(\phi_{t_i})\boldsymbol{\eta} + \mathbf{R}(\phi_{t_i})\boldsymbol{\epsilon}_{t_i},$$

which is how the ST approach models the coordinates (see for example Mastrantonio et al. (2019)). From (1) we can compute the *displacement-coordinates* \mathbf{y}_{t_i} ,

$$\mathbf{y}_{t_i} = \mathbf{R}(\phi_{t_i})^{-1} (\mathbf{s}_{t_{i+1}} - \mathbf{s}_{t_i}) = \boldsymbol{\eta} + \boldsymbol{\epsilon}_{t_i}, \quad (4)$$

which are coordinates that are centered on \mathbf{s}_{t_i} and x -axis that is on the direction of $\mathbf{s}_{t_{j+1}} - \mathbf{s}_{t_{i,j}}$. The displacement-coordinates are normally distributed and time-independent: the relation between \mathbf{s}_{t_i} and \mathbf{y}_{t_i} is depicted in Figure 1.

From $\mathbf{y}_{t_i} = (y_{t_i,1}, y_{t_i,2})'$ we can compute the movement-metrics (r_{t_i}, θ_{t_i}) , which are the polar coordinates representation of \mathbf{y}_{t_i} , where $\theta_{t_i} = \text{atan}^*(y_{t_i,2}, y_{t_i,1})$ is interpreted as the turning-angle, i.e., change in direction, and $r_{t_i} = \|\mathbf{y}_{t_i}\|_2$ as the step-length, i.e., the animal speed. The previous two locations, needed to compute the rotation matrix in (4), introduce dependence in the movement direction, i.e., directional persistence. For example, if the distribution of θ has circular mean $\pi/4$ and small circular variance, the animal tends to turn left at each time-point.

For any value $\rho \in (0, 1)$, the directional persistence decreases, since the angle of the rotation matrix is multiplied by ρ , and the strength of attraction to $\boldsymbol{\mu}$ is weakened by $(1 - \rho)$.

3. The proposed approach

It is unrealistic to assume that the parameters describing the movement do not change with time, since different behaviours can be observed in a time-window. For this reason, often heterogeneity is introduced with a mixture-type model, where the latent classification is the behaviour exhibited by the animal at a given time-point. Different approaches have been proposed, see for example [Patterson et al. \(2017\)](#), [Harris and Blackwell \(2013\)](#) or [Mastrantonio et al. \(2019\)](#), but the most commonly used is the HMM, which is the one we use in our proposal. We introduce novelties in the way that the priors over the STAP parameters are defined, to allow the sharing of behavioural features between animals and behaviours.

3.1. The model

Let assume we have m animals, and for the j -th animal the set of spatial locations that describe the movement is indicated with $\mathbf{s}_j = (\mathbf{s}_{j,t_{j,1}}, \mathbf{s}_{j,t_{j,2}}, \dots, \mathbf{s}_{j,t_{j,n_j}})$, where $(t_{j,1}, t_{j,2}, \dots, t_{j,n_j}) \equiv \mathcal{T}_j$ is a set of equally-spaced temporal indices.

We introduce a discrete random variables $z_{j,t_{j,i}} \in \mathbb{N}$ that indicates the behaviour assumed by the j -th animal at time-point $t_{j,i}$. For each behaviour, we assume that the conditional distribution of the j -th animal is STAP with vector of parameters that changes accordingly to $z_{j,t_{j,i}}$. The time evolution of $z_{j,t_{j,i}}$ is described by a first-order Markov chain with an infinite number of possible states; the emission-distribution and the Markov chain on the latent variables define an HMM. To complete the model we have to specify the distribution over the STAP and the Markov chains parameters; with the latter we introduce the features of our proposal. The model is

$$f(\mathbf{s}|\boldsymbol{\theta}, \mathbf{z}) = \prod_{j=1}^m \prod_{i=1}^{n_j-1} f(\mathbf{s}_{j,t_{j,i+1}}|\mathbf{s}_{j,t_{j,i}}, \mathbf{s}_{j,t_{j,i-1}}, \boldsymbol{\theta}_{z_{j,t_{j,i}}}) \quad (5)$$

$$\mathbf{s}_{j,t_{j,i+1}}|\mathbf{s}_{j,t_{j,i}}, \mathbf{s}_{j,t_{j,i-1}}, \boldsymbol{\theta}_k \sim \text{STAP}(\boldsymbol{\theta}_k), \quad \mathbf{s}_{j,t_{j,0}} \sim \text{Unif}(\mathcal{D}), \quad (6)$$

$$z_{j,t_{j,i}}|z_{j,t_{j,i-1}}, \boldsymbol{\pi}_{j,z_{j,t_{j,i-1}}} \sim \text{Multinomial}(1, \boldsymbol{\pi}_{j,z_{j,t_{j,i-1}}}), \quad z_{j,t_{j,0}} = 1, \quad (7)$$

$$\boldsymbol{\pi}_{j,l}|\alpha, \tau, \boldsymbol{\beta} \sim \text{DP}\left(\alpha + \tau, \frac{\alpha\boldsymbol{\beta} + \tau\delta_l}{\alpha + \tau}\right), \quad (8)$$

$$\{\beta_k\}_{k \in \mathbb{N}} = C_1(\boldsymbol{\beta}_\mu^*, \boldsymbol{\beta}_\eta^*, \boldsymbol{\beta}_\Sigma^*, \boldsymbol{\beta}_\nu^*, \boldsymbol{\beta}_\rho^*), \quad (9)$$

$$\{\boldsymbol{\theta}_k\}_{k \in \mathbb{N}} = C_2(\boldsymbol{\mu}^*, \boldsymbol{\eta}^*, \boldsymbol{\Sigma}^*, \boldsymbol{\nu}^*, \boldsymbol{\rho}^*), \quad (10)$$

$$\boldsymbol{\beta}_\mu^*|\gamma \sim \text{Gem}(\gamma), \boldsymbol{\beta}_\eta^*|\gamma \sim \text{Gem}(\gamma), \boldsymbol{\beta}_\Sigma^*|\gamma \sim \text{Gem}(\gamma), \quad (11)$$

$$\boldsymbol{\beta}_\nu^*|\gamma \sim \text{Gem}(\gamma), \boldsymbol{\beta}_\rho^*|\gamma \sim \text{Gem}(\gamma),$$

$$\boldsymbol{\mu}_p^*|H_\mu \sim H_\mu, \boldsymbol{\eta}_p^*|H_\eta \sim H_\eta, \boldsymbol{\Sigma}_p^*|H_\Sigma \sim H_\Sigma, \quad (12)$$

$$\boldsymbol{\nu}_p^*|H_\nu \sim H_\nu, \boldsymbol{\rho}_p^*|H_\rho \sim H_\rho,$$

where we assume $p \in \mathbb{N}$, $j = 1, \dots, m$, $l \in \mathbb{N}$, and $i = 1, \dots, n_j - 1$. Each level of the model hierarchy is explained below.

The DPs With equation (12) we indicate that the p -th possible value for a STAP parameter is sampled from a distribution H_\cdot , independently from the others. A vector of

probabilities β , Gem distributed (Gnedin et al., 2001), is associated to each parameter.

Equations (11) and (12) can be combined to define draws from DPs (Ferguson, 1973), one for each STAP parameter. For example, for parameter μ we can say that the discrete distribution

$$G_{\mu} = \sum_{p \in \mathbb{N}} \beta_{\mu_p}^* \delta_{\mu_p^*}, \quad (13)$$

where $\beta_{\mu}^* = \{\beta_{\mu_p}^*\}_{p \in \mathbb{N}}$ and δ is the Dirac delta function, is from a $\text{DP}(\gamma, H_{\mu})$. The sets of atoms and weights of the DPs, respectively $\mu^* = \{\mu_p^*\}_{p \in \mathbb{N}}$ and β_{μ}^* in (13), contain the possible values that the parameters can assume in a behaviour (μ_p^*) and the ‘‘base’’ probabilities ($\beta_{\mu_p}^*$) that a particular value of the parameter is selected in a behaviour (see equation (17)).

The functions $C_1(\cdot)$ and $C_2(\cdot)$ In equation (10) we define the set of possible STAP parameters $\theta_k = (\mu_k, \eta_k, \Sigma_k, \nu_k, \rho_k)$, see equation (6), using the function $C_2(\cdot)$. This function produces the set by creating all possible combinations, without repetition (i.e., $\theta_k \neq \theta_{k'}$, if $k \neq k'$), of the elements in the 5 sets $\{\mu_p^*\}_{p \in \mathbb{N}}$, $\{\eta_p^*\}_{p \in \mathbb{N}}$, $\{\Sigma_p^*\}_{p \in \mathbb{N}}$, $\{\nu_p^*\}_{p \in \mathbb{N}}$, $\{\rho_p^*\}_{p \in \mathbb{N}}$. Notice that, even if $\theta_k \neq \theta_{k'}$, a subset of parameters can be the same, e.g., we can have $\nu_k \equiv \nu_{k'}$. We can then introduce new variables, $w_{\mu,k}$, $w_{\eta,k}$, $w_{\Sigma,k}$, $w_{\nu,k}$ and $w_{\rho,k}$, whose values represent which one of the p -th parameter is in θ_k :

$$\mu_k = \mu_{w_{\mu,k}}^*, \quad \eta_k = \eta_{w_{\eta,k}}^*, \quad \Sigma_k = \Sigma_{w_{\Sigma,k}}^*, \quad \nu_k = \nu_{w_{\nu,k}}^*, \quad \rho_k = \rho_{w_{\rho,k}}^*. \quad (14)$$

Using these new variables, function $C_1(\cdot)$, in equation (9), defines the weight β_k as:

$$\beta_k = \beta_{\mu_{w_{\mu,k}}}^* \beta_{\eta_{w_{\eta,k}}}^* \beta_{\Sigma_{w_{\Sigma,k}}}^* \beta_{\nu_{w_{\nu,k}}}^* \beta_{\rho_{w_{\rho,k}}}^*, \quad (15)$$

where β_k is a weight associated with θ_k . Notice that, by definition, β_k is obtained by multiplying the β^* associated to the parameters in θ_k . The vector $\{\beta_k\}_{k \in \mathbb{N}}$ is a probability vector and then $\{\theta_k, \beta_k\}_{k \in \mathbb{K}}$ can be used to define the discrete distribution

$$G_0 = \sum_{k \in \mathbb{N}} \beta_k \delta_{\theta_k}. \quad (16)$$

Given G_0 , the model can be seen as a version of the sHDP-HMM of Fox et al. (2011), where the base distribution of the first level DP is in our case G_0 , i.e., a combination of DPs, while in Fox et al. (2011) G_0 is DP distributed. The distribution G_0 is the one that allows the sharing of behavioural feature, i.e., STAP parameters.

The transition matrix For each animal j , we indicate the animal-specific HMM transition-matrix as $\mathbf{\Pi}_j$, and we assume that the l -th row is given by $\pi_{j,l} = \{\pi_{j,l,k}\}_{k \in \mathbb{N}}$. Matrix $\mathbf{\Pi}_j$ rules the switching between behaviours, as shown in equation (7), and the row $\pi_{j,l}$ is DP distributed, see equation (8). The expected value of the vector $\pi_{j,l}$ is equal to

$$\mathbb{E}(\pi_{j,l} | \alpha, \kappa, \beta) = \frac{\alpha \beta + \tau \delta_l}{\alpha + \tau}. \quad (17)$$

From (17) we can see that the k -th element of β is associated to the expected value of the k -th element of $\pi_{j,l}$, and a larger β_k increases the expected value of $\pi_{j,l,k}$, i.e., the

Table 1. Predictive performances of the two models.

	Woody	Sherlock	Alvin	Rosie	Bear	Lucy	Mean
M1	4.1036	4.2202	0.3369	6.9323	4.2679	4.4961	4.0595
M2	4.1049	4.2419	0.3279	6.9072	4.3276	4.5106	4.0700

probability to switch from behaviour l to k , for all $l \in \mathbb{N}$ and $j = 1, \dots, m$. Given equation (15), we can see why β^* is the “base probability” since, for example, if we increase the value of $\beta_{\nu,p}^*$, we will also increase the value of the β_k that contains ν_p^* . Parameter α is the scaling parameter of the DP while κ is a weight added to the self transitions; for more details on the parameters α and κ see Fox et al. (2011).

The emission-distribution The model specification is concluded with the emission distribution, given by (5) and (6). Notice that, given the latent behaviours, we consider the animal independent but, since the animal share the same set of atoms $\{\theta_k\}_{k \in \mathbb{N}}$, behaviour in different animals can be described by the same STAP distribution. Moreover, from equation (14), we know that θ_k can have elements in common with $\theta_{k'}$, meaning that, even if the behaviours are different, they can share features, e.g., the same attractive-point or the movement-metrics, which is the main novelty of our proposal, not possible with other proposals.

Even if the set of possible parameters is the same for all animals, the transition probability Π_j are different and then, the switching between behaviour, as well as the probabilities to stay in a particular state, are animal-specific, as we can see from equation (8).

Notice that the number of possible behaviors is infinite, since $\pi_{j,l}$ is infinite-dimensional. Nonetheless, in the observed time-window, only a finite number of behaviours can be observed. The K_j unique values assumed by z_{j,t_i} is then a random variable that we use to estimate the number of latent behaviours.

4. Motivating data

Maremma Sheepdogs are dogs, which originate from Europe, that have been used for centuries to protect livestock from potential predators (Gehring et al., 2017). They live with the livestock since birth and, as a result, they develop a strong bond and an instinct to protect it. It is possible to fence-trained them, to remain in proximity of the paddock, but they are generally allowed to move freely. Outside Europe, especially in Australia, the use of livestock guardian dogs is relatively new and, due to their effectiveness, the interest is increasing (van Bommel and Invasive Animals Cooperative Research Centre, 2010; van Bommel and Johnson, 2016). Since in Australia the properties extension can be several thousand hectares, it is hard for the owner to supervision the dogs (van Bommel and Johnson, 2012) and to know their behaviour (van Bommel and Invasive Animals Cooperative Research Centre, 2010).

To analyse the behaviour, we use data, freely available at the movebank repository[†].

[†]<https://www.datarepository.movebank.org/handle/10255/move.395>

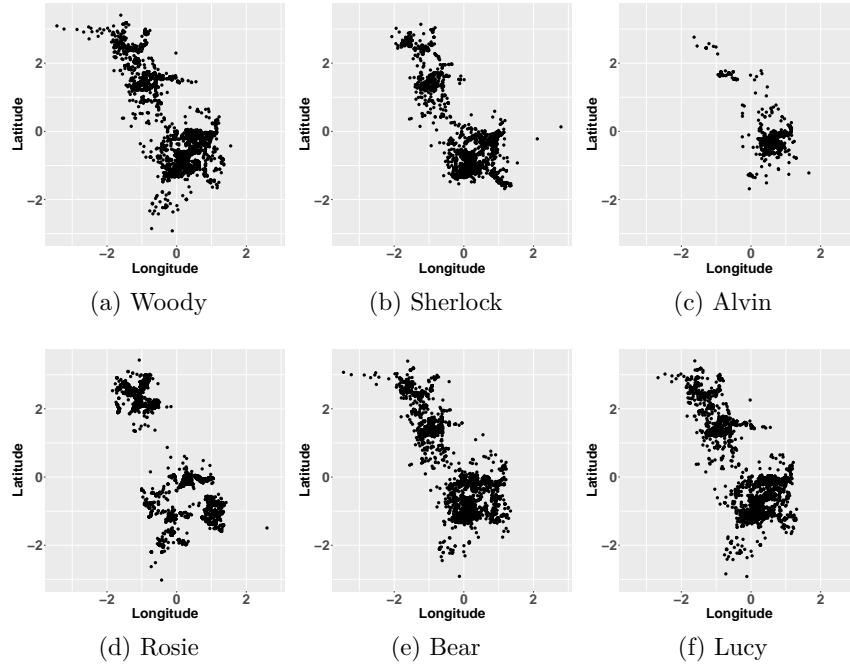


Fig. 2. Observed spatial locations.

In the dataset we use, there are the recorded coordinates of 6 dogs, taken at the Heatherlie property in Australia, between the 2012-11-10 15:30 and the 2012-08-02 15:30, every 30 minutes. The data consist of 4801 observations for each dog, with less than 1% of missing points. In the dataset, the dogs are called Woody, Sherlock, Alvin, Rosie, Bear, and Lucy. Rosie and Lucy are female while the other four are male; the observed coordinates are shown in Figure 2. As observed in [van Bommel and Johnson \(2016\)](#), Woody, Sherlock, Bear and Lucy formed a cohesive group, responsible for the livestock protection, while Rosie, due to its old age, is solitary, and Alvin suffers a social exclusion, which restricted its movement; see Figure 2.

To facilitate the priors specification, we standardise the data. The coordinates are centered using the bivariate sample mean and scaled with a common standard deviation, computed using both X and Y coordinates. The common standard deviation is used to maintain the relative scale between the two coordinate since, otherwise, we introduce bias in the movement. The model is implemented assuming a $N(\mathbf{0}, 1000\mathbf{I})$ for $\boldsymbol{\mu}_h^*$ and $\boldsymbol{\eta}_h^*$, $U(0, 1)$ for ν_h^* and $IW(3, \mathbf{I})$ for $\boldsymbol{\Sigma}_j^*$. Parameter ρ_h^* is assumed to come from a mixture of a $U(0, 1)$ and two bulks of probability on 0 and 1, with the 3 mixture weights equal to 1/3. This prior allows ρ_{k,t_i} to be, at posteriori, equal to 0 or 1 with probability greater than 0, which gives us the possibility to detect if a behaviour is a pure OU or ST. For the DP parameters, following [Fox et al. \(2011\)](#), we use $\alpha + \tau, \gamma \sim G(1.1, 0.1)$ and $\tau/(\alpha + \tau) \sim B(1, 1)$. Posterior estimates are obtained with 75000 iterations, burnin 37500, thin 15, having then 2500 samples for posterior inference.

Table 2. Woody: posterior means and CIs of the model parameters ($j=1$).

	k=1	k=2	k=3
$\mu_{j,1}$	0.59	0.559	-0.073
(CI)	(-0.825 7.322)	(-0.845 7.293)	(-0.23 0.088)
$\mu_{j,2}$	0.336	0.286	0.265
(CI)	(-1.277 4.801)	(-1.277 4.933)	(0.081 0.455)
$\eta_{j,1}$	-0.001	-0.002	-0.005
(CI)	(-0.002 -0.001)	(-0.002 -0.001)	(-0.015 -0.001)
$\eta_{j,2}$	0	0	-0.018
(CI)	(0 0)	(0 0)	(0 0.005)
ν_j	0.345	0.355	0.092
(CI)	(0.002 0.999)	(0.003 0.999)	(0.072 0.109)
ρ_j	1	0.999	0.035
(CI)	[1 1]	[1 1]	[0 0.122)
$\Sigma_{1,1}$	0	0.014	0.135
(CI)	(0 0)	(0.012 0.016)	(0.124 0.147)
$\Sigma_{1,2}$	0	0	-0.023
(CI)	(0 0)	(0 0.001)	(-0.031 -0.016)
$\Sigma_{2,2}$	0	0.01	0.198
(CI)	(0 0)	(0.008 0.011)	(0.175 0.218)
π_1	0.761	0.181	0.056
(CI)	(0.743 0.779)	(0.163 0.199)	(0.044 0.069)
π_2	0.383	0.392	0.217
(CI)	(0.35 0.419)	(0.345 0.437)	(0.18 0.257)
π_3	0.142	0.3	0.538
(CI)	(0.114 0.17)	(0.251 0.353)	(0.487 0.586)
π_4	0.46	0	0.003
(CI)	(0.251 0.967)	(0 0)	(0 0.044)
n_j	2695	1225	813

For comparison, on the same dataset we also estimate a model where each animal follows a sHDP-HMM with STAP density, i.e. the animals are completely independent, having than six different models without parameters sharing across animals. To evaluate the model performances, for each animal we select randomly 10% of the observations and we estimate the models considering them as missing. The posterior samples are then used to compute the MSE. We indicate our proposal with M1, while the model where the animals are completely independent as M2. The results are shown in Table 1 where we can see that our proposal is the one with the lowest mean value, i.e., and then describe better the data. The results in the next section are obtained using the entire dataset, without setting 10% of the observations as missing. All models are implemented in Julia 1.3 (Bezanson et al., 2017).

4.1. Results

To facilitate the discussion, we decide to analyse only behaviours observed at least once a day, on average. For this reason, from the MCMC output, and for each time-point and

Table 3. Sherlock: posterior means and CIs of the model parameters ($j=2$).

	k=1	k=2	k=3
$\mu_{j,1}$	0.52	0.539	-0.072
(CI)	(-0.847 6.35)	(-0.845 6.973)	(-0.229 0.09)
$\mu_{j,2}$	0.322	0.259	0.263
(CI)	(-1.277 4.747)	(-1.277 4.544)	(0.078 0.453)
$\eta_{j,1}$	-0.001	-0.013	-0.01
(CI)	(-0.002 -0.001)	(-0.017 -0.009)	(-0.016 -0.001)
$\eta_{j,2}$	0	0.003	0.002
(CI)	(0 0)	(0 0.006)	(0 0.005)
ν_j	0.36	0.354	0.092
(CI)	(0.002 0.999)	(0.002 0.999)	(0.072 0.11)
ρ_j	1	1	0.035
(CI)	[1 1]	[1 1]	[0 0.129)
$\Sigma_{1,1}$	0	0.009	0.131
(CI)	(0 0)	(0.008 0.01)	(0.089 0.146)
$\Sigma_{1,2}$	0	0	-0.019
(CI)	(0 0)	(0 0.001)	(-0.03 0.017)
$\Sigma_{2,2}$	0	0.006	0.194
(CI)	(0 0)	(0.005 0.007)	(0.113 0.224)
π_1	0.772	0.152	0.075
(CI)	(0.756 0.789)	(0.135 0.168)	(0.063 0.09)
π_2	0.386	0.477	0.135
(CI)	(0.354 0.418)	(0.442 0.511)	(0.108 0.16)
π_3	0.229	0.238	0.523
(CI)	(0.192 0.27)	(0.194 0.283)	(0.46 0.574)
π_4	0.186	0	0
(CI)	(0 0.757)	(0 0)	(0 0)
n_j	2856	1199	741

Table 4. Alvin: posterior means and CIs of the model parameters ($j=3$).

	k=1	k=2	k=3	k=4
$\mu_{j,1}$	0.622	5.022	0.575	0.575
(CI)	(-0.831 7.477)	(-0.092 21.167)	(0.574 0.576)	(0.574 0.576)
$\mu_{j,2}$	0.307	2.683	-0.38	-0.38
(CI)	(-1.277 5.322)	(-0.381 11.332)	(-0.381 -0.379)	(-0.381 -0.379)
$\eta_{j,1}$	-0.001	0.003	-0.015	0.007
(CI)	(-0.002 -0.001)	(-0.015 -0.001)	(-0.016 -0.001)	(-0.016 -0.001)
$\eta_{j,2}$	0	0.001	-0.004	-0.028
(CI)	(0 0)	(0 0.005)	(0 0.005)	(0 0.005)
ν_j	0.337	0.029	0.997	0.367
(CI)	(0.003 0.999)	(0.001 0.105)	(0.993 1]	(0.299 0.451)
ρ_j	1	0.064	0	0.015
(CI)	[1 1]	[0 1]	[0 0]	[0 0.11)
$\Sigma_{1,1}$	0	0.009	0	0.086
(CI)	(0 0)	(0.008 0.01)	(0 0)	(0.073 0.106)
$\Sigma_{1,2}$	0	0	0	0.016
(CI)	(0 0)	(0 0.001)	(0 0)	(0.007 0.03)
$\Sigma_{2,2}$	0	0.006	0	0.092
(CI)	(0 0)	(0.005 0.007)	(0 0)	(0.073 0.132)
π_1	0.747	0.098	0.123	0.031
(CI)	(0.689 0.829)	(0.084 0.113)	(0.046 0.173)	(0.021 0.043)
π_2	0.196	0.302	0.357	0.128
(CI)	(0.161 0.234)	(0.253 0.353)	(0.313 0.403)	(0.094 0.165)
π_3	0.594	0.134	0.268	0.003
(CI)	(0.373 0.832)	(0.101 0.173)	(0.016 0.506)	(0 0.022)
π_4	0.143	0.175	0.279	0.401
(CI)	(0.098 0.194)	(0.114 0.243)	(0.222 0.341)	(0.321 0.478)
π_5	0.005	0.051	0	0.34
(CI)	(0 0.072)	(0 0.296)	(0 0)	(0.106 0.58)
π_6	0.581	0	0	0
(CI)	(0.168 0.947)	(0 0)	(0 0)	(0 0)
n_j	3336	653	519	267

Table 5. Rosie: posterior means and CIs of the model parameters ($j=4$).

	k=1	k=2	k=3
$\mu_{j,1}$	0.566	0.411	0.592
(CI)	(-0.818 7.378)	(-0.845 5.292)	(-0.82 7.107)
$\mu_{j,2}$	0.266	0.216	0.338
(CI)	(-1.278 4.357)	(-1.278 3.567)	(-1.277 5.105)
$\eta_{j,1}$	-0.001	-0.013	-0.01
(CI)	(-0.002 -0.001)	(-0.017 -0.009)	(-0.016 -0.001)
$\eta_{j,2}$	0	0.003	-0.004
(CI)	(0 0)	(0 0.006)	(0 0.005)
ν_j	0.346	0.339	0.328
(CI)	(0.002 0.999)	(0.002 0.999)	(0.002 0.999)
ρ_j	1	1	0.926
(CI)	[1 1]	[1 1]	[0 1]
$\Sigma_{1,1}$	0	0.01	0.089
(CI)	(0 0)	(0.008 0.015)	(0.073 0.135)
$\Sigma_{1,2}$	0	0	0.013
(CI)	(0 0)	(0 0.001)	(-0.024 0.024)
$\Sigma_{2,2}$	0	0.007	0.096
(CI)	(0 0)	(0.005 0.01)	(0.072 0.196)
π_1	0.827	0.147	0.025
(CI)	(0.814 0.841)	(0.131 0.166)	(0.009 0.038)
π_2	0.428	0.504	0.069
(CI)	(0.395 0.461)	(0.457 0.558)	(0.031 0.1)
π_3	0.25	0.281	0.468
(CI)	(0.182 0.317)	(0.201 0.372)	(0.39 0.547)
n_j	3356	1179	265

Table 6. Bear: posterior means and CIs of the model parameters (j=5).

	k=1	k=2	k=3
$\mu_{j,1}$	0.686	0.604	-0.073
(CI)	(-0.791 7.705)	(-0.82 7.57)	(-0.23 0.088)
$\mu_{j,2}$	0.327	0.286	0.265
(CI)	(-1.277 5.282)	(-1.278 5.467)	(0.081 0.455)
$\eta_{j,1}$	-0.001	-0.009	0.01
(CI)	(-0.002 -0.001)	(-0.016 -0.001)	(-0.015 -0.001)
$\eta_{j,2}$	0	0.002	0.04
(CI)	(0 0)	(0 0.006)	(0 0.005)
ν_j	0.351	0.36	0.092
(CI)	(0.002 0.999)	(0.002 0.999)	(0.072 0.109)
ρ_j	1	1	0.027
(CI)	[1 1]	[1 1]	[0 0.117]
$\Sigma_{1,1}$	0	0.014	0.135
(CI)	(0 0)	(0.012 0.016)	(0.124 0.147)
$\Sigma_{1,2}$	0	0	-0.023
(CI)	(0 0)	(0 0.001)	(-0.031 -0.016)
$\Sigma_{2,2}$	0	0.01	0.198
(CI)	(0 0)	(0.008 0.011)	(0.175 0.218)
π_1	0.768	0.194	0.038
(CI)	(0.751 0.783)	(0.177 0.211)	(0.028 0.051)
π_2	0.411	0.472	0.117
(CI)	(0.381 0.441)	(0.435 0.508)	(0.093 0.144)
π_3	0.125	0.296	0.579
(CI)	(0.089 0.163)	(0.237 0.369)	(0.516 0.635)
n_j	2820	1395	585

Table 7. Lucy: posterior means and CIs of the model parameters (j=6).

	k=1	k=2	k=3
$\mu_{j,1}$	0.526	0.575	-0.073
(CI)	(-0.829 6.625)	(-0.807 7.441)	(-0.23 0.088)
$\mu_{j,2}$	0.276	0.252	0.265
(CI)	(-1.277 4.862)	(-1.278 4.865)	(0.081 0.455)
$\eta_{j,1}$	-0.001	-0.013	0.013
(CI)	(-0.002 -0.001)	(-0.017 -0.009)	(-0.016 -0.001)
$\eta_{j,2}$	0	0.003	0.021
(CI)	(0 0)	(0 0.006)	(0 0.005)
ν_j	0.348	0.35	0.092
(CI)	(0.003 0.999)	(0.002 0.999)	(0.072 0.109)
ρ_j	1	1	0.03
(CI)	[1 1]	[1 1]	[0 0.121]
$\Sigma_{1,1}$	0	0.014	0.135
(CI)	(0 0)	(0.01 0.016)	(0.124 0.147)
$\Sigma_{1,2}$	0	0	-0.023
(CI)	(0 0)	(0 0.001)	(-0.031 -0.016)
$\Sigma_{2,2}$	0	0.009	0.198
(CI)	(0 0)	(0.007 0.011)	(0.175 0.218)
π_1	0.725	0.216	0.059
(CI)	(0.706 0.743)	(0.194 0.237)	(0.044 0.077)
π_2	0.366	0.479	0.155
(CI)	(0.338 0.396)	(0.44 0.515)	(0.13 0.184)
π_3	0.162	0.291	0.547
(CI)	(0.132 0.193)	(0.24 0.349)	(0.494 0.596)
π_4	0.004	0.17	0.204
(CI)	(0 0.023)	(0 0.763)	(0 0.986)
n_j	2492	1550	757

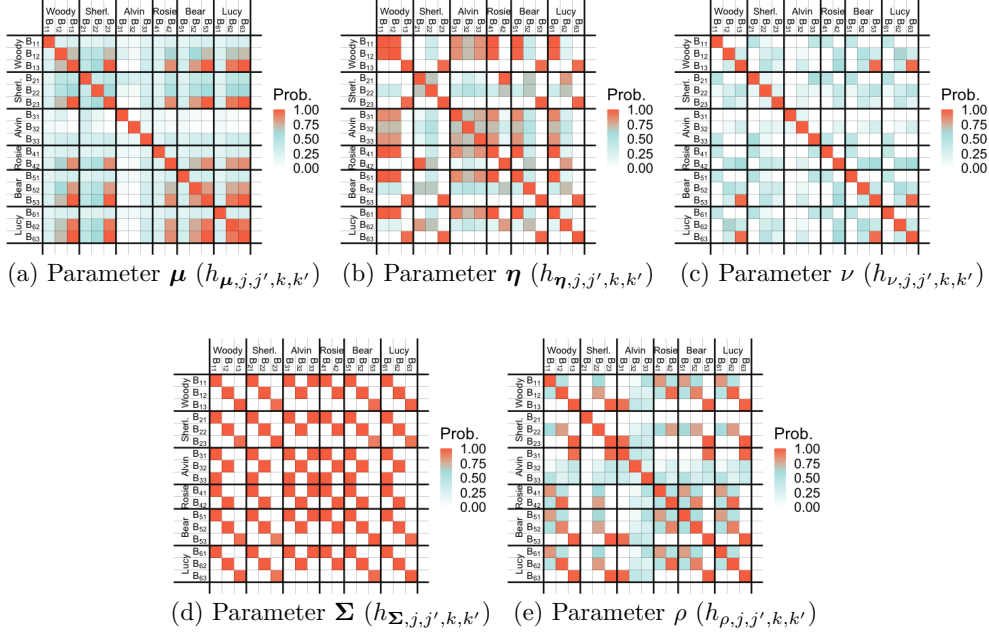


Fig. 3. Graphical representation of the posterior mean of $h_{\mu,j,j',k,k'}$ (a), $h_{\eta,j,j',k,k'}$ (b), $h_{\nu,j,j',k,k'}$ (c), $h_{\Sigma,j,j',k,k'}$ (d), $h_{\rho,j,j',k,k'}$ (e), which are the probabilities that the parameter has the same value in different behaviours.

animal, we compute the maximum-at-posterior (MAP) estimate of the behaviour (the MAP of $z_{j,t_{j,i}}$) and this is considered as the estimated behaviour of the j -th animal at time $t_{j,i}$. We indicated with $n_{j,k}$ the number of times each (MAP) behaviour is observed and we describe only behaviours with $n_{j,k} > 100$. We have than 4 behaviours for Alvin and 3 for the others. The cumulative sums of the number of time-points discarded are 67 for Woody, 4 for Sherlock, 25 for Alvin, and 1 for Lucy.

With a slight abuse of notation, we assume $n_{j,1} > n_{j,2} > \dots$, meaning that the k -th behaviour of the j -th dog is not necessarily equal to the k -th of the others 5. We then indicate with $(\boldsymbol{\mu}_{j,k}, \boldsymbol{\eta}_{j,k}, \nu_{j,k}, \rho_{j,k}, \boldsymbol{\Sigma}_{j,k})$ the set of parameters of the k -th behaviour of the j -th animal, and with $\boldsymbol{\pi}_{j,l}$ the l -th row of the transition matrix $\boldsymbol{\Pi}_j$. The posterior estimates and credible intervals (CIs) for the STAP parameters, $n_{j,k}$ and the transition probabilities are shown in Tables 2-7.

Let indicate with Bjk , the k -th behaviour of the j -th animal, and with $h_{\mu,j,j',k,k'}^b, h_{\eta,j,j',k,k'}^b, h_{\nu,j,j',k,k'}^b, h_{\Sigma,j,j',k,k'}^b, h_{\rho,j,j',k,k'}^b \in \{0, 1\}$ the variables that have value 1 if, in the b -th MCMC posterior sample, the associated parameter has the same value in Bjk and $Bj'k'$. Since $\boldsymbol{\mu}$ and ν are identifiable only if $\rho \neq 1$, then we assume $h_{\mu,j,j',k,k'}^b = 0$ and $h_{\nu,j,j',k,k'}^b = 0$ if $\rho_{j,k}^b$ or $\rho_{j',k'}^b$ is equal to 1 and, for similar reasons, we assume $h_{\eta,j,j',k,k'}^b = 0$ if $\rho_{j,k}^b$ or $\rho_{j',k'}^b$ is equal to 0. The posterior mean of h . (i.e. its sample mean across MCMC samples) can be used as an estimate of the probability that Bjk and $Bj'k'$ have the same

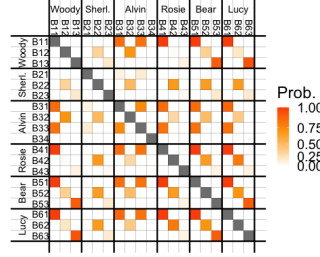


Fig. 4. Graphical representation of the posterior mean of $h_{j,j',k,k'}$, which is the probability that two behaviours are the same.

value of the parameter. These probabilities are shown in Figures 3 (a)-(e). We can also combine the variables h . in the following way:

$$h_{j,j',k,k'}^b = \begin{cases} h_{\mu,j,j',k,k'}^b h_{\nu,j,j',k,k'}^b h_{\Sigma,j,j',k,k'}^b, h_{\rho,j,j',k,k'}^b & \text{if } \rho_{j,k}^b = 0 \text{ or } \rho_{j',k'}^b = 0, \\ h_{\eta,j,j',k,k'}^b h_{\Sigma,j,j',k,k'}^b, h_{\rho,j,j',k,k'}^b & \text{if } \rho_{j,k}^b = 1 \text{ or } \rho_{j',k'}^b = 1, \\ h_{\mu,j,j',k,k'}^b h_{\eta,j,j',k,k'}^b h_{\nu,j,j',k,k'}^b h_{\Sigma,j,j',k,k'}^b, h_{\rho,j,j',k,k'}^b & \text{otherwise.} \end{cases}$$

Notice that $h_{j,j',k,k'}^b \in \{0, 1\}$ and it is equal to 1 only if all parameters of Bjk and $Bj'k'$ are the same, with the exception of the non-identifiable parameters (η if $\rho = 0$ and (μ, ν if $\rho = 1$). We can use the posterior mean of $h_{j,j',k,k'}$ has an estimate of the probability that Bjk is equal to $Bj'k'$, i.e., probability that the two behaviours are the same (or, equivalently, the entire set of STAP parameters is the same); the results are in Figure 4.

From a descriptive point of view, we can use the CI of ρ to identify the type of behaviour. If its right limit is approximatively 0, the behaviour is a *pure* OU, if the left one is approximatively 1, it can be considered as a *pure* ST, otherwise the behaviour shows both ST and OU characteristics and we call it OU-ST behaviour. For the ST behaviours, we plotted in Figures 5 and 6 the posterior predictive distributions of the movement-metrics, i.e. turning-angles (Figures 5) and step-lengths (Figures 6). Notice that, the step-length distributions have on the x-axis the dogs speed in meters/hour.

4.2. Output description and interpretation

The four dogs that form a cohesive group (Woody, Sherlock, Bear and Lucy) have the first two behaviours that are *pure* ST (see Tables 2-7), while the third one is OU with a slight directional persistence. Alvin, the socially excluded dog, is the only one with four behaviours and its first is a pure ST, the second is OU-ST, the third is a pure OU, while the last one is an OU with a slight directional persistence. On the other hand, Rosie, the eldest dog, has the first two that are pure ST, while the third one is OU-ST (CI $\approx [0, 1]$).

From Figures 3 (b), (d) and Figure 4, we see that the ST specific parameters (η and Σ) of the first behaviours, for each dogs, are almost the same. This is also confirmed by the predictive distributions of step-length and turning-angle, in Figure 5 and 6. The speed is very low, with mean value ≈ 15.53 meters/hour, and a unimodal circular distribution with circular mean $\approx -\pi$, indicating a change of direction of half a circle between consecutive

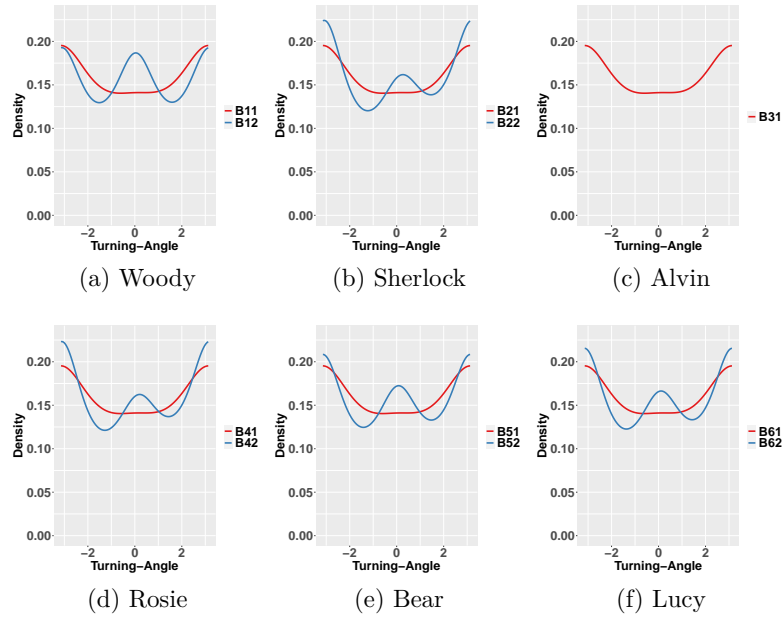


Fig. 5. Posterior predictive densities of the turning-angles for selected behaviours.

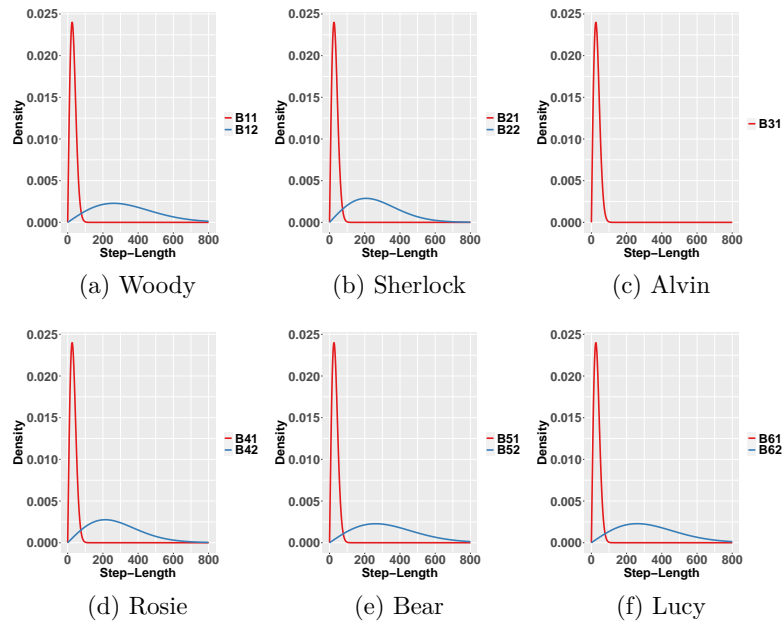


Fig. 6. Posterior predictive densities of the step-lengths for selected behaviours. The x-axis represent the animal speed expressed in meters/hour.

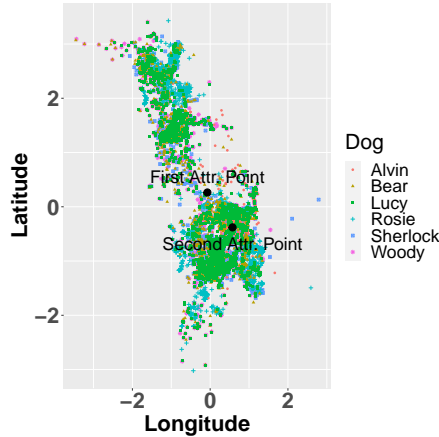


Fig. 7. Observed spatial locations and coordinates of the 2 spatial attractors.

time-points. This behaviour is coherent with the dogs resting or attending livestock (see [van Bommel and Invasive Animals Cooperative Research Centre, 2010](#)). Even if in the second behaviours the speeds are almost identical for all dogs, there are differences in the direction, see Figure 6. All dogs have a bimodal distribution with major mode at $\approx -\pi$ and the other at ≈ 0 , which indicates a movement over a straight line with changes in direction. With respect to Bj1, the mean speed is now 141.07 and the variance is higher. Owing to the higher speed and probability to have movements in a straight line, we can interpret these behaviours as the dog performing boundary patrolling or seeing off predator (see [van Bommel and Invasive Animals Cooperative Research Centre, 2010](#)).

For the dogs in the cohesive group, the OU behaviours (B13, B23, B53, B63) have the same attractive point μ , Figure 3 (a). The strength of attraction, measured by ν , is also similar (as we can see from Figure 3 (c)) and, since the CIs are $\approx [0.07, 0.11]$, it is very weak; the movement closely resembles a random walk with a weak attraction to μ . Alvin has two OU behaviours, that share the same attractive point, see Figure 3 (a), with different ν ; in B33 the attraction to μ is strong, with $\nu \approx 1$ while in B34 is weak and similar to the OU behaviours of the cohesive group. The extreme social exclusion that the dog suffers can be the reason why its attractive-point is different from the one of the others. These two spatial points are indicated as *first attractive point* and *second attractive point*, respectively, in Figure 7. As we can see from Figure c2 of [van Bommel and Johnson \(2012\)](#), the two attractive points are close to where the livestock is, and the second one is particularly close to the owner homestead. These behaviours can be easily interpreted as the dogs attending livestock or spending time with the owner.

In the two OU-ST behaviour, B33 and B43, there are not well defined attractive-points (see the CI of μ) and not even a directional persistence (CI of $\rho \approx [0, 1]$). These behaviours, due to the lack of structure in the movement patterns, represent the dogs exploring the property.

From the model output is clear that these dogs tend to behave in a similar way, as we can see from the first two behaviours (especially Bj1 and, partially, also Bj2) that

are very similar. We also found evidence that most of the dog spend time close to the livestock and they are attracted to the same spatial point, see Figure 7. Given that for 4 dogs most of the behaviours are very similar, we consider this further evidence that, as pointed out by van Bommel and Johnson (2012), these form a cohesive social group that is in charge of keeping the livestock safe.

It is of interesting to note that, even if our model has the better overall value of MSE (see Table 1) it is out-performed by M2 for the 2 animals that are not part of the social group. Since they do not share many features with the other dogs, they do not take advantage from the parameters sharing feature of our hierarchical prior G_0 (equation (16)), and an independent HMM, which is a more parsimonious model, is preferable for these two dogs.

5. Final remarks

In this work, we proposed a new approach that can be used to model multiple animals that, under the classification given by Scharf and Buderman (2020), is part of the indirect approach.

Our model is similar to the sHDP-HMM but, while models based on the HDP allow only the sharing of the entire vector of parameters between groups, in our proposal also subset can be shared. Although we define our model using a STAP emission-distribution, our approach is general and can be used with other proposals. We decided to use the STAP since it allows us to model ST and OU movement patterns at the same time.

The model is then used to understand the behaviour of 6 Maremma Sheepdog, observed in a property in Australia. The results show that there are many common features between animals, i.e. subset of parameters, such as similar predictive distributions for the movement-metrics or attractive-points, and also between behaviours of the same dog. The results obtained are easily interpretable, and having a rich output, can give an insight into the similarities between animals, which make its use interesting in an applied context. We compare our model with a competitive approach, where an HMM is fitted independently to each dog, and we have shown that our proposal is preferable

In our proposal, we cannot evaluate if two animals change behaviour at the same time-point. This is a possible extension that we are currently working on. Another possibility is in the use of covariate to model the probabilities that behaviours share parameters.

Implementation

The codes that can be used to replicate the results, tables, and figures, are available at https://github.com/GianlucaMastrantonio/multiple_animals_movement_model.

Acknowledgments

The work of the author is partially developed under the MIUR grant Dipartimenti di Eccellenza 2018 - 2022 (E11G18000350001), conferred to the Dipartimento di Scienze Matematiche - DISMA, Politecnico di Torino.

References

- Anderson, C. R. and Lindzey, F. G. (2003). “Estimating Cougar Predation Rates from GPS Location Clusters.” *The Journal of Wildlife Management*, 67(2): 307–316.
- Bezanson, J., Edelman, A., Karpinski, S., and Shah, V. B. (2017). “Julia: A fresh approach to numerical computing.” *SIAM review*, 59(1): 65–98.
- Blackwell, P. (1997). “Random diffusion models for animal movement.” *Ecological Modelling*, 100(1): 87 – 102.
- Blackwell, P. G. (2003). “Bayesian inference for Markov processes with diffusion and discrete components.” *Biometrika*, 90(3): 613–627.
- Buderman, F. E., Hooten, M. B., Alldredge, M. W., Hanks, E. M., and Ivan, J. S. (2018). “Time-varying predatory behavior is primary predictor of fine-scale movement of wildland-urban cougars.” *Movement Ecology*, 6(1): 22.
- Calabrese, J. M., Fleming, C. H., Fagan, W. F., Rimmler, M., Kaczensky, P., Bewick, S., Leimgruber, P., and Mueller, T. (2018). “Disentangling social interactions and environmental drivers in multi-individual wildlife tracking data.” *Philosophical Transactions of the Royal Society B: Biological Sciences*, 373(1746): 20170007.
- Christ, A., Hoef, J. V., and Zimmerman, D. L. (2008). “An animal movement model incorporating home range and habitat selection.” *Environmental and Ecological Statistics*, 15(1): 27–38.
- Dunn, J. E. and Gipson, P. S. (1977). “Analysis of radiotelemetry data in studies of home range.” *Biometrics*, 33(1).
- Ferguson, T. S. (1973). “A Bayesian analysis of some nonparametric problems.” *The Annals of Statistics*, 1(2): 209–230.
- Fleming, C. H., Calabrese, J. M., Mueller, T., Olson, K. A., Leimgruber, P., and Fagan, W. F. (2014). “Non-Markovian maximum likelihood estimation of autocorrelated movement processes.” *Methods in Ecology and Evolution*, 5(5): 462–472.
- Fox, E. B., Sudderth, E. B., Jordan, M. I., and Willsky, A. S. (2011). “A sticky HDP-HMM with application to speaker diarization.” *The Annals of Applied Statistics*, 5(2A): 1020–1056.
- Gehring, T. M., VerCauteren, K. C., and Cellar, A. C. (2017). “Good Fences Make Good Neighbors: Implementation of Electric Fencing for Establishing Effective Livestock-Protection Dogs.” *Human-Wildlife Interactions*, 5(1): 106–111.
- Gnedin, A., Gnedin, E., and Kerov, S. (2001). “A Characterization of GEM Distributions.” *Combin. Probab. Comp.*, 10: 213–217.
- Harris, K. J. and Blackwell, P. G. (2013). “Flexible continuous-time modelling for heterogeneous animal movement.” *Ecological Modelling*, 255: 29 – 37.

- Hebblewhite, M. and Merrill, E. (2008). “Modelling wildlife and human relationships for social species with mixed-effects resource selection models.” Journal of Applied Ecology, 45(3): 834–844.
- Hooten, M., Johnson, D., McClintock, B., and Morales, J. (2017). Animal Movement: Statistical Models for Telemetry Data. CRC Press.
- Hooten, M. B., Scharf, H. R., Hefley, T. J., Pearse, A. T., and Weegman, M. D. (2018). “Animal movement models for migratory individuals and groups.” Methods in Ecology and Evolution, 9(7): 1692–1705.
- Iglehart, D. L. (1968). “Limit Theorems for the Multi-urn Ehrenfest Model.” Ann. Math. Statist., 39(3): 864–876.
- Jammalamadaka, S. R. and Kozubowski, T. J. (2004). “New Families of Wrapped Distributions for Modeling Skew Circular Data.” Communications in Statistics - Theory and Methods, 33(9): 2059–2074.
- Johnson, D. S., London, J. M., Lea, M.-A., and Durban, J. W. (2008). “Continuous-time correlated random walk model for animal telemetry data.” Ecology, 89(5): 1208–1215.
- Jonsen, I. D., Flemming, J. M., and Myers, R. A. (2005). “Robust state-space modeling of animal movement data.” Ecology, 86(11): 2874–2880.
- Langrock, R., King, R., Matthiopoulos, J., Thomas, L., Fortin, D., and Morales, J. M. (2012). “Flexible and practical modeling of animal telemetry data: hidden Markov models and extensions.” Ecology, 93(11): 2336–2342.
- Maruotti, A., Punzo, A., Mastrantonio, G., and Lagona, F. (2016). “A time-dependent extension of the projected normal regression model for longitudinal circular data based on a hidden Markov heterogeneity structure.” Stochastic Environmental Research and Risk Assessment, 30: 1725–1740.
- Mastrantonio, G. (2018). “The joint projected normal and skew-normal: A distribution for poly-cylindrical data.” Journal of Multivariate Analysis, 165: 14 – 26.
- (2020). “Modeling animal movement with directional persistence and attractive points.” arXiv. 2012.03248.
- Mastrantonio, G., Grazian, C., Mancinelli, S., and Bibbona, E. (2019). “New formulation of the logistic-Gaussian process to analyze trajectory tracking data.” Ann. Appl. Stat., 13(4): 2483–2508.
- McClintock, B. T., King, R., Thomas, L., Matthiopoulos, J., McConnell, B. J., and Morales, J. M. (2012). “A general discrete-time modeling framework for animal movement using multistate random walks.” Ecological Monographs, 82(3): 335–349.
- McClintock, B. T., Russell, D. J. F., Matthiopoulos, J., and King, R. (2013). “Combining individual animal movement and ancillary biotelemetry data to investigate population-level activity budgets.” Ecology, 94(4): 838–849.

- Merrill, S. B. and David Mech, L. (2000). “Details of Extensive Movements by Minnesota Wolves (*Canis lupus*).” The American Midland Naturalist, 144(2): 428–433.
- Michelot, T., Langrock, R., and Patterson, T. A. (2016). “moveHMM: an R package for the statistical modelling of animal movement data using hidden Markov models.” Methods in Ecology and Evolution, 7(11): 1308–1315.
- Morales, J. M., Haydon, D. T., Frair, J., Holsinger, K. E., and Fryxell, J. M. (2004). “Extracting more out of relocation data: building movement models as mixtures of random walks.” Ecology, 85(9): 2436–2445.
- Patterson, T. A., Parton, A., Langrock, R., Blackwell, P. G., Thomas, L., and King, R. (2017). “Statistical modelling of individual animal movement: an overview of key methods and a discussion of practical challenges.” AStA Advances in Statistical Analysis, 101(4): 399–438.
- Scharf, H. R. and Buderman, F. E. (2020). “Animal movement models for multiple individuals.” WIREs Computational Statistics.
- Teh, Y. W., Jordan, M. I., Beal, M. J., and Blei, D. M. (2006). “Hierarchical Dirichlet processes.” Journal of the American Statistical Association, 101(476): 1566–1581.
- van, L., Bommel and Johnson, C. (2014). “Data from: Where do livestock guardian dogs go? Movement patterns of free-ranging Maremma sheepdogs, doi:10.5441/001/1.pv048q7v.”
- van Bommel, L. and Invasive Animals Cooperative Research Centre (2010). Guardian Dogs: Best Practice Manual for the Use of Livestock Guardian Dogs. Invasive Animals Cooperative Research Centre.
- van Bommel, L. and Johnson, C. N. (2012). “Good dog! Using livestock guardian dogs to protect livestock from predators in Australia’s extensive grazing systems.” Wildlife Research, 39(3): 220–229.
- (2014). “Where Do Livestock Guardian Dogs Go? Movement Patterns of Free-Ranging Maremma Sheepdogs.” PLOS ONE, 9(10): 1–12.
- (2016). “Livestock guardian dogs as surrogate top predators? How Maremma sheepdogs affect a wildlife community.” Ecology and Evolution, 6(18): 6702–6711.
- Westley, P. A. H., Berdahl, A. M., Torney, C. J., and Biro, D. (2018). “Collective movement in ecology: from emerging technologies to conservation and management.” Philosophical Transactions of the Royal Society B: Biological Sciences, 373(1746): 20170004.

The modeling of multiple animals that share behavioral features

Gianluca Mastrantonio

Politecnico di Torino, Dipartimento di Scienze Matematiche

Abstract

In this work, we propose a model that can be used to infer the behavior of multiple animals. Our proposal is defined as a set of hidden Markov models that are based on the sticky hierarchical Dirichlet process, with a shared base-measure, and a STAP emission distribution. The latent classifications are representative of the behavior assumed by the animals, which is described by the STAP parameters. Given the latent classifications, the animals are independent.

As a result of the way we formalize the distribution over the STAP parameters, the animals may share, in different behaviors, the set or a subset of the parameters, thereby allowing us to investigate the similarities between them. The hidden Markov models, based on the Dirichlet process, allow us to estimate the number of latent behaviors for each animal, as a model parameter.

This proposal is motivated by a real data problem, where the GPS coordinates of six Maremma Sheepdogs have been observed. Among the other results, we show that four dogs share most of the behavior characteristics, while two have specific behaviors.

1 Introduction

Movement data are often based on a time-series of 2-dimensional spatial coordinates recorded using a GPS device attached to an animal. Since the first paper by Dunn and Gipson (1977), the statistical models used to analyze such data have become increasingly popular, and are used to understand different aspects of the movement of animals, ranging from habitat selection (Hebblewhite and Merrill, 2008) to behavior analysis (Merrill and David Mech, 2000; Anderson and Lindzey, 2003; Maruotti et al., 2016; Mastrantonio, 2018); for a detailed review, the reader may refer to Hooten et al. (2017).

Three major categories of movement-description models can be identified in the behavior modeling framework: biased random walks (BRWs), correlated random walks (CRWs), and bias and correlated random walks (BCRWs). In a BRW, the animal movement is attracted (or biased) toward a point in space, which is called *center-of-attraction* (see, for example, Blackwell, 1997; Dunn and Gipson, 1977). The center-of-attraction can be interpreted as a proxy of the home-range (Christ et al., 2008) or it can describe a movement toward a patch of space (McClintock et al., 2012). In a CRW, the movement direction, at any given time, depends on the previous direction. This characteristic is called *directional persistence* (Jonsen et al., 2005) and it is useful to describe a constant change in direction between consecutive observations. If both directional persistence and attractors are used to describe a movement, the model is a BCRW (Fortin et al., 2005; Codling et al., 2008; McClintock et al., 2012). A movement-description model is generally used as an emission distribution of a mixture-type model, where a latent cluster-membership variable is used to identify the behavior assumed by an animal. If the observed time-window is wide enough, the use of a mixture-type model is justified by the assumption that an animal exhibits more than one behavior during the day (Patterson et al., 2008), e.g., sleeping and hunting. The switching between behaviors is often temporally structured and, if formulated in a discrete-time framework, the model is usually the hidden Markov model (HMM) (Michelot et al., 2016; Langrock et al., 2012).

The literature on the modeling of multiple animals is not as extensive as that on single individuals,

even though coordinates of different animals are often recorded. Nonetheless, interest in this topic is increasing (see, for example, Westley et al., 2018) since, as shown by (Jonsen, 2016), the joint modeling of multiple animals often increases the precision of the estimates. By adopting the classification given by Scharf and Buderman (2020), it is possible to model multiple animals using two approaches. In the first approach, called *indirect*, the parameters that govern the behaviors are seen as random effects across animals, i.e., they come from a common distribution, whose parameters must be estimated, and the animals are conditionally independent (see, for example, McClintock et al., 2013; Michelot et al., 2017; Buderman et al., 2018). On the other hand, in the *direct* approach, the dependence between animals is described by an unobserved graph or social network, see, for example, Calabrese et al. (2018) Hooten et al. (2018), Milner et al. (2021) and Niu et al. (2020).

We here propose a Bayesian model which can be used to describe multiple animals that share certain movement characteristics, observed over different time-windows. The model is based on the hierarchical Dirichlet process (HDP) (Teh et al., 2006) and it is a generalization of the sticky hierarchical Dirichlet process HMM (sHDP-HMM) of Fox et al. (2011). In the model, given the latent classification and likelihood parameters, the animals are independent and the behaviors are described by the five parameters of the STAP distribution, which is a BCRW emission-distribution that has recently been proposed by Mastrantonio (2020). The main contributions of the present proposal are the possibility of estimating the number of latent behaviors of each animal as model parameters, and of introducing the sharing of parameters between behaviors and animals in HMMs based on Dirichlet processes (DPs). The former is a by-product of the DP modeling, which allows us to avoid the use of information criteria to select the number of behaviors, which has been shown to be problematic in this context (Pohle et al., 2017), or a trans-dimensional Markov chain Monte Carlo (MCMC) algorithm, such as the reversible jump MCMC (RJMCMC), which presents challenges in its implementation (Hastie and Green, 2012). The sharing of parameters is introduced in the lower level of the model hierarchy, where the distribution over the STAP parameters is defined by combining five different DPs. This distribution is discrete, with a countable number of atoms being defined so that they can share some of their multivariate components. This approach is similar to the one proposed by Mastrantonio et al. (2021), which was used to model climate data in a change-point framework. Therefore, the behaviors within or between animals can have the same value of an STAP parameter, and this allows us to investigate similarities and differences between the analyzed animals. Other approaches also exist that have the sharing of parameters as one of their characteristics (see, for example, Jonsen (2016) or Milner et al. (2021)), but they require one to select, a priori, what parameters are allowed to change and the number of values that a parameter can assume. On the other hand, in our proposal, everything is done during the model fitting and driven by the information within the data.

Our proposal has been used to model the trajectories of 6 Maremma Sheepdogs, observed in Australia with recorded coordinates every 30 minutes. These dogs are used all over Europe and Asia to protect livestock from possible predators and, in recent years, also in Australia (see, for example, van Bommel and Johnson, 2016; Gehring et al., 2017). Maremma Sheepdogs are able to work in synergy with the shepherd to keep the stock together but this is not always possible when the property is too large. For this reason, the dogs are often left alone and are rarely visited by the shepherd. The owner has no supervision over the dogs and it is therefore interesting to analyze and understand their behavior. The used dataset was taken from the movebank repository (www.movebank.org) and is described in detail in van Bommel and Johnson (2014a) and van Bommel and Johnson (2014b). With our model, we have identified many similarities and some specific features between dogs, that are easy to interpret and which give a better insight into the behavior of the dogs. Two competitive models have also been estimated on the same data and the results are compared with our proposal.

The paper is organized as follows. We introduce the STAP density in Section 2, and the hierarchical formalization of our proposal in Section 3, while Section 4 contains the results of the real data application. The paper ends with some conclusive remarks in Section 5. The Appendix contain details of the MCMC algorithm and on the results of the competitive models.

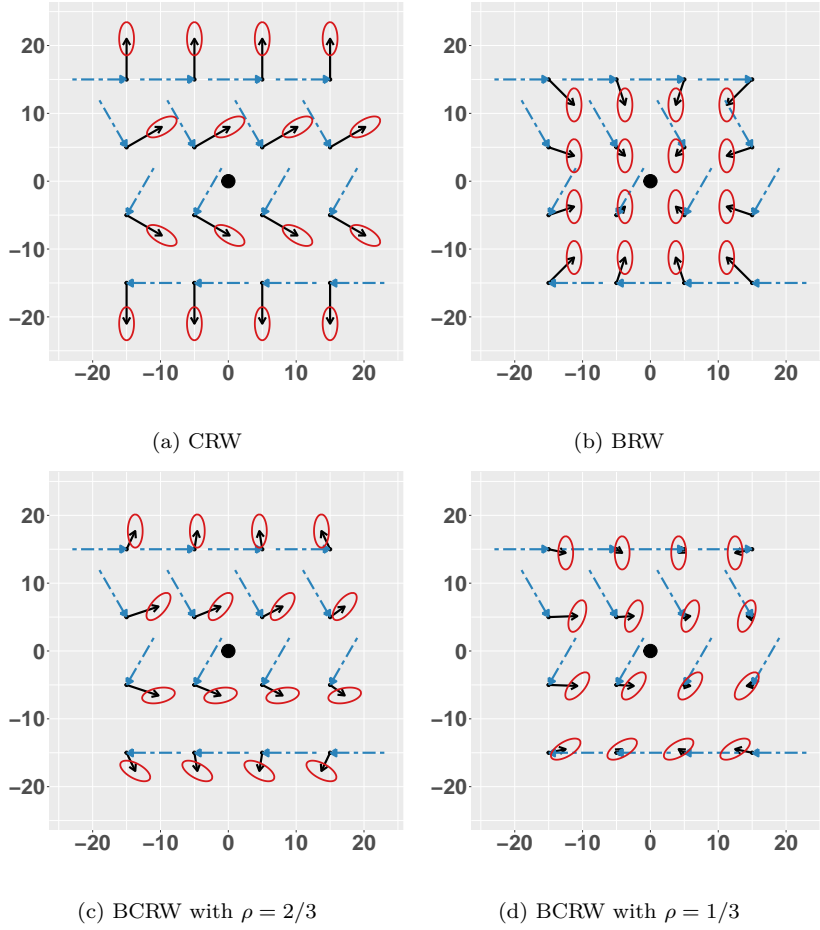


Figure 1: Graphical representation of the conditional distribution of \mathbf{s}_{i+1} for different possible values of \mathbf{s}_i and the previous directions. The dashed arrow represents the movement between \mathbf{s}_{i-1} and \mathbf{s}_i . The solid arrow is $\bar{\mathbf{F}}_i$, while the ellipse is the area containing 95% of the probability mass of the conditional distribution of \mathbf{s}_{i+1} . $\boldsymbol{\mu} = (0, 0)'$, $\boldsymbol{\eta} = (0, 6)'$, $\tau = 0.25$, $\boldsymbol{\Sigma} = \begin{pmatrix} 0.2 & 0 \\ 0 & 1 \end{pmatrix}$ in all figures, and the central dot is the location $\boldsymbol{\mu}$, which is the attractor in the BRW and the BCRW.

2 The STAP distribution

With the aim of better understanding the results of the real data application (Section 4) and the formalization of our proposal, we briefly describe the STAP distribution, which was introduced in Mastrantonio (2020), and its parameters; for a more detailed description the reader may refer to Mastrantonio (2020).

We assume we have a time-series of two-dimensional spatial locations $\mathbf{s} = (\mathbf{s}_{t_1}, \dots, \mathbf{s}_{t_T})'$ that represent an animal's path, where $\mathbf{s}_{t_i} = (s_{t_i,1}, s_{t_i,2}) \in \mathcal{D} \subset \mathbb{R}^2$, and t_i is a temporal index. The coordinates are recorded without any measurement error and the time difference between consecutive points is constant. In order to formalize the STAP, we introduce the bearing angle

$$\phi_{t_i} = \text{atan}^*(s_{t_{i+1},2} - s_{t_i,2}, s_{t_{i+1},1} - s_{t_i,1}) \in [-\pi, \pi),$$

and the rotation matrix

$$\mathbf{R}(x) = \begin{pmatrix} \cos(x) & -\sin(x) \\ \sin(x) & \cos(x) \end{pmatrix},$$

where $\text{atan}^*(\cdot)$ is the two-argument tangent function (Jammalamadaka and Kozubowski, 2004). The bearing-angle measures the direction of the movement between time t_i and t_{i+1} , and the rotation matrix can be used to perform a rotation in a two-dimensional space, so that if it multiplies a two-dimensional vector, the vector is rotated anti-clockwise by an angle x . The conditional distribution of $\mathbf{s}_{t_{i+1}}$ is assumed to be second-order Markovian, with the following specification:

$$\begin{aligned} \mathbf{s}_{t_{i+1}} | \mathbf{s}_{t_i}, \mathbf{s}_{t_{i-1}} &\sim N(\mathbf{s}_{t_i} + \mathbf{M}_{t_i}, \mathbf{V}_{t_i}), \quad i \in \{1, \dots, T-1\}, \\ \mathbf{M}_{t_i} &= (1 - \rho)\tau(\boldsymbol{\mu} - \mathbf{s}_{t_i}) + \rho\mathbf{R}(\phi_{t_{i-1}})\boldsymbol{\eta}, \\ \mathbf{V}_{t_i} &= \mathbf{R}(\rho\phi_{t_{i-1}})\boldsymbol{\Sigma}\mathbf{R}'(\rho\phi_{t_{i-1}}), \end{aligned} \quad (1)$$

where $\boldsymbol{\mu}, \boldsymbol{\eta} \in \mathbb{R}^2$, $\tau \in (0, 1)$, $\rho \in [0, 1]$, and $\boldsymbol{\Sigma}$ is a 2-dimensional covariance matrix. The location \mathbf{s}_{t_1} is fixed, and \mathbf{s}_{t_0} is another parameters that is needed to compute ϕ_{t_0} in the conditional distribution of \mathbf{s}_{t_2} . If the path follows equation (1), we write $\mathbf{s}_{t_{i+1}} | \mathbf{s}_{t_i}, \mathbf{s}_{t_{i-1}} \sim \text{STAP}(\boldsymbol{\theta})$, with $\boldsymbol{\theta} = (\boldsymbol{\mu}, \boldsymbol{\eta}, \boldsymbol{\Sigma}, \tau, \rho)$.

The movement described by the STAP can have directional-persistence and attraction to a point in space, therefore, the STAP is a BCRW. To better understand these two properties and how they are formalized in equation (1), we introduce the vector $\vec{\mathbf{F}}_{t_i}$, which is a vector with initial and terminal points equal to \mathbf{s}_{t_i} and $\mathbf{s}_{t_i} + \mathbf{M}_{t_i}$, respectively. This vector represents the expected movement between time t_i and t_{i+1} , since its initial point is the previously observed location \mathbf{s}_{t_i} and the terminal one is equal to $\mathbb{E}(\mathbf{s}_{t_{i+1}} | \mathbf{s}_{t_i})$. If $\rho = 0$, the STAP reduces to a two-dimensional AR(1) (a BRW), and $\vec{\mathbf{F}}_{t_i}$ points to the spatial location $\boldsymbol{\mu}$, which is therefore the attractor. The length of $\vec{\mathbf{F}}_{t_i}$ is $\tau \|(\boldsymbol{\mu} - \mathbf{s}_{t_i})\|$, which shows that τ measures how much of the total distance between the last observation (\mathbf{s}_{t_i}) and the attractor ($\boldsymbol{\mu}$) is expected to be covered or, in other words, how strong the attraction to $\boldsymbol{\mu}$ is. If $\rho = 1$, the STAP reduces to a CRW, based on a normal density. In this case, the direction of $\vec{\mathbf{F}}_{t_i}$ is the same as the direction of $\mathbf{R}(\phi_{t_{i-1}})\boldsymbol{\eta}$, which depends on the previous bearing angle $\phi_{t_{i-1}}$, and thus induces a directional-correlation between consecutive points. If $\rho \in (0, 1)$, $\vec{\mathbf{F}}_{t_i}$ is a weighted mean between its value in a BRW and a CRW, with weights given by $(1 - \rho)$ and ρ , respectively. The covariance matrix of the conditional distribution of $\mathbf{s}_{t_{i+1}}$ is fixed in a BRW ($\text{Cov}(\mathbf{s}_{t_{i+1}} | \mathbf{s}_{t_i}) = \boldsymbol{\Sigma}$), while it rotates with the bearing-angle for any $\rho > 0$ ($\text{Cov}(\mathbf{s}_{t_{i+1}} | \mathbf{s}_{t_i}) = \mathbf{R}(\rho\phi_{t_{i-1}})\boldsymbol{\Sigma}\mathbf{R}'(\rho\phi_{t_{i-1}})$): for more details, the reader may refer to Mastrantonio (2020).

We show examples of STAP densities, and the associated BRW ($\rho = 0$) and CRW ($\rho = 1$) in Figure 1, to better understand the differences between the BRW, CRW and BCRW. The dashed arrow in the figure is the movement between times t_{i-1} and t_i , the solid arrow is $\vec{\mathbf{F}}_{t_i}$, and the ellipse is a contour of the conditional distribution of $\mathbf{s}_{t_{i+1}}$ with a constant density containing 95% of the total probability mass. From 1 (a), we can see that the direction of $\vec{\mathbf{F}}_{t_i}$ and the ellipse change according to $\phi_{t_{i-1}}$ in a CRW. On the other hand $\vec{\mathbf{F}}_{t_i}$ and the ellipse are independent from the previous direction in a BRW (Figure 1 (b)), and $\vec{\mathbf{F}}_{t_i}$ points to the spatial attractor $\boldsymbol{\mu} = (0, 0)'$. When $\rho \in (0, 1)$, the ellipse and $\vec{\mathbf{F}}_{t_i}$ are dependent on both the previous direction and the spatial attractor, see Figures 1 (c) and (d).

3 The proposed model

In this section, we introduce the components of the model and how they are used to introduce the characteristics of our proposal. We extend the notation of the previous section to describe the path of m animals, and to allow changes in the behavior to be considered.

We indicate the path of the j -th animal with $\mathbf{s}_j = (\mathbf{s}_{j,t_{j,1}}, \mathbf{s}_{j,t_{j,2}}, \dots, \mathbf{s}_{j,t_{j,T_j}})$, where $j = 1, \dots, m$, and $\mathcal{T}_j \equiv (t_{j,1}, t_{j,2}, \dots, t_{j,T_j})$ is the set of temporal points, equally spaced in time, where the position of the j -th dog is recorded. The sets \mathcal{T}_j and $\mathcal{T}_{j'}$ can contain different time-points, but the time difference must be constant across animals, i.e., $t_{j,i+1} - t_{j,i} = c$ for all $j = 1, \dots, m$ and $i = 1, \dots, T_j - 1$. We

introduce a discrete random variable $z_{j,t_j,i} \in \mathbb{N}$ to represent the animal behavior at time $t_{j,i}$, where $z_{j,t_j,i} = k$ indicates that animal j follows behavior k at time $t_{j,i}$. Given the behavior assumed by each animal, the paths are independent and

$$\mathbf{s}_{j,t_{j,i+1}} | \mathbf{s}_{j,t_{j,i}}, \mathbf{s}_{j,t_{j,i-1}}, z_{j,t_{j,i}} \sim \text{STAP}(\boldsymbol{\theta}_{z_{j,t_{j,i}}})$$

where $\boldsymbol{\theta}_k = (\boldsymbol{\mu}_k, \boldsymbol{\eta}_k, \boldsymbol{\Sigma}_k, \tau_k, \rho_k)$. In other words, if the j -th animal is following the k -th behavior at time $t_{j,i}$ (i.e., $z_{j,t_{j,i}} = k$), the path is described by the set $\boldsymbol{\theta}_k$ of STAP parameters. It should be noted that the k -th behaviors are represented by the same set of parameters $\boldsymbol{\theta}_k$ for all animals.

Let $\mathbf{s} = \{\mathbf{s}_j\}_{j=1}^m$, $\mathbf{z}_j = \{z_{j,t}\}_{t \in \mathcal{T}_j}$, $\mathbf{z} = \{\mathbf{z}_j\}_{j=1}^m$, and $\boldsymbol{\theta} = \{\boldsymbol{\theta}_k\}_{k \in \mathbb{N}}$, then the model we propose is

$$f(\mathbf{s} | \boldsymbol{\theta}, \mathbf{z}) = \prod_{j=1}^m \prod_{i=1}^{T_j-1} f(\mathbf{s}_{j,t_{j,i+1}} | \mathbf{s}_{j,t_{j,i}}, \mathbf{s}_{j,t_{j,i-1}}, \boldsymbol{\theta}_{z_{j,t_{j,i}}}), \quad (2)$$

$$\mathbf{s}_{j,t_{j,i+1}} | \mathbf{s}_{j,t_{j,i}}, \mathbf{s}_{j,t_{j,i-1}}, z_{j,t_{j,i}}, \boldsymbol{\theta}_{z_{j,t_{j,i}}} \sim \text{STAP}(\boldsymbol{\theta}_{z_{j,t_{j,i}}}), \quad \mathbf{s}_{j,t_{j,0}} \sim \text{Unif}(\mathcal{D}), \quad (3)$$

$$z_{j,t_{j,i}} | z_{j,t_{j,i-1}}, \boldsymbol{\pi}_{j,z_{j,t_{j,i-1}}} \sim \text{Multinomial}(1, \boldsymbol{\pi}_{j,z_{j,t_{j,i-1}}}), \quad (4)$$

$$z_{j,t_{j,0}} \sim \text{Geom}(\epsilon),$$

$$\boldsymbol{\pi}_{j,l} | \alpha, \nu, \boldsymbol{\beta} \sim \text{DP} \left(\alpha + \nu, \frac{\alpha \boldsymbol{\beta} + \nu \delta_l}{\alpha + \nu} \right), \quad (5)$$

$$\{\beta_k\}_{k \in \mathbb{N}} = C_1(\boldsymbol{\beta}_\mu^*, \boldsymbol{\beta}_\eta^*, \boldsymbol{\beta}_\Sigma^*, \boldsymbol{\beta}_\tau^*, \boldsymbol{\beta}_\rho^*), \quad (6)$$

$$\{\boldsymbol{\theta}_k\}_{k \in \mathbb{N}} = C_2(\boldsymbol{\mu}^*, \boldsymbol{\eta}^*, \boldsymbol{\Sigma}^*, \boldsymbol{\tau}^*, \boldsymbol{\rho}^*), \quad (7)$$

$$\boldsymbol{\beta}_\mu^* | \gamma_\mu \sim \text{Gem}(\gamma_\mu), \boldsymbol{\beta}_\eta^* | \gamma_\eta \sim \text{Gem}(\gamma_\eta), \boldsymbol{\beta}_\Sigma^* | \gamma_\Sigma \sim \text{Gem}(\gamma_\Sigma), \quad (8)$$

$$\boldsymbol{\beta}_\tau^* | \gamma_\tau \sim \text{Gem}(\gamma_\tau), \boldsymbol{\beta}_\rho^* | \gamma_\rho \sim \text{Gem}(\gamma_\rho),$$

$$\boldsymbol{\mu}_p^* | H_\mu \sim H_\mu, \boldsymbol{\eta}_p^* | H_\eta \sim H_\eta, \boldsymbol{\Sigma}_p^* | H_\Sigma \sim H_\Sigma, \quad (9)$$

$$\boldsymbol{\tau}_p^* | H_\tau \sim H_\tau, \boldsymbol{\rho}_p^* | H_\rho \sim H_\rho,$$

where $p \in \mathbb{N}$, $l \in \mathbb{N}$, and $i = 1, \dots, T_j - 1$. A full description of the components of the model and how they are used to introduce the main novelties of our model is given below.

The DPs. In order to simplify the description of the lower levels of the model hierarchy, we use χ as a variable that can be $\boldsymbol{\mu}$, $\boldsymbol{\eta}$, $\boldsymbol{\Sigma}$, ν , or ρ , and it is used when whatever is described can be applied to any of the five parameters. In equation (9), the values of the STAP parameter χ_p are sampled from the distribution H_χ , and the infinite-dimensional vector of probabilities $\boldsymbol{\beta}_\chi^* = \{\beta_{\chi,p}^*\}_{p \in \mathbb{N}}$, associated with parameter χ , is Gem distributed (Gnedin et al., 2001) with *scaling parameter* γ_χ . The scaling parameter can easily be interpreted with the stick-breaking representation of the GEM distribution, defined as follows:

$$\beta_{\chi,1}^* \sim \text{B}(1, \gamma_\chi), \quad (10)$$

$$\frac{\beta_{\chi,p}^*}{1 - \sum_{h=1}^{p-1} \beta_{\chi,h}^*} \sim \text{B}(1, \gamma_\chi), \quad p \neq 1.$$

From (10), we see that the smaller γ_χ is, and the smaller is the number of elements of $\boldsymbol{\beta}_\chi^*$ that contains most of the probability mass with $\lim_{\gamma_\chi \rightarrow 0} \beta_{\chi,1}^* = 1$ and $\lim_{\gamma_\chi \rightarrow 0} \beta_{\chi,p}^* = 0$ for all $p \neq 1$. The vectors $\boldsymbol{\beta}_\chi^*$ and $\boldsymbol{\chi}^* = \{\chi_p^*\}_{p \in \mathbb{N}}$ can be used to define the discrete distribution

$$G_\chi = \sum_{p \in \mathbb{N}} \beta_{\chi,p}^* \delta_{\chi_p^*}, \quad (11)$$

where δ is the Dirac delta function. Equation (11) is a draw from a $\text{DP}(\gamma_\chi, H_\chi)$, and thus we can equivalently describe $\boldsymbol{\beta}_\chi^*$ and χ_p as the components of a sample from $\text{DP}(\gamma_\chi, H_\chi)$, or as equations (8)

and (9). The vectors $\boldsymbol{\chi}^*$ and $\boldsymbol{\beta}_{\chi}^*$ contain, respectively, the values that the parameters can assume (χ_p^*) and the “base” probability ($\beta_{\chi_p}^*$) that a particular value of the parameter is selected in a behavior (see equation (15) below).

The functions $C_1(\cdot)$ and $C_2(\cdot)$. The function $C_1(\cdot)$ and $C_2(\cdot)$ (equations (6) and (7)) introduce the sharing of parameters between behaviors, which is one of the novelties of our proposal. The role of function $C_2(\cdot)$ is to produce the set of STAP parameters $\{\boldsymbol{\theta}_k\}_{k \in \mathbb{N}}$, where we remind the reader that $\boldsymbol{\theta}_k = (\boldsymbol{\mu}_k, \boldsymbol{\eta}_k, \boldsymbol{\Sigma}_k, \tau_k, \rho_k)$. The set $\{\boldsymbol{\theta}_k\}_{k \in \mathbb{N}}$ is comprised of all the possible combinations of the 5 STAP parameters, without repetitions. This means that $\boldsymbol{\theta}_k \neq \boldsymbol{\theta}_{k'}$, if $k \neq k'$, but we can have a subset of elements that has the same value, e.g., $\tau_k \equiv \tau_{k'}$. Hence, since each behavior selects its STAP parameters in $\boldsymbol{\theta} = \{\boldsymbol{\theta}_k\}_{k \in \mathbb{N}}$, different behaviors can share parameters, even though they are described by a different $\boldsymbol{\theta}_k$.

Function $C_1(\cdot)$ is closely related to $C_2(\cdot)$ since, if we introduce the new variables $\lambda_{\boldsymbol{\mu},k}$, $\lambda_{\boldsymbol{\eta},k}$, $\lambda_{\boldsymbol{\Sigma},k}$, $\lambda_{\tau,k}$ and $\lambda_{\rho,k}$ that represent what parameter is in $\boldsymbol{\theta}_k$, i.e.,

$$\boldsymbol{\mu}_k = \boldsymbol{\mu}_{\lambda_{\boldsymbol{\mu},k}}^*, \quad \boldsymbol{\eta}_k = \boldsymbol{\eta}_{\lambda_{\boldsymbol{\eta},k}}^*, \quad \boldsymbol{\Sigma}_k = \boldsymbol{\Sigma}_{\lambda_{\boldsymbol{\Sigma},k}}^*, \quad \tau_k = \tau_{\lambda_{\tau,k}}^*, \quad \rho_k = \rho_{\lambda_{\rho,k}}^*, \quad (12)$$

we can associate a value β_k to $\boldsymbol{\theta}_k$ which is computed as

$$\beta_k = \beta_{\boldsymbol{\mu}, \lambda_{\boldsymbol{\mu},k}}^* \beta_{\boldsymbol{\eta}, \lambda_{\boldsymbol{\eta},k}}^* \beta_{\boldsymbol{\Sigma}, \lambda_{\boldsymbol{\Sigma},k}}^* \beta_{\tau, \lambda_{\tau,k}}^* \beta_{\rho, \lambda_{\rho,k}}^*.$$

The set $\{\beta_k\}_{k \in \mathbb{N}}$ is the output of $C_1(\cdot)$ and it is a probability vector, since $\sum_{k \in \mathbb{N}} \beta_k = 1$ and $\beta_k \in (0, 1)$. We can define the discrete distribution

$$G_0 = \sum_{k \in \mathbb{N}} \beta_k \delta_{\boldsymbol{\theta}_k}, \quad (13)$$

where, similarly to (11), its atoms contain all the possible values that $\boldsymbol{\theta}_k$ can assume and β_k is connected to the expected value of the probability of selection $\boldsymbol{\theta}_k$ as the vector of parameter in a behavior (see equation (14) below). This way to define the distribution G_0 is closely related to the shared base-distribution of the change-point model of Mastrantonio et al. (2021).

Behavior switching. Let $\boldsymbol{\Pi}_j$ be the matrix that has $\boldsymbol{\pi}_{j,l} = \{\pi_{j,l,k}\}_{k \in \mathbb{N}}$ as l -th row. Matrix $\boldsymbol{\Pi}_j$ rules the switching between the behaviors of animal j (equation (4)) and if the j -th animal is following behavior l at time $t_{j,i-1}$, the probability of switching to behavior k is given by the element of $\boldsymbol{\Pi}_j$ in row l and column k . Hence, the time evolution of $z_{j,t_j,i}$ is modeled by a discrete first-order Markov process, which defines an HMM with transition matrix $\boldsymbol{\Pi}_j$ and initial state $z_{j,t_j,0}$. The initial state is drawn from a Geometric distribution with parameter ϵ , which is defined as the number of Bernoulli trials needed to have one success. The row $\boldsymbol{\pi}_{j,l}$ is DP distributed (see equation (5)) and the expected value of $\pi_{j,l,k}$ is equal to

$$\mathbb{E}(\pi_{j,l,k} | \alpha, \boldsymbol{\kappa}, \boldsymbol{\beta}) = \frac{\alpha \beta_k + \nu \delta(l, k)}{\alpha + \nu} \quad (14)$$

(see Fox et al., 2011), where $\delta(l, k)$ is equal to 1 if $l = k$, and 0 otherwise. From (14), we can see that the k -th element of $\boldsymbol{\beta}$ is associated with the expected value of $\pi_{j,l,k}$, for all the animals ($j = 1, \dots, m$) and $l \in \mathbb{N}$. Hence, a larger β_k increases the probability of switching from any behavior l to the k -th, described by $\boldsymbol{\theta}_k$. On the other hand, equation (14) can also be stated as

$$\mathbb{E}(\pi_{j,l,k} | \alpha, \boldsymbol{\kappa}, \boldsymbol{\beta}) = \frac{\alpha \beta_{\boldsymbol{\mu}, \lambda_{\boldsymbol{\mu},k}}^* \beta_{\boldsymbol{\eta}, \lambda_{\boldsymbol{\eta},k}}^* \beta_{\boldsymbol{\Sigma}, \lambda_{\boldsymbol{\Sigma},k}}^* \beta_{\tau, \lambda_{\tau,k}}^* \beta_{\rho, \lambda_{\rho,k}}^* + \nu \delta(l, k)}{\alpha + \nu}, \quad (15)$$

which highlights how the value $\beta_{\chi,p}^*$ is connected to all $\pi_{j,l,k}$, with $l, k \in \mathbb{N}$ and $j = 1, \dots, m$, so that $\lambda_{\chi,k} = p$. Therefore, a larger $\beta_{\chi,p}^*$ increases the expected values of all these probabilities, and for this reason we call β_{χ}^* the “base probability” as χ_p^* . The variable α is the scaling parameter of the DP of

equation (5), which has the same interpretation of γ_χ , while κ is a weight that is added to the self transitions $\pi_{j,l,l}$ to increase their expected value, see equation (14), which in turn is used to reduce the tendency of the HDP-HMM to create redundant behaviors, i.e., behaviors with similar parameter vectors. For a more detailed description of parameters α and ν , the reader may refer to Fox et al. (2011).

It should be noted that, in most applications, see, for example, McClintock et al. (2012) and Leos-Barajas et al. (2017), $z_{j,t_j,i} \in \{1, 2, \dots, K^*\}$ is assumed, where K^* indicates the maximum number of behaviors, while we have $z_{j,t_j,i} \in \mathbb{N}$ in this work, since we define the HMM using DPs. Thus, the model assumes an infinite and countable number of possible behaviors for each animal, but, since we have a finite number of observed time-points, only a finite number K_j of them can be “occupied”; these are generally called “non-empty states” (Frühwirth-Schnatter and Malsiner-Walli, 2019), or, in this context, “non-empty behaviors”. The random variable K_j is used to estimate the number of latent behaviors of the j -th animal. Parameters α , κ and γ (through β) determine the number of non-empty states K_j , since they are responsible with the total mass associated with each of the Π_j elements.

The emission-distribution. The model specification is concluded with the emission distribution, which is given by (2) and (3). It should be noted that, given the latent behaviors, we consider the animals independent but, since they share the same set of atoms $\{\theta_k\}_{k \in \mathbb{N}}$, the behaviors of the different animals can be described by the same STAP distribution. From equation (12), we know that θ_k and $\theta_{k'}$ can have common components and therefore, when an animal changes behavior, it is not necessary for all the parameters to change and, more importantly, we can also identify the features that two animals share for different behaviors, e.g., two behaviors can have the same attractive-point (μ_p^*), even though the strength of attraction (τ_p^*) is different. This feature is one of the main novelties of our proposal, and, although other approaches have a similar characteristic (see, for example, Jonsen (2016) or Milner et al. (2021)), they do not allow the number of latent behaviors to be estimate, which is the other main novelty of our proposal, the possibility of evaluating, during model fitting, what parameters are allowed to change, or the number of values that a parameter can assume. The sharing of a subset of the parameters between states is new in the context of HMMs based on DPs.

Connection to the sHDP-HMM. To conclude this section, we would like to show that our proposal can be considered as a generalization of the sHDP-HMM. The model of Fox et al. (2011) is defined for a single time-series, and G_0 is a draw from a DP. It is easy to see that, if we consider only one animal and use only one multivariate parameter in equation (9), e.g., $\theta_p^* = (\mu_p^*, \eta_p^*, \Sigma_p^*, \tau_p^*, \rho_p^*)$, with the associated vector of probability β_{θ^*} , the distribution G_0 is a draw from a DP, since $\beta_k = \beta_{\theta^*,p}^*$ and $\theta_k = \theta_p^*$. Hence, the model reduces to a sHDP-HMM.

4 Real data application

We have the recorded coordinates of 6 dogs, taken every 30 minutes at the Heatherlie property in Australia, between 2012-11-10 15:30 and 2012-08-02 15:30. The data¹ consist of 4801 observations for each dog, with less than 1% of missing points. To facilitate the specification of the prior the coordinates are centered using the bivariate sample mean and scaled with a common standard deviation, computed using both the X and Y coordinates, to maintain the relative scale between the two coordinates; the recorded locations are shown in Figure 2. The dogs are called Woody, Sherlock, Alvin, Rosie, Bear, and Lucy. Rosie and Lucy are female, while the other four are male, and Woody, Sherlock, Bear and Lucy form a cohesive group, which is responsible for livestock protection, while Rosie, due to her advanced age, is solitary, and Alvin suffers from social exclusion, which restricted his movement (van Bommel and Johnson, 2016).

Maremma Sheepdogs originate from Europe, and have been used for centuries to protect livestock

¹The dataset is freely available from the movebank repository <https://www.datarepository.movebank.org/handle/10255/move.395>

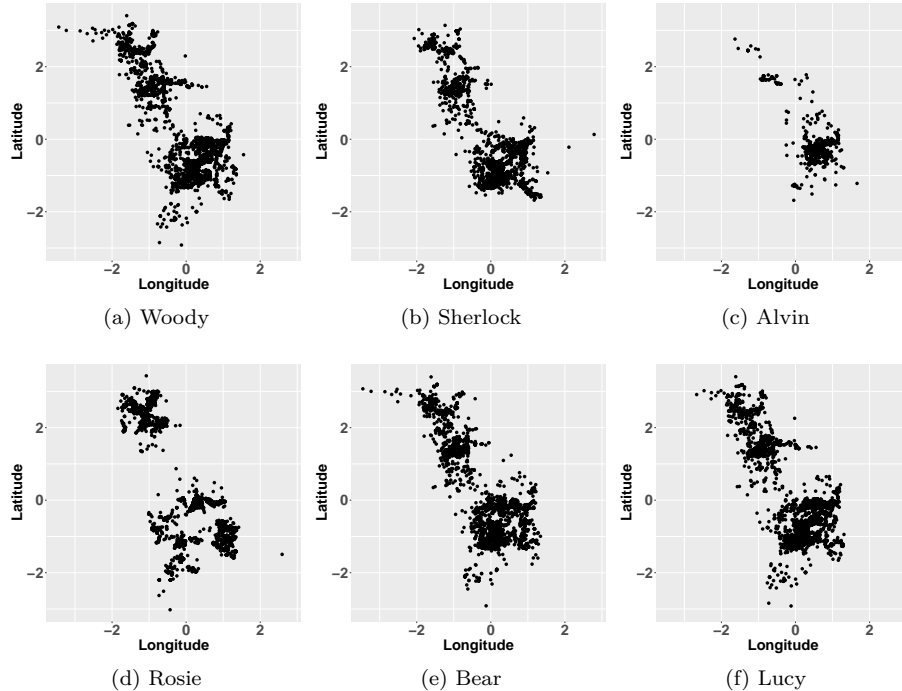


Figure 2: The observed spatial locations of the six dogs.

Table 1: Information criteria for the proposed model (M1), sHDP-HHMMs with a common G_0 (M2), sHDP-HHMMs with animal-specific $G_{0,j}$ (M3). The model selected by each index is indicated in bold.

	M1	M2	M3
ICL	209593	201880	192145
DIC5	-457502	-441264	-407823
DIC7	-417544	-400786	-376037

from potential predators (Gehring et al., 2017). They are trained to live with the livestock from birth and, as a result, they develop a strong bond with them and an instinct to protect them. They can be fence-trained, but are generally allowed to move freely. The use of livestock guardian dogs is relatively new outside Europe, especially in Australia, and, due to their effectiveness, interest in their use is increasing (van Bommel and Invasive Animals Cooperative Research Centre, 2010; van Bommel and Johnson, 2016). Since the extension of properties in Australia can be as much as several thousand hectares, it is hard for the owner to supervise the dogs (van Bommel and Johnson, 2012) and to have information about their behavior (van Bommel and Invasive Animals Cooperative Research Centre, 2010).

4.1 Comparison of the model and implementation details

We compare the predictive performances between our proposal (M1) and two competitive models (M2 and M3), using the integrated completed likelihood (ICL) (Biernacki et al., 2000) and the deviance information criteria (DIC) DIC₅ and DIC₇ (Celeux et al., 2006). In the first competitive model (M2),

we assume that only the entire vector of STAP parameters can be shared between animals, which means that each time-series is an sHDP-HMM with a share based distribution. In terms of model formalization, we assume

$$\{\beta_k\}_{k \in \mathbb{N}} | \gamma \sim \text{Gem}(\gamma),$$

$$\boldsymbol{\theta}_k | H_\mu, H_\eta, H_\Sigma, H_\tau, H_\rho \sim H_\mu \times H_\eta \times H_\Sigma \times H_\tau \times H_\rho,$$

for the set of atoms and weights of G_0 (equation (13)). In the second competitor (M3), each animal follows the model of Mastrantonio (2020), which means they are completely independent, and there is no sharing of parameters. Hence, we substitute G_0 with the animal-specific distribution

$$G_{0,j} = \sum_{k \in \mathbb{N}} \beta_{j,k} \delta_{\tilde{\boldsymbol{\theta}}_{j,k}},$$

where

$$\{\beta_{j,k}\}_{k \in \mathbb{N}} | \gamma_j \sim \text{Gem}(\gamma_j),$$

$$\tilde{\boldsymbol{\theta}}_{j,k} | H_\mu, H_\eta, H_\Sigma, H_\tau, H_\rho \sim H_\mu \times H_\eta \times H_\Sigma \times H_\tau \times H_\rho,$$

$$\tilde{\boldsymbol{\theta}}_{j,k} = (\boldsymbol{\mu}_{j,k}, \boldsymbol{\eta}_{j,k}, \boldsymbol{\Sigma}_{j,k}, \tau_{j,k}, \rho_{j,k}),$$

and then

$$\mathbf{s}_{j,t_j,i+1} | \mathbf{s}_{j,t_j,i}, \mathbf{s}_{j,t_j,i-1}, z_{j,t_j,i}, \tilde{\boldsymbol{\theta}}_{j,z_{j,t_j,i}} \sim \text{STAP}(\tilde{\boldsymbol{\theta}}_{j,z_{j,t_j,i}}).$$

By changing the way distribution G_0 is defined, we aim to show that the main feature of our proposal, i.e., the sharing of sets and subsets of parameters, improves the model fitting and leads to a better description of the data.

The models are implemented assuming $H_\mu \equiv N(\mathbf{0}, 20\mathbf{I})$, $H_\eta \equiv N(\mathbf{0}, 20\mathbf{I})$, $H_\tau \equiv U(0, 1)$, and $H_\Sigma \equiv IW(3, \mathbf{I})$. The distribution H_ρ is assumed to be a mixture of a $U(0, 1)$ and two bulks of probability on 0 and 1, with the 3 mixture weights equal to 1/3. This allows ρ_k (in M1 and M2) and $\rho_{j,k}$ (in M3) to be, a posteriori, equal to 0 or 1 with a greater probability than 0, which allows us to detect a pure CRW or BRW behavior. We assume $\alpha + \nu, \gamma_\mu, \gamma_\eta, \gamma_\Sigma, \gamma_\rho, \gamma_\tau, \gamma, \gamma_1, \dots, \gamma_m \sim G(0.01, 0.01)$ and $\nu / (\alpha + \nu) \sim B(1, 1)$, which allows us to easily sample from their full conditionals, see Fox et al. (2011) and Section A of the Appendix. All the distributions are chosen to be weakly informative. The domain \mathcal{D} is a square $[-5, 5] \times [-5, 5]$ and the parameter ϵ of the Geometric distribution is equal to 0.00001, which means that the distribution over the initial state, $z_{j,t_j,0}$, is approximately uniform over the positive integers. Posterior estimates are obtained with 15000 iterations, burnin 7500, thin 3, and thus 2500 samples are available for posterior inference. Convergence has been checked by means of a visual inspection of the posterior chains and using the \hat{R} statistics (Gelman et al., 2013). Details on the MCMC algorithm, implemented in Julia 1.3 (Bezanson et al., 2017), can be found in the Appendix, Section A, and the codes used to replicate the results, tables, and figures are available at https://github.com/GianlucaMastrantonio/multiple_animals_movement_model.

In Table 1, we can see that the three indices indicate that our model is the one with the best fit², model M2 is the second, while M3 is always the last. Therefore, the joint modeling of the six dogs improves the performances of the model (since M2 is always preferable to M3), but the sharing of a subset of parameters also leads to a better description of the data (since M1 is better than M2). We provide a description of the results obtained with M2 and M3 in the Appendix, Section B.

4.2 Description and interpretation of the output

Using the algorithm proposed by Wade and Ghahramani (2018), we find a representative behavior $\hat{z}_{j,t_j,i}$ associated with each animal and time, that we indicate as *MAP behavior*. We indicate the k -th

²It should be noted that a higher ICL and a lower DIC indicate a better fit.

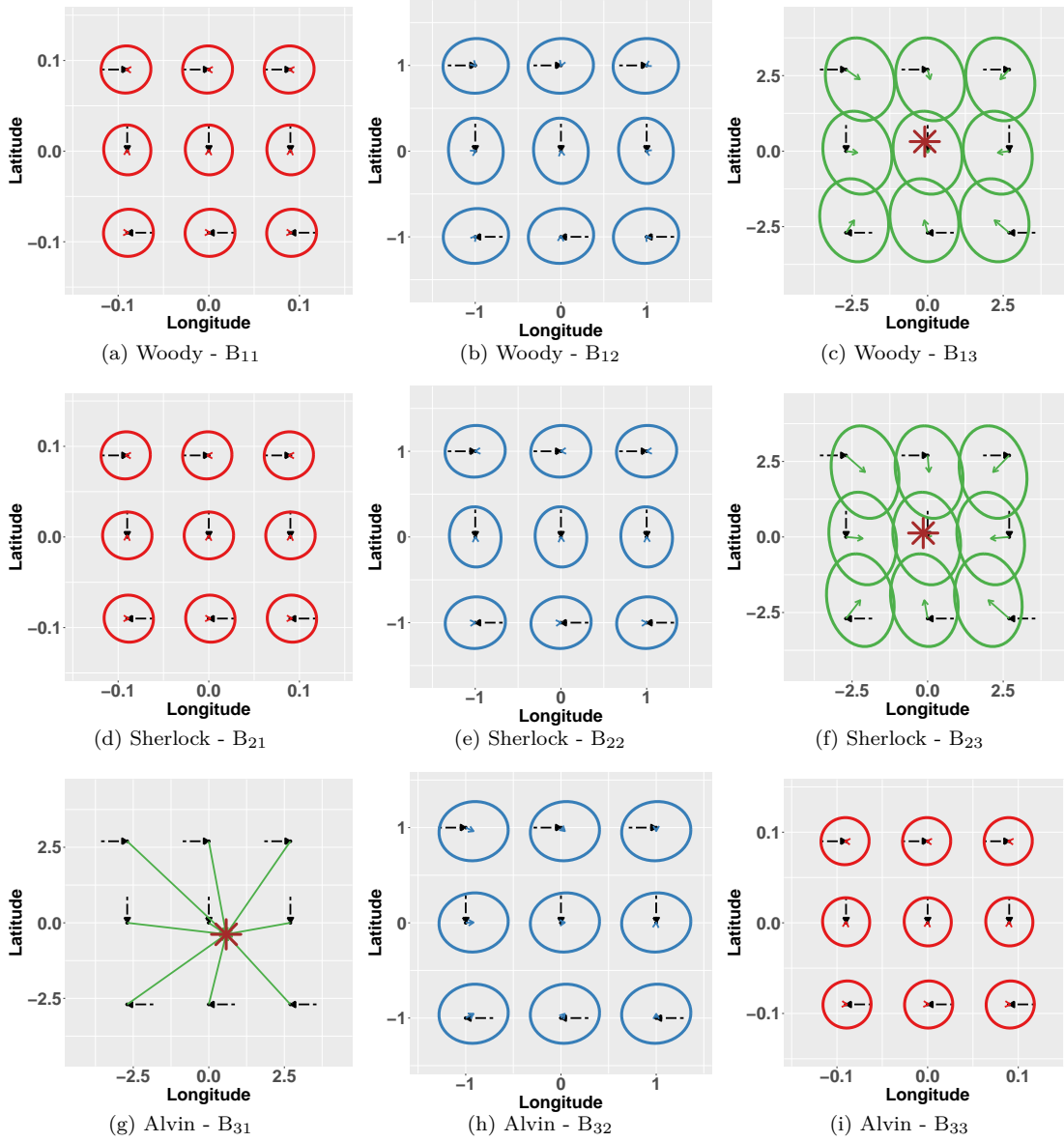


Figure 3: Graphical representation of the conditional distribution of $\mathbf{s}_{j,t_j,i+1}$ for the first three dogs, for different possible values of $\mathbf{s}_{j,t_j,i}$ and previous directions. The images has been obtained by using the posterior values that maximize the data likelihood of each animal, given the representative clusterization $\hat{z}_{j,t_j,i}$. The dashed arrow represents the movement between $\mathbf{s}_{j,t_j,i-1}$ and $\mathbf{s}_{j,t_j,i}$. The solid arrow is $\vec{\mathbf{F}}_{j,t_j,i}$, while the ellipse is an area containing 95% of the probability mass of the conditional distribution of $\mathbf{s}_{j,t_j,i+1}$. The asterisk represents the attractor, and it is only shown for behaviors that have posterior values of $\rho_{j,k} < 0.9$ and $\tau_{j,k} > 0.1$.

behavior of the j -th dog based on $\hat{z}_{j,t_j,i}$ as B_{jk} , and let $n_{j,k}$ be the number of times we have $\hat{z}_{j,t_j,i} = k$, without any loss of generality, we assume $n_{j,1} > n_{j,2} > \dots$, i.e., the behaviors are ordered with respect to the number of times they are observed. It should be noted that B_{jk} is not the same as $B_{j'k}$, if $j \neq j'$, and therefore, to avoid confusion, we indicate the vector of STAP parameters for B_{jk} with $\boldsymbol{\theta}_{j,k} = (\boldsymbol{\mu}_{j,k}, \boldsymbol{\eta}_{j,k}, \boldsymbol{\Sigma}_{j,k}, \tau_{j,k}, \rho_{j,k})$. For easiness of interpretation, we only discuss behaviors that have

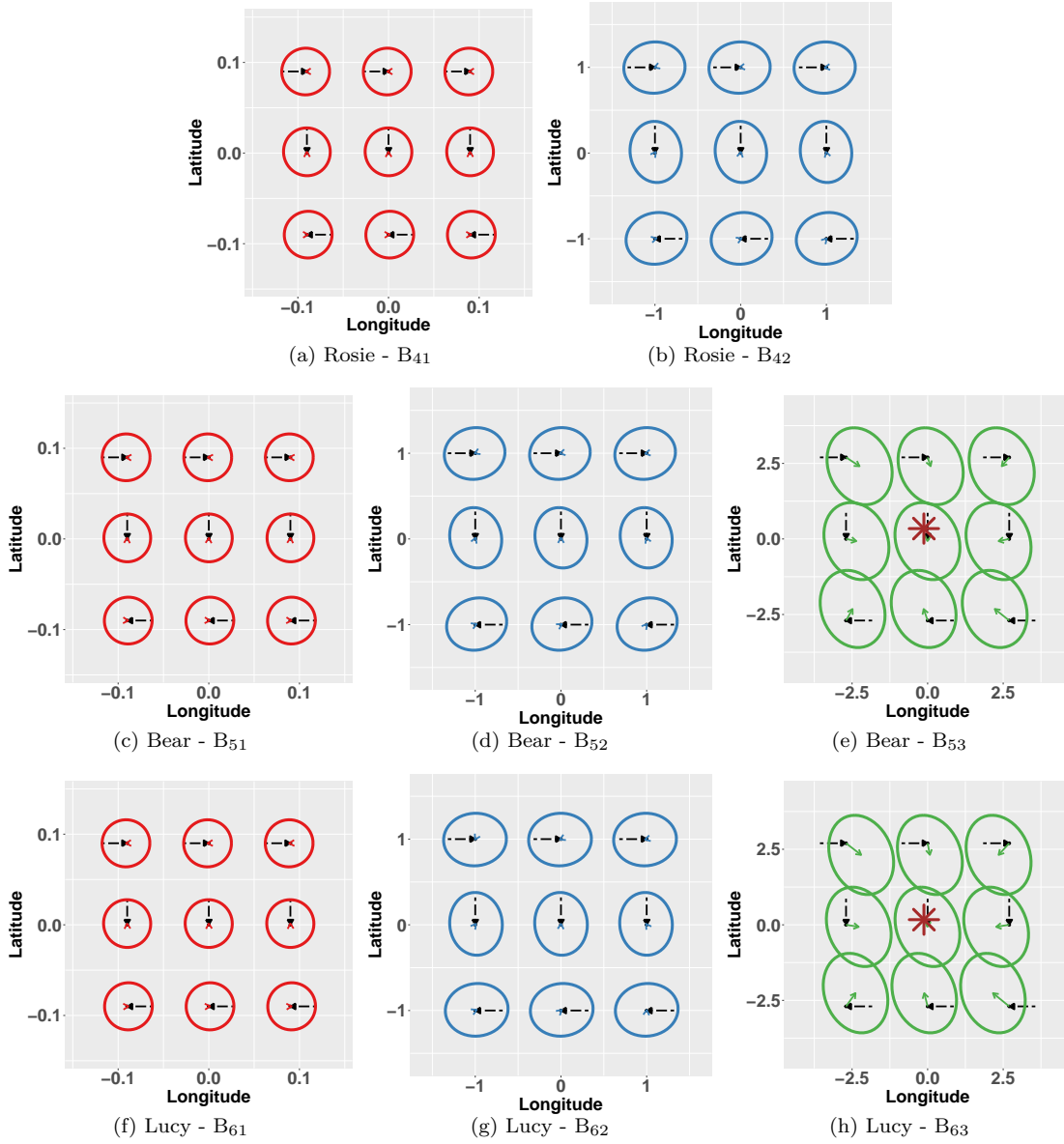


Figure 4: Graphical representation of the conditional distribution of $\mathbf{s}_{j,t_j,i+1}$ for the last three dogs, for different possible values of $\mathbf{s}_{j,t_j,i}$ and previous directions. The images has been obtained by using the posterior values that maximize the data likelihood of each animal, given the representative clusterization $\hat{z}_{j,t_j,i}$. The dashed arrow represents the movement between $\mathbf{s}_{j,t_j,i-1}$ and $\mathbf{s}_{j,t_j,i}$. The solid arrow is $\vec{\mathbf{F}}_{j,t_j,i}$, while the ellipse is an area containing 95% of the probability mass of the conditional distribution of $\mathbf{s}_{j,t_j,i+1}$. The asterisk represents the attractor, and it is only shown for behaviors that have posterior values of $\rho_{j,k} < 0.9$ and $\tau_{j,k} > 0.1$.

been observed, on average, at least once a day ($n_{j,k} > 100$), thus obtaining then 3 behaviors for each dogs, with the exception of Rosie (dog 4) that has 2 behaviors; see Tables 3-8 in the Appendix, where the posterior means ($\hat{\cdot}$) and credible intervals (CIs) for the STAP parameters, $n_{j,k}$, and the transition probabilities for all the dogs and behaviors are shown. Using similar pictures to the ones used in Figure 1, we show a graphical description of the behaviors found by the model in Figures 3 and 4;

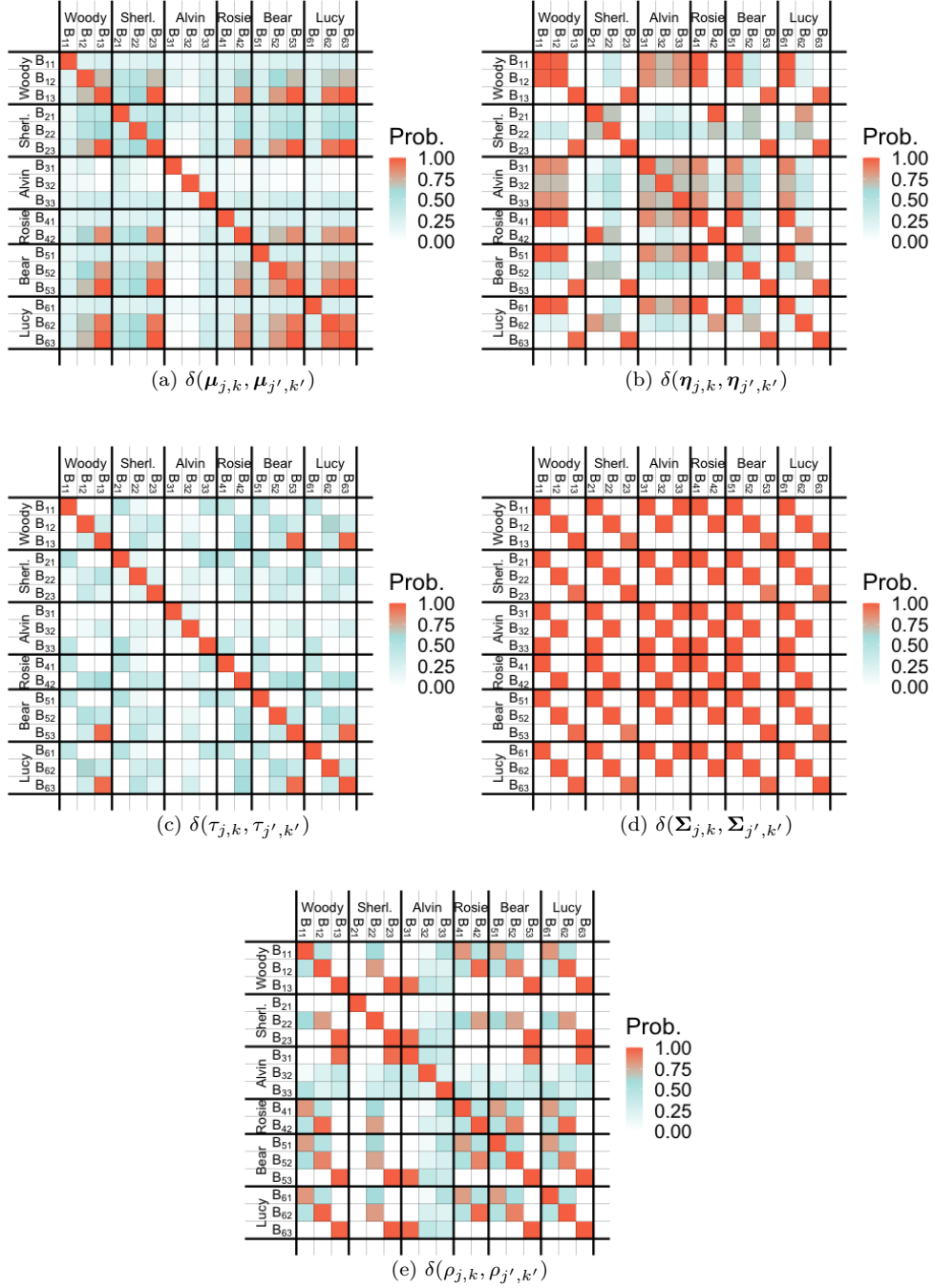


Figure 5: Graphical representation of the posterior mean of $\delta(\cdot, \cdot)$, which represents the probability of the parameters in its argument having the same value for two behaviors.

the behaviors are represented on different spatial scales. From the model output, we computed the posterior mean of the variable $\delta(\chi_{j,k}, \chi_{j',k'})$, which is the posterior probability that a STAP parameter assumes the same value in B_{jk} and $B_{j'k'}$. These probabilities are depicted in Figure 5 for all possible

Table 2: The Adjusted Rand Index for all the pairs of dogs.

	Woody	Sherlock	Alvin	Rosie	Bear	Lucy
Woody	1.000	0.094	0.006	0.030	0.181	0.414
Sherlock	0.094	1.000	-0.004	0.015	0.125	0.081
Alvin	0.006	-0.004	1.000	0.047	-0.002	0.003
Rosie	0.030	0.015	0.047	1.000	0.021	0.021
Bear	0.181	0.125	-0.002	0.021	1.000	0.159
Lucy	0.414	0.081	0.003	0.021	0.159	1.000

combinations of behaviors and animals. To take into account that identifiability for $\boldsymbol{\mu}_{j,k}$ and $\boldsymbol{\eta}_{j,k}$ is only granted if $\rho_{j,k} < 1$ and $\rho_{j,k} > 0$, respectively (see equation (1)), we assume $\delta(\boldsymbol{\mu}_{j,k}, \boldsymbol{\mu}_{j',k'}) = 0$, if $\rho_{j,k} = 1$ or $\rho_{j',k'} = 1$, and $\delta(\boldsymbol{\eta}_{j,k}, \boldsymbol{\eta}_{j',k'}) = 0$ if $\rho_{j,k} = 0$ or $\rho_{j',k'} = 0$, for $(i, j) \neq (i', j')$.

Similarities between the MAP behaviors. One of the assumptions of our proposal is that the temporal evolution of the behaviors are independent. To have a posterior confirmation that this hypothesis is true, we computed the Adjusted Rand Index (Gates and Ahn, 2017) for the MAP behaviors of each pair of animals. The Adjusted Rand Index, which is a measure of similarity (or agreement) between two clusterizations, has a value close to one, if there is a strong agreement, while its value is close to zero (even negative) if the clusterization is very dissimilar. It should be noted that we are able to compute the index because the animals are observed in the same temporal-window. The results in Table 2 show that the values of the index are very low, with the exception of dogs 1 and 6, where the index is 0.414. We can conclude that our hypothesis is reasonable.

The dogs in the cohesive group. We can clearly see, from Figures 3 and 4, that the four dogs that form a cohesive group (dog 1 Woody, dog 2 Sherlock, dog 5 Bear and dog 6 Lucy) have similar behaviors. In behavior B_{j1} , the length of $\vec{\mathbf{F}}_{j,t_j,i}$ is ≈ 0 , which means that the distribution of $\mathbf{s}_{j,t_j,i+1}$ is centered on the previous location ($\mathbf{s}_{j,t_j,i}$), there is no a preferable direction, since the ellipses are very close to a circle, the speed is very low (see the size of the ellipses), and there is no attractor. Hence, the movement is only determined by the covariance matrix $\boldsymbol{\Sigma}_{j,1}$, which is the same for all the first behaviors (B_{j1}), see Figure 5 (d). The first behavior of the cohesive group can easily be interpreted as boundary-patrolling- or scent-marking-behavior, which is a common behavior in this dog breed, and it has already been observed and with similar movement characteristics (McGrew and Blakesley, 1982; Mastrantonio, 2020).

As in B_{j1} , the length of $\vec{\mathbf{F}}_{j,t_j,i}$ is ≈ 0 in B_{j2} , there is no attractor but, since the ellipses rotate according to the previous directions, there is directional persistence. The major and minor axes of the ellipses have different lengths, with the major one in the same direction as $\phi_{j,t_j,i-1}$, which means that we can expect to observe more movements on a straight line, i.e., in the same direction as the previous bearing angle $\phi_{j,t_j,i-1}$, or in direction $\phi_{j,t_j,i-1} - \pi$. The strength of directional persistence, measured by parameter $\rho_{j,2}$, is very similar for all the B_{j2} , as we can see from Figure 5 (e), where the probability values are close to 1. The movement speed in B_{j2} increases compared to B_{j1} , and B_{j2} is fully characterized by $\boldsymbol{\Sigma}_{j,2}$ and $\rho_{j,2}$. The strong directional persistence, the movement along a straight line, and the higher speed can lead to B_{j2} being interpreted as a defending-behavior, where the dog defends the territory and livestock from predators, that is, mostly wild dogs and foxes that are present in the area (see Brook et al., 2012; Walton et al., 2017), or an explore-behavior (van Bommel and Invasive Animals Cooperative Research Centre, 2010; Mastrantonio, 2020).

The third behavior is a BRW, since the CIs of $\rho_{j,3}$ are very close to 0 and the ellipses are independent of the previous direction (see Figures 3 and 4). The CIs of $\tau_{j,3}$, which are in $[0.1, 0.28]$, indicate a moderate attraction to $\boldsymbol{\mu}_{j,3}$, see Tables 3, 4, 7 and 8 in the Appendix. The four dogs have the same spatial attractor, $\boldsymbol{\mu}_{j,3}$, the same covariance matrix, $\boldsymbol{\Sigma}_{j,3}$, the same parameter $\rho_{j,k}$ and, with

the exception of the second dog, the same $\tau_{j,k}$, as we can see from Figures 3, 4, and 5. The spatial attractor, due to the large variance of the movement (the ellipses size), can be considered as a tendency of these dogs to move to the central patch of the space and, since we can see from Figure c2 of van Bommel and Johnson (2012) that the attractor is close to where the livestock is, it is easy to interpret this behavior as the dog attending livestock.

It is interesting to note that the parameters that define the three behaviors, i.e., $\Sigma_{j,k}$ in B_{j1} , $(\Sigma_{j,k}, \rho_{j,k})$ in B_{j2} , $(\mu_{j,k}, \tau_{j,k}, \Sigma_{j,k}, \rho_{j,k})$ in B_{j3} , have a high probability of being the same between dogs, see Figure 5, which means that they behave in a similar manner. In transition matrix terms, we can see, from Tables 3, 4, 7 and 8 in the Appendix, that $\hat{\pi}_{j,1,2} > \hat{\pi}_{j,1,3}$ and $\hat{\pi}_{j,3,2} > \hat{\pi}_{j,3,1}$. Then, after patrolling (B_{j1}), it is more probable that the dog begins to explore the space, or to defend the property from predators spotted during patrolling (B_{j2}), than to guard livestock (B_{j3}). After attending livestock, it is more probable that the dog switches to B_{j2} .

The socially excluded dog and the old one. The socially excluded dog ($j=3$) has 3 behaviors, one of which, B_{31} , is different from all the other dogs' behaviors, while the other two, B_{32} and B_{33} , are similar to the ones of the cohesive group, e.g., B_{32} is similar to B_{j2} and B_{33} is similar to B_{j1} , with $j = 1, 2, 5, 6$, see Figures 3 and 4. B_{33} is only characterized by the covariance matrix $\Sigma_{j,3}$, since like B_{j1} in the cohesive group, $\vec{F}_{3,t_{3,i}}$ is ≈ 0 and there is no attractor or directional persistence. Therefore, due to the high probability of $\Sigma_{3,3}$ having the same value as $\Sigma_{j,3}$, with $j = 1, 2, 5, 6$, see Figure 5 (d), B_{33} may be interpreted in the same way as the first behaviors of the cohesive group, i.e., a boundary-patrolling behavior.

B_{32} is similar to the second behavior of the cohesive group in terms of covariance matrix, see Figure 5 (d), but there is a lack of directional persistence, and a slight bias toward an attractor located in the central area, see the direction of $\vec{F}_{3,t_{3,i}}$. With this behavior, the dog is exploring but, at the same time, staying in the proximity of the sheep paddock, see Figure 2 (c).

The CI of $\tau_{3,1}$ is very close to 1 and B_{31} therefore has a strong attraction to the coordinates $\hat{\mu}_{3,1} = (0.575, -381)'$, as we can see from Table 5 of the Appendix. The CIs of $\mu_{3,1,1}$ and $\mu_{3,1,2}$ are very small and equal to $(0.575, 0.576)$ and $(-0.381, 0.380)$, respectively, which means that the attractor is well localized in space. We can see from Figure c2 of van Bommel and Johnson (2012), that $\hat{\mu}_{3,1}$ is close to the owner's homestead. This behavior cannot be interpreted as the dog attending livestock since, once it reaches the spatial attractor, it does not move very much, i.e., the sizes of the ellipses are very small. Hence, this is probably a behavior in which the dog stays close to the owner's house, and rests.

For the last dog, that is the old one, the model has found only two behaviors. B_{41} has the same characteristics as the first behavior of the cohesive group, with the same values of the covariance matrix, while B_{42} is similar to the second behavior of the cohesive group, with the same covariance matrix and similar directional persistence, see Figures 3, 4, and 5. Hence, they can be interpreted as the first and second behaviors of the cohesive group. It is interesting to note that, since this dog is very old, she is no longer able to attend livestock, which is the activity that requires the most energy (higher speed), but she is still working, that is, checking the boundaries (B_{41}), exploring the space, and defending the territory (B_{42}).

5 Final remarks

In this work, we have proposed a new HMM which can be used to model trajectory-tracking data of multiple animals and which, according to the classification given by Scharf and Buderman (2020), is part of the indirect approach. Our model allows subsets of parameters to be shared between animals and behaviors, and the number of latent behaviors to be selected during the model fitting. The emission distribution is the STAP, but other distributions can be used by changing the model formalization accordingly.

The model was used to help understand the behavior of 6 Maremma Sheepdogs, observed in a

property in Australia. The results show that there are many common features between the animals, such as the attractive point, and most of them share the same number of behaviors as well as the same parameter values. The obtained results are easily interpretable, and the rich output offers an insight into the similarities between animals.

As a possible extension, we are currently exploring the use of covariates to model the probability that behaviors share parameters, and we are working on a different formalization that makes the model able to detect whether different animals tend to follow the same behaviors at the same time-points.

Acknowledgments

The author would like to thank the Editor-in-Chief, the Associate Editor and the two anonymous reviewers for their comments that have greatly improved the manuscript. The work of the author has partially been developed under the MIUR grant Dipartimenti di Eccellenza 2018 - 2022 (E11G18000350001), conferred to the Dipartimento di Scienze Matematiche - DISMA, Politecnico di Torino.

Appendix A Markov chain Monte Carlo algorithm

In the next two sections, we show how to sample the posterior values of the HMM parameters, Section A.1, and STAP parameters, Section A.2. The algorithm is based on the works of Mastrantonio (2020) and Fox et al. (2011).

A.1 HMM

In order to implement the sample of the HMM parameters, we use the *degree L weak limit approximation* (Ishwaran and Zarepour, 2002) of a DP, which approximates the distribution of the infinite-dimensional probability vector GEM distributed, with a finite one of dimension L. We thus obtain

$$\begin{aligned}
 \beta_{\mu}^* | \gamma_{\mu} &\sim \text{Dir} \left(\frac{\gamma_{\mu}}{L}, \dots, \frac{\gamma_{\mu}}{L} \right), \\
 \beta_{\eta}^* | \gamma_{\eta} &\sim \text{Dir} \left(\frac{\gamma_{\eta}}{L}, \dots, \frac{\gamma_{\eta}}{L} \right), \\
 \beta_{\Sigma}^* | \gamma_{\Sigma} &\sim \text{Dir} \left(\frac{\gamma_{\Sigma}}{L}, \dots, \frac{\gamma_{\Sigma}}{L} \right), \\
 \beta_{\tau}^* | \gamma_{\tau} &\sim \text{Dir} \left(\frac{\gamma_{\tau}}{L}, \dots, \frac{\gamma_{\tau}}{L} \right), \\
 \beta_{\rho}^* | \gamma_{\rho} &\sim \text{Dir} \left(\frac{\gamma_{\rho}}{L}, \dots, \frac{\gamma_{\rho}}{L} \right),
 \end{aligned} \tag{16}$$

and

$$\pi_{j,l} | \alpha, \nu, \beta \sim \text{Dir}(\alpha\beta_1 + \nu\delta(l, 1), \alpha\beta_2 + \nu\delta(l, 2), \dots, \alpha\beta_{L^5} + \nu\delta(l, L^5)). \tag{17}$$

Hence, β and $\pi_{j,l}$ are both finite-dimensional (see Fox et al. (2011)) with L and L^5 elements. As $L \rightarrow \infty$, the Dirichlet distributions in (16) converges to the associated GEMs, and equation (17) converges to a DP $\left(\alpha + \nu, \frac{\alpha\beta + \nu\delta_l}{\alpha + \nu} \right)$. This approximation greatly simplifies the implementation, and it is accurate as long as the number of unique values of each STAP parameter, estimated by means of the model, is $\ll L$. For our implementation, we assume $L = 100$.

Sampling $\pi_{j,l}$ Let $n_{j,l,k}$ be the number of transitions of the j -th animal from behavior l to behavior k :

$$n_{j,l,k} = \sum_{i=1}^{T-1} \delta(z_{j,t_{j,i-1}}, l) \delta(z_{j,t_{j,i}}, k).$$

Since (17) has a finite dimension, $\boldsymbol{\pi}_{j,l}$ can be sampled as in a standard HMM, and its full conditional is

$$\boldsymbol{\pi}_{j,l} \sim \text{Dir}(\alpha\boldsymbol{\beta}_1 + \nu\delta(l, 1) + n_{j,l,1}, \alpha\boldsymbol{\beta}_2 + \nu\delta(l, 2) + n_{j,l,2}, \dots, \alpha\boldsymbol{\beta}_{L^5} + \nu\delta(l, L^5) + n_{j,l,L^5}).$$

It should be noted that, even though the dimension of $\boldsymbol{\pi}_{j,l}$ is very large, we do not have to sample all of its components but only the ones with $n_{j,l,k} > 0$. This can easily be done using the stick-breaking sample scheme (Sethuraman, 1994).

Sampling β_μ^* , β_η^* , β_Σ^* , β_τ^* , β_ρ^* In order to be able to sample these parameters, we use the results of Fox et al. (2011), which show that, by introducing the latent variables

$$\begin{aligned} x_{j,l,k,h} &\sim \text{Ber}\left(\frac{\alpha\beta_k + \nu\delta(l, k)}{h - 1 + \alpha\beta_k + \nu\delta(l, k)}\right), h = 1, \dots, n_{j,l,k}, \\ w_{j,l} &\sim \text{Binomial}\left(b_{j,l,l}, \frac{\nu}{\nu + \beta_j\alpha}\right), \end{aligned} \quad (18)$$

where the variables $x_{j,l,k,h}$ in (18) only need to be sampled if $n_{j,l,k} > 0$, the vector $\boldsymbol{\beta}$ enters into the density of $\{\boldsymbol{\pi}_{j,l}\}_{l=1}^{L^5}$ as

$$\prod_{l=1}^{L^5} \prod_{k=1}^{L^5} \beta_k^{\bar{b}_{j,l,k}} = \prod_{k=1}^{L^5} \beta_k^{\bar{b}_{j,\cdot,k}} = \prod_{k=1}^{L^5} \left(\beta_{\mu,\lambda_{\mu,k}}^* \beta_{\eta,\lambda_{\eta,k}}^* \beta_{\Sigma,\lambda_{\Sigma,k}}^* \beta_{\tau,\lambda_{\tau,k}}^* \beta_{\rho,\lambda_{\rho,k}}^* \right)^{\bar{b}_{j,\cdot,k}},$$

where

$$\begin{aligned} \bar{b}_{j,\cdot,k} &= \sum_{l=1}^{L^5} \bar{b}_{j,l,k}, \\ \bar{b}_{j,l,k} &= \begin{cases} b_{j,l,k} & \text{if } l \neq k, \\ b_{j,l,k} - w_{j,l} & \text{if } l = k, \end{cases} \\ b_{j,l,k} &= \begin{cases} 0 & \text{if } n_{j,l,k} = 0, \\ \sum_{h=1}^{n_{j,l,k}} x_{j,l,k,h} & \text{otherwise.} \end{cases} \end{aligned}$$

Hence, the full conditionals are

$$\begin{aligned} \beta_\mu^* &\sim \text{Dir}\left(\frac{\gamma_\mu}{L} + \bar{b}_{\mu,1}, \frac{\gamma_\mu}{L} + \bar{b}_{\mu,2}, \dots, \frac{\gamma_\mu}{L} + \bar{b}_{\mu,L}\right), \\ \beta_\eta^* &\sim \text{Dir}\left(\frac{\gamma_\eta}{L} + \bar{b}_{\eta,1}, \frac{\gamma_\eta}{L} + \bar{b}_{\eta,2}, \dots, \frac{\gamma_\eta}{L} + \bar{b}_{\eta,L}\right), \\ \beta_\Sigma^* &\sim \text{Dir}\left(\frac{\gamma_\Sigma}{L} + \bar{b}_{\Sigma,1}, \frac{\gamma_\Sigma}{L} + \bar{b}_{\Sigma,2}, \dots, \frac{\gamma_\Sigma}{L} + \bar{b}_{\Sigma,L}\right), \\ \beta_\tau^* &\sim \text{Dir}\left(\frac{\gamma_\tau}{L} + \bar{b}_{\tau,1}, \frac{\gamma_\tau}{L} + \bar{b}_{\tau,2}, \dots, \frac{\gamma_\tau}{L} + \bar{b}_{\tau,L}\right), \\ \beta_\rho^* &\sim \text{Dir}\left(\frac{\gamma_\rho}{L} + \bar{b}_{\rho,1}, \frac{\gamma_\rho}{L} + \bar{b}_{\rho,2}, \dots, \frac{\gamma_\rho}{L} + \bar{b}_{\rho,L}\right), \end{aligned}$$

where

$$\begin{aligned}\bar{b}_{\boldsymbol{\mu},p} &= \sum_{j=1}^m \sum_{k=1}^{L^5} \bar{b}_{j,\cdot,k} \delta(\lambda_{\boldsymbol{\mu},k}, p), \\ \bar{b}_{\boldsymbol{\eta},p} &= \sum_{j=1}^m \sum_{k=1}^{L^5} \bar{b}_{j,\cdot,k} \delta(\lambda_{\boldsymbol{\eta},k}, p), \\ \bar{b}_{\boldsymbol{\Sigma},p} &= \sum_{j=1}^m \sum_{k=1}^{L^5} \bar{b}_{j,\cdot,k} \delta(\lambda_{\boldsymbol{\Sigma},k}, p), \\ \bar{b}_{\boldsymbol{\tau},p} &= \sum_{j=1}^m \sum_{k=1}^{L^5} \bar{b}_{j,\cdot,k} \delta(\lambda_{\boldsymbol{\tau},k}, p), \\ \bar{b}_{\boldsymbol{\rho},p} &= \sum_{j=1}^m \sum_{k=1}^{L^5} \bar{b}_{j,\cdot,k} \delta(\lambda_{\boldsymbol{\rho},k}, p).\end{aligned}$$

Sampling $\gamma_{\boldsymbol{\mu}}, \gamma_{\boldsymbol{\eta}}, \gamma_{\boldsymbol{\Sigma}}, \gamma_{\boldsymbol{\tau}}, \gamma_{\boldsymbol{\rho}}$ Since each γ_{χ} is the hyperparameter of a DP, we can use the approach proposed by Escobar and West (1995), which was later extended to the sHDP-HMM framework by Fox et al. (2011). If the prior is $G(a_{\gamma}, b_{\gamma})$ and if we introduce the latent variables

$$\begin{aligned}\xi_{\boldsymbol{\mu}} &\sim \text{B}(\gamma_{\boldsymbol{\mu}} + 1, \sum_{p=1}^L \bar{b}_{\boldsymbol{\mu},p}), \\ \xi_{\boldsymbol{\eta}} &\sim \text{B}(\gamma_{\boldsymbol{\eta}} + 1, \sum_{p=1}^L \bar{b}_{\boldsymbol{\eta},p}), \\ \xi_{\boldsymbol{\Sigma}} &\sim \text{B}(\gamma_{\boldsymbol{\Sigma}} + 1, \sum_{p=1}^L \bar{b}_{\boldsymbol{\Sigma},p}), \\ \xi_{\boldsymbol{\tau}} &\sim \text{B}(\gamma_{\boldsymbol{\tau}} + 1, \sum_{p=1}^L \bar{b}_{\boldsymbol{\tau},p}), \\ \xi_{\boldsymbol{\rho}} &\sim \text{B}(\gamma_{\boldsymbol{\rho}} + 1, \sum_{p=1}^L \bar{b}_{\boldsymbol{\rho},p}),\end{aligned}$$

and let

$$\begin{aligned}
K_{\boldsymbol{\mu}} &= \sum_{p=1}^L \mathbb{I}(\bar{b}_{\boldsymbol{\mu},p} > 0), \\
K_{\boldsymbol{\eta}} &= \sum_{p=1}^L \mathbb{I}(\bar{b}_{\boldsymbol{\eta},p} > 0), \\
K_{\boldsymbol{\Sigma}} &= \sum_{p=1}^L \mathbb{I}(\bar{b}_{\boldsymbol{\Sigma},p} > 0), \\
K_{\boldsymbol{\tau}} &= \sum_{p=1}^L \mathbb{I}(\bar{b}_{\boldsymbol{\tau},p} > 0), \\
K_{\boldsymbol{\rho}} &= \sum_{p=1}^L \mathbb{I}(\bar{b}_{\boldsymbol{\rho},p} > 0).
\end{aligned}$$

where $\mathbb{I}(\cdot)$ is equal to 1 if the argument is true, and zero otherwise, the full conditionals become

$$\begin{aligned}
\gamma_{\boldsymbol{\mu}} &\sim \pi_{\boldsymbol{\mu}} \text{G}(a_{\gamma} + K_{\boldsymbol{\mu}}, b_{\gamma} - \log(\xi_{\boldsymbol{\mu}})) + (1 - \pi_{\boldsymbol{\mu}}) \text{G}(a_{\gamma} + K_{\boldsymbol{\mu}} - 1, b_{\gamma} - \log(\xi_{\boldsymbol{\mu}})), \\
\gamma_{\boldsymbol{\eta}} &\sim \pi_{\boldsymbol{\eta}} \text{G}(a_{\gamma} + K_{\boldsymbol{\eta}}, b_{\gamma} - \log(\xi_{\boldsymbol{\eta}})) + (1 - \pi_{\boldsymbol{\eta}}) \text{G}(a_{\gamma} + K_{\boldsymbol{\eta}} - 1, b_{\gamma} - \log(\xi_{\boldsymbol{\mu}})), \\
\gamma_{\boldsymbol{\Sigma}} &\sim \pi_{\boldsymbol{\Sigma}} \text{G}(a_{\gamma} + K_{\boldsymbol{\Sigma}}, b_{\gamma} - \log(\xi_{\boldsymbol{\Sigma}})) + (1 - \pi_{\boldsymbol{\Sigma}}) \text{G}(a_{\gamma} + K_{\boldsymbol{\Sigma}} - 1, b_{\gamma} - \log(\xi_{\boldsymbol{\Sigma}})), \\
\gamma_{\boldsymbol{\tau}} &\sim \pi_{\boldsymbol{\tau}} \text{G}(a_{\gamma} + K_{\boldsymbol{\tau}}, b_{\gamma} - \log(\xi_{\boldsymbol{\tau}})) + (1 - \pi_{\boldsymbol{\tau}}) \text{G}(a_{\gamma} + K_{\boldsymbol{\tau}} - 1, b_{\gamma} - \log(\xi_{\boldsymbol{\tau}})), \\
\gamma_{\boldsymbol{\rho}} &\sim \pi_{\boldsymbol{\rho}} \text{G}(a_{\gamma} + K_{\boldsymbol{\rho}}, b_{\gamma} - \log(\xi_{\boldsymbol{\rho}})) + (1 - \pi_{\boldsymbol{\rho}}) \text{G}(a_{\gamma} + K_{\boldsymbol{\rho}} - 1, b_{\gamma} - \log(\xi_{\boldsymbol{\rho}})),
\end{aligned}$$

where

$$\begin{aligned}
\pi_{\boldsymbol{\mu}} &= \frac{a_{\gamma} + K_{\boldsymbol{\mu}} - 1}{(b_{\gamma} - \log(\xi_{\boldsymbol{\mu}})) \sum_{p=1}^L \bar{b}_{\boldsymbol{\mu},p}}, \\
\pi_{\boldsymbol{\eta}} &= \frac{a_{\gamma} + K_{\boldsymbol{\eta}} - 1}{(b_{\gamma} - \log(\xi_{\boldsymbol{\eta}})) \sum_{p=1}^L \bar{b}_{\boldsymbol{\eta},p}}, \\
\pi_{\boldsymbol{\Sigma}} &= \frac{a_{\gamma} + K_{\boldsymbol{\Sigma}} - 1}{(b_{\gamma} - \log(\xi_{\boldsymbol{\Sigma}})) \sum_{p=1}^L \bar{b}_{\boldsymbol{\Sigma},p}}, \\
\pi_{\boldsymbol{\tau}} &= \frac{a_{\gamma} + K_{\boldsymbol{\tau}} - 1}{(b_{\gamma} - \log(\xi_{\boldsymbol{\tau}})) \sum_{p=1}^L \bar{b}_{\boldsymbol{\tau},p}}, \\
\pi_{\boldsymbol{\rho}} &= \frac{a_{\gamma} + K_{\boldsymbol{\rho}} - 1}{(b_{\gamma} - \log(\xi_{\boldsymbol{\rho}})) \sum_{p=1}^L \bar{b}_{\boldsymbol{\rho},p}}.
\end{aligned}$$

Sampling $\nu/(\alpha + \nu)$ The sampling of this parameter follows directly from Fox et al. (2011), if we assume a $B(a_{\nu}, b_{\nu})$ prior. This parameter enters into the distribution of the transition matrix as in the model of Fox et al. (2011), with the only difference being that we have to take into consideration that m different HMMs are used. Hence, the full conditional of $\nu/(\alpha + \nu)$ is

$$\text{B} \left(\sum_{j=1}^m \sum_{l=1}^{K_j} w_{j,l} + a_{\nu}, \sum_{l=1}^L \sum_{k=1}^L b_{j,l,k} - \sum_{j=1}^m \sum_{l=1}^{K_j} w_{j,l} + b_{\nu} \right).$$

Sampling $\alpha + \nu$ Fox et al. (2011) showed that the contribution of the j -th transition matrix to the full conditional of $\alpha + \nu$ is

$$(\alpha + \nu) \sum_{l=1}^L \sum_{k=1}^L b_{j,l,k} \prod_{l=1}^{K_j} \frac{\Gamma(\alpha + \nu)}{\Gamma(\alpha + \nu + \sum_{k=1}^L n_{j,l,k})}.$$

Since conditionally to β the animals are independent, we can use the results of Fox et al. (2011). Hence, if we introduce the following latent variables

$$r_{1,j,l} \sim B(\alpha + \nu + 1, \sum_{k=1}^L n_{j,l,k}),$$

$$r_{2,j,l} \sim \text{Ber}\left(\frac{\sum_{k=1}^L n_{j,l,k}}{\sum_{k=1}^L n_{j,l,k} + \alpha + \nu}\right),$$

we can express the full conditional of $\alpha + \nu$ as

$$G\left(a_{\alpha+\nu} + \sum_{j=1}^m \sum_{l=1}^{K_j} w_{j,l} - \sum_{j=1}^m \sum_{l=1}^L r_{2,j,l}, b_{\alpha+\nu} - \sum_{j=1}^m \sum_{l=1}^L \log(r_{1,j,l})\right).$$

Sampling $z_{j,t_j,i}$ The full conditional of $z_{j,t_j,i}$ is multinomial, with one trial and the k -th probability proportional to

$$\begin{cases} \pi_{j,z_j,t_j,i-1,k} \pi_{j,k,z_j,t_j,i+1} f(s_{j,t_j,i+1} | s_{j,t_j,i}, s_{j,t_j,i-1}, \theta_k) & \text{if } i \geq 1, \\ (1 - \epsilon)^{k-1} \epsilon \pi_{j,k,z_j,t_j,1} & \text{otherwise,} \end{cases} \quad (19)$$

where $f(s_{j,t_j,i+1} | s_{j,t_j,i}, s_{j,t_j,i-1}, \theta_k)$ is the STAP density and $((1 - \epsilon)^{k-1} \epsilon)$ is the Geometric probability mass over the value k . In order to be able to sample from the full conditional, we have to compute (19) for all the possible L^5 behaviors, which is unfeasible. For this reason, we decided to exploit the beam sample scheme of Van Gael et al. (2008) which, as a result of the introduction of latent variables, is able to drastically reduce the number of elements that need to be computed. The idea is to introduce the variables

$$u_{j,t_j,i} \sim U(0, \pi_{j,z_j,t_j,i-1,z_j,t_j,i}),$$

and then, conditionally to all $u_{j,t_j,i}$, the variable $z_{j,t_j,i}$ is only allowed to assume values that satisfy the constraints $\pi_{j,z_j,t_j,i-1,z_j,t_j,i} > u_{j,t_j,i}$ and $\pi_{j,z_j,t_j,i,z_j,t_j,i+1} > u_{j,t_j,i+1}$. Hence, equation (19) only needs to be evaluated for a finite set of elements, which is often very small. The values of $\pi_{j,l,k}$ for empty behaviors can easily be obtained using the stick breaking sample scheme.

In order to increase the convergence speed, we also suggest using another updating strategy for $z_{j,t_j,i}$. Let us introduce the new random variables $z_{\mu,j,t_j,i}$, $z_{\eta,j,t_j,i}$, $z_{\Sigma,j,t_j,i}$, $z_{\tau,j,t_j,i}$, and $z_{\rho,j,t_j,i}$, whose values represent what elements of μ^* , η^* , Σ^* , τ^* , and ρ^* , respectively, are in θ , at time t_j,i and for the j -th animal. There is a one-to-one relationship between $z_{j,t_j,i}$ and $(z_{\mu,j,t_j,i}, z_{\eta,j,t_j,i}, z_{\Sigma,j,t_j,i}, z_{\tau,j,t_j,i}, z_{\rho,j,t_j,i})$, i.e., if we know the value of $z_{j,t_j,i}$, we also know $(z_{\mu,j,t_j,i}, z_{\eta,j,t_j,i}, z_{\Sigma,j,t_j,i}, z_{\tau,j,t_j,i}, z_{\rho,j,t_j,i})$, and vice-versa, and sampling the former or the latter is therefore equivalent, but if we use $(z_{\mu,j,t_j,i}, z_{\eta,j,t_j,i}, z_{\Sigma,j,t_j,i}, z_{\tau,j,t_j,i}, z_{\rho,j,t_j,i})$, we have the possibility of updating a parameter at the time which, according to our experience, increases the convergence speed.

A.2 STAP parameters

Conditionally to the latent behaviors, the animals are independent and, therefore, the sampling of the STAP parameters follows directly from Mastrantonio (2020), if we take into account that the parameters are shared between animals and behaviors. For this reasons, let us define $\mathcal{I}_{\mu,j,p}$ as the set

of indices i of the j -th animal, so that $\boldsymbol{\mu}_{z_j, t_j, i} = \boldsymbol{\mu}_p^*$; the sets $\mathcal{I}_{\boldsymbol{\eta}, j, p}$, $\mathcal{I}_{\boldsymbol{\Sigma}, j, p}$, $\mathcal{I}_{\boldsymbol{\tau}, j, p}$, and $\mathcal{I}_{\boldsymbol{\rho}, j, p}$ are defined in a similar way. If the sets $\mathcal{I}_{\chi, j, p}$ are empty for a given parameter χ_p^* and all animals, then the full conditional is equal to the distribution H_χ which, given the chosen distributions, is easy to sample from. We do not need to sample all the L parameters, but only the ones that are observed in at least one of the non-empty behaviors, or the ones that are needed to sample the variables z_j, t_j, i .

Sampling $\boldsymbol{\mu}_p^*$ If we assume $\boldsymbol{\mu}_p^* \sim N(\mathbf{B}_\mu, \mathbf{W}_\mu)$, the full conditional is $N(\mathbf{B}_{\mu, p}, \mathbf{W}_{\mu, p})$ with

$$\mathbf{W}_{\mu, p} = \left(\sum_{j=1}^m \sum_{i \in \mathcal{I}_{\mu, j, p}} (1 - \rho_{z_j, t_j, i})^2 \tau_{z_j, t_j, i}^2 \mathbf{V}_{\mu, j, t_j, i}^{-1} + \mathbf{W}_\mu^{-1} \right)^{-1},$$

$$\mathbf{B}_{\mu, p} = \mathbf{W}_{\mu, p} \left(\sum_{j=1}^m \sum_{i \in \mathcal{I}_{\mu, j, p}} (1 - \rho_{z_j, t_j, i}) \tau_{z_j, t_j, i} \mathbf{V}_{\mu, j, t_j, i}^{-1} \mathbf{M}_{\mu, j, t_j, i} + \mathbf{W}_\mu^{-1} \mathbf{B}_\mu \right).$$

and

$$\mathbf{V}_{\mu, j, t_j, i} = \mathbf{R}(\rho_{z_j, t_j, i} \phi_{j, t_j, i-1}) \boldsymbol{\Sigma}_{z_j, t_j, i}^{-1} \mathbf{R}'(\rho_{z_j, t_j, i} \phi_{j, t_j, i-1})$$

$$\mathbf{M}_{\mu, j, t_j, i} = \mathbf{s}_{j, t_j, i+1} - \mathbf{s}_{j, t_j, i} + (1 - \rho_{z_j, t_j, i}) \tau_{z_j, t_j, i} \mathbf{s}_{j, t_j, i} - \rho_{z_j, t_j, i} \mathbf{R}(\phi_{j, t_j, i-1}) \boldsymbol{\eta}_{z_j, t_j, i}$$

Sampling $\boldsymbol{\eta}_p^*$ If we assume $\boldsymbol{\eta}_p^* \sim N(\mathbf{B}_\eta, \mathbf{W}_\eta)$, the full conditional is $N(\mathbf{B}_{\eta, p}, \mathbf{W}_{\eta, p})$ with

$$\mathbf{W}_{\eta, p} = \left(\sum_{j=1}^m \sum_{i \in \mathcal{I}_{\eta, j, p}} \rho_{z_j, t_j, i}^2 \mathbf{R}'(\phi_{j, t_j, i-1}) \mathbf{V}_{\eta, j, t_j, i}^{-1} \mathbf{R}(\phi_{j, t_j, i-1}) + \mathbf{W}_\eta^{-1} \right)^{-1},$$

$$\mathbf{B}_{\eta, p} = \mathbf{W}_{\eta, p} \left(\sum_{j=1}^m \sum_{i \in \mathcal{I}_{\eta, j, p}} \rho_{z_j, t_j, i} \mathbf{R}'(\phi_{j, t_j, i-1}) \mathbf{V}_{\eta, j, t_j, i}^{-1} \mathbf{M}_{\eta, j, t_j, i} + \mathbf{W}_\eta^{-1} \mathbf{B}_\eta \right).$$

and

$$\mathbf{V}_{\eta, j, t_j, i} = \mathbf{R}(\rho_{z_j, t_j, i} \phi_{j, t_j, i-1}) \boldsymbol{\Sigma}_{z_j, t_j, i}^{-1} \mathbf{R}'(\rho_{z_j, t_j, i} \phi_{j, t_j, i-1})$$

$$\mathbf{M}_{\eta, j, t_j, i} = \mathbf{s}_{j, t_j, i+1} - \mathbf{s}_{j, t_j, i} - (1 - \rho_{z_j, t_j, i}) \tau_{z_j, t_j, i} (\boldsymbol{\mu}_{z_j, t_j, i} - \mathbf{s}_{j, t_j, i})$$

Sampling τ_p^* If we assume $\tau_p^* \sim U(0, 1)$, the full conditional is therefore a truncated normal $N(\mathbf{B}_{\tau, p}, \mathbf{W}_{\tau, p}) I(0, 1)$ with

$$\mathbf{W}_{\tau, p} = \left(\sum_{j=1}^m \sum_{i \in \mathcal{I}_{\tau, j, p}} (1 - \rho_{z_j, t_j, i})^2 (\boldsymbol{\mu}_{z_j, t_j, i} - \mathbf{s}_{j, t_j, i})' \mathbf{V}_{\tau, j, t_j, i}^{-1} (\boldsymbol{\mu}_{z_j, t_j, i} - \mathbf{s}_{j, t_j, i}) \right)^{-1},$$

$$\mathbf{B}_{\tau, p} = \mathbf{W}_{\tau, p} \left(\sum_{j=1}^m \sum_{i \in \mathcal{I}_{\tau, j, p}} (1 - \rho_{z_j, t_j, i}) (\boldsymbol{\mu}_{z_j, t_j, i} - \mathbf{s}_{j, t_j, i})' \mathbf{V}_{\tau, j, t_j, i}^{-1} \mathbf{M}_{\tau, j, t_j, i} \right).$$

and

$$\mathbf{V}_{\tau, j, t_j, i} = \mathbf{R}(\rho_{z_j, t_j, i} \phi_{j, t_j, i-1}) \boldsymbol{\Sigma}_{z_j, t_j, i}^{-1} \mathbf{R}'(\rho_{z_j, t_j, i} \phi_{j, t_j, i-1})$$

$$\mathbf{M}_{\tau, j, t_j, i} = \mathbf{s}_{j, t_j, i+1} - \mathbf{s}_{j, t_j, i} - \rho_{z_j, t_j, i} \mathbf{R}(\phi_{j, t_j, i-1}) \boldsymbol{\eta}_{z_j, t_j, i}$$

Sampling Σ_p^* Since $\Sigma_p^* \sim IW(a_{\Sigma}, \mathbf{C}_{\Sigma})$, the full conditional is $IW(a_{\Sigma,p}, \mathbf{C}_{\Sigma,p})$ with

$$a_{\Sigma,j} = a_{\Sigma} + \sum_{j=1}^m \sum_{i \in \mathcal{I}_{\Sigma,j,p}} 1,$$

$$\mathbf{C}_{\Sigma,j} = \mathbf{C}_{\Sigma} + \sum_{j=1}^m \sum_{i \in \mathcal{I}_{\Sigma,j,p}} \left(\mathbf{R}'(\rho_{z_j,t_{j,i}}) \mathbf{M}_{\Sigma,j,t_{j,i}} \right) \left(\mathbf{R}'(\rho_{z_j,t_{j,i}}) \mathbf{M}_{\Sigma,j,t_{j,i}} \right)'.$$

and

$$\mathbf{M}_{\Sigma,j,t_{j,i}} = \mathbf{s}_{j,t_{j,i+1}} - \mathbf{s}_{j,t_{j,i}} - (1 - \rho_{z_j,t_{j,i}}) \tau_{z_j,t_{j,i}} (\boldsymbol{\mu}_{z_j,t_{j,i}} - \mathbf{s}_{j,t_{j,i}}) - \rho_{z_j,t_{j,i}} \mathbf{R}(\phi_{j,t_{i-1}}) \boldsymbol{\eta}_{z_j,t_{j,i}}$$

Sampling ρ_p^* It is not possible to find a closed-form update for ρ_p^* , since it is part of the rotation matrix argument, and a Metropolis algorithm should therefore be used. Special care should be taken in defining the proposal in order to be able to propose a value in $[0,1]$.

Sampling the missing locations It is not possible to derive a closed-form full conditional for a missing $\mathbf{s}_{j,t_{j,i}}$, and a Metropolis algorithm should therefore be used.

Appendix B Real data application - Additional results

In this section, we show the posterior means and CIs of the model parameters of our proposal (M1) (Tables 3-8), model M2 (Tables 9-14), and model M3 (Tables 15-15). We also show the graphical description of the behaviors found for M2 and M3 in Figures 6-7 and Figures 8-9, respectively. As in the main manuscript, we only discuss behaviors with $n_{j,k} > 100$, and in order to distinguish between the results of different models, we use the superscript to indicate which model we are referring to.

M2 description The model M2 finds the same number of behaviors as M1, and similar parameters. The major difference between the two is in the ordering of the behaviors of the third dog, since the boundary-patrolling behavior of M2 (B_{31}^{M2}) is the one with the largest number of temporal points ($n_{3,1}^{M2} = 3537$), while it is the third ($n_{3,3}^{M1} = 608$) in M1. The behavior with the strongest attraction to the central tendency is B_{32}^{M2} (the second) in M2, with only $n_{3,2}^{M2} = 818$ temporal-points, while it is B_{31}^{M1} (the first) in M1. It is interesting to note that all the boundary-patrolling behaviors of the 6 dogs are described by the same set of parameters, i.e., they are the same behaviors, and the same is also true for the explore-behaviors. On the other hand, the attending-livestock behaviors, B_{13}^{M2} , B_{23}^{M2} , and B_{53}^{M2} , are the same, while B_{63}^{M2} has its own set of parameters, with a slightly different attractor.

A possible explanation for why, unlike our proposal, the boundary-patrolling behavior of the third dog has the highest number of temporal points, can be found in the way the model is formalized. All the animals, in M2, share the same set of parameters, and 5 of them have the same boundary-patrolling behavior as the first one. This means that the expected value of the probability of remaining in this behavior, or of moving to this behavior from any other, is also very high for the third dog, which may lead to an overestimation of the number of temporal-points that belong to this behavior. This problem is not present in M1 because, even though all the boundary-patrolling behaviors are very similar, they only share the covariance matrix $\boldsymbol{\Sigma}_{j,k}^{M1}$, but all the other parameters are different, see, for example, parameters $\rho_{j,k}^{M1}$ and $\tau_{j,k}^{M1}$ in Figure 5 (c) and (e) of the Manuscript. This means that there is only the probability of that specific covariance matrix to be higher. It is also interesting to note that the CIs of the spatial attractors are wider in M2, in the behaviors where they are relevant, than for M1, especially for dog 3.

Table 3: M1 - Woody: posterior means and CIs of the model parameters (j=1).

	k=1	k=2	k=3
$\mu_{j,k,1}$	0.088	0.082	-0.147
(CI)	(-2.536 1.164)	(-0.268 0.752)	(-0.282 -0.007)
$\mu_{j,k,2}$	0.151	0.011	0.148
(CI)	(-0.381 3.043)	(-0.381 0.31)	(-0.013 0.33)
$\eta_{j,k,1}$	-0.001	-0.001	13.688
(CI)	(-0.001 -0.001)	(-0.002 -0.001)	(4.141 18.192)
$\eta_{j,k,2}$	0	0	1.444
(CI)	(0 0)	(0 0)	(-1.857 4.694)
$\tau_{j,k}$	0.151	0.281	0.128
(CI)	(0 0.992)	(0.11 0.589)	(0.102 0.159)
$\rho_{j,k}$	0.984	0.965	0.008
(CI)	(0.948 1)	(0.941 0.984)	(0.005 0.01)
$\Sigma_{j,k,1,1}$	0	0.022	0.201
(CI)	(0 0)	(0.02 0.025)	(0.178 0.23)
$\Sigma_{j,k,1,2}$	0	0.001	-0.037
(CI)	(0 0)	(0 0.001)	(-0.053 -0.025)
$\Sigma_{j,k,2,2}$	0	0.016	0.29
(CI)	(0 0)	(0.014 0.018)	(0.251 0.335)
$\pi_{j,1,k}$	0.772	0.197	0.03
(CI)	(0.755 0.789)	(0.18 0.215)	(0.02 0.042)
$\pi_{j,2,k}$	0.354	0.49	0.156
(CI)	(0.325 0.384)	(0.442 0.539)	(0.123 0.19)
$\pi_{j,3,k}$	0.149	0.388	0.462
(CI)	(0.116 0.187)	(0.318 0.467)	(0.381 0.534)
$n_{j,k}$	2745	1553	502

M3 description The results of M3 are very different from those obtained from the other two models, since dog 3 has 3 behaviors, while the others only have 2. The first behavior of the 6 dogs is similar to the boundary-patrolling-behavior of M1 and M2, but the ellipses are much wider, i.e., the variances in $\Sigma_{j,k}^{M3}$ are larger. With the exception of dog 2, the second behaviors lack directional persistence and attractors. On the other hand, B_{32}^{M3} and B_{33}^{M3} each have an attractor, located in a similar place to the one in B_{31}^{M1} , and the attraction is strong in B_{32}^{M3} and weak in B_{33}^{M3} . The CI of the spatial attractor is wider than the one in B_{31}^{M1} .

The difference between the results of M3 and those of M2 and M1 can be explained by the independence between animals since, as already pointed out by Jonsen (2016), the inference and description of behaviors improve if multiple animals are considered. M3 fails especially in the description of the dogs in the cohesive group, which could point out the benefits of a joint modeling. This is further highlighted by the values of the information criteria shown in Table 1 in the Manuscript, which indicate that M3 always has the worst goodness-of-fit.

References

- Anderson, C. R. and Lindzey, F. G. (2003). “Estimating Cougar Predation Rates from GPS Location Clusters.” *The Journal of Wildlife Management*, 67(2): 307–316.
- Bezanson, J., Edelman, A., Karpinski, S., and Shah, V. B. (2017). “Julia: A fresh approach to numerical computing.” *SIAM review*, 59(1): 65–98.

Table 4: M1 - Sherlock: posterior means and CIs of the model parameters (j=2).

	k=1	k=2	k=3
$\mu_{j,k,1}$	0.34	0.056	-0.147
(CI)	(-0.265 1.207)	(-0.289 0.852)	(-0.282 -0.007)
$\mu_{j,k,2}$	-0.03	0.069	0.147
(CI)	(-0.381 0.368)	(-0.381 0.344)	(-0.014 0.33)
$\eta_{j,k,1}$	-0.012	-0.008	14.055
(CI)	(-0.018 -0.007)	(-0.016 -0.001)	(10.181 18.192)
$\eta_{j,k,2}$	0.002	0.001	1.551
(CI)	(-0.001 0.004)	(-0.001 0.004)	(-1.773 4.827)
$\tau_{j,k}$	0	0.169	0.204
(CI)	(0 0)	(0 0.983)	(0.129 0.277)
$\rho_{j,k}$	0.139	0.972	0.007
(CI)	(0.086 0.233)	(0.942 1)	(0.005 0.01)
$\Sigma_{j,k,1,1}$	0	0.022	0.204
(CI)	(0 0)	(0.02 0.025)	(0.18 0.24)
$\Sigma_{j,k,1,2}$	0	0.001	-0.038
(CI)	(0 0)	(0 0.001)	(-0.056 -0.024)
$\Sigma_{j,k,2,2}$	0	0.016	0.296
(CI)	(0 0)	(0.014 0.018)	(0.256 0.381)
$\pi_{j,1,k}$	0.781	0.179	0.039
(CI)	(0.766 0.796)	(0.162 0.196)	(0.028 0.052)
$\pi_{j,2,k}$	0.374	0.521	0.104
(CI)	(0.346 0.402)	(0.49 0.553)	(0.083 0.128)
$\pi_{j,3,k}$	0.213	0.385	0.402
(CI)	(0.169 0.261)	(0.295 0.492)	(0.301 0.485)
$n_{j,k}$	2927	1473	400

- Biernacki, C., Celeux, G., and Govaert, G. (2000). “Assessing a Mixture Model for Clustering with the Integrated Completed Likelihood.” *IEEE Trans. Pattern Anal. Mach. Intell.*, 22(7): 719–725.
- Blackwell, P. (1997). “Random diffusion models for animal movement.” *Ecological Modelling*, 100(1): 87 – 102.
- Brook, L. A., Johnson, C. N., and Ritchie, E. G. (2012). “Effects of predator control on behaviour of an apex predator and indirect consequences for mesopredator suppression.” *Journal of Applied Ecology*, 49(6): 1278–1286.
- Buderman, F. E., Hooten, M. B., Alldredge, M. W., Hanks, E. M., and Ivan, J. S. (2018). “Time-varying predatory behavior is primary predictor of fine-scale movement of wildland-urban cougars.” *Movement Ecology*, 6(1): 22.
- Calabrese, J. M., Fleming, C. H., Fagan, W. F., Rimpler, M., Kaczensky, P., Bewick, S., Leimgruber, P., and Mueller, T. (2018). “Disentangling social interactions and environmental drivers in multi-individual wildlife tracking data.” *Philosophical Transactions of the Royal Society B: Biological Sciences*, 373(1746): 20170007.
- Celeux, G., Forbes, F., Robert, C. P., Titterton, D. M., Futurs, I., and Rhône-alpes, I. (2006). “Deviance information criteria for missing data models.” *Bayesian Analysis*, 4: 651–674.
- Christ, A., Hoef, J. V., and Zimmerman, D. L. (2008). “An animal movement model incorporating home range and habitat selection.” *Environmental and Ecological Statistics*, 15(1): 27–38.

Table 5: M1 - Alvin: posterior means and CIs of the model parameters (j=3).

	k=1	k=2	k=3	k=4	k=5
$\mu_{j,k,1}$	0.575	0.921	0.168	0.625	-2.344
(CI)	(0.575 0.576)	(0.577 2.02)	(-0.329 1.078)	(0.557 0.835)	(-6.044 -0.793)
$\mu_{j,k,2}$	-0.381	0.094	0.061	-0.225	3.651
(CI)	(-0.381 -0.38)	(-0.186 0.987)	(-0.381 1.014)	(-0.381 0.122)	(1.556 8.708)
$\eta_{j,k,1}$	0.144	0.014	0.012	0.866	1.133
(CI)	(-0.013 -0.001)	(-0.015 -0.001)	(-0.015 -0.001)	(-0.016 14.445)	(-0.016 14.947)
$\eta_{j,k,2}$	0.025	0.003	0.001	0.128	0.097
(CI)	(0 0.003)	(0 0.003)	(0 0.003)	(-0.001 2.61)	(-0.002 2.252)
$\tau_{j,k}$	0.991	0.258	0.125	0.435	0.663
(CI)	(0.984 0.997)	(0.024 0.994)	(0 0.991)	(0.224 0.585)	(0.222 0.995)
$\rho_{j,k}$	0.007	0.454	0.617	0.022	0.029
(CI)	(0 0.01)	(0.005 0.97)	(0.005 1)	(0.004 0.142)	(0 0.233)
$\Sigma_{j,k,1,1}$	0	0.022	0	0.214	0.023
(CI)	(0 0)	(0.02 0.025)	(0 0)	(0.181 0.326)	(0.02 0.025)
$\Sigma_{j,k,1,2}$	0	0.001	0	-0.046	0
(CI)	(0 0)	(0 0.001)	(0 0)	(-0.142 -0.025)	(0 0.001)
$\Sigma_{j,k,2,2}$	0	0.016	0	0.32	0.017
(CI)	(0 0)	(0.014 0.018)	(0 0)	(0.258 0.568)	(0.014 0.018)
$\pi_{j,1,k}$	0.89	0.096	0.009	0.004	0.001
(CI)	(0.878 0.901)	(0.085 0.107)	(0.004 0.015)	(0.002 0.007)	(0 0.002)
$\pi_{j,2,k}$	0.318	0.421	0.21	0.05	0
(CI)	(0.282 0.354)	(0.377 0.463)	(0.18 0.243)	(0.027 0.079)	(0 0)
$\pi_{j,3,k}$	0.112	0.209	0.659	0.019	0
(CI)	(0.086 0.14)	(0.176 0.244)	(0.619 0.699)	(0.007 0.036)	(0 0)
$\pi_{j,4,k}$	0.3	0.18	0.121	0.396	0
(CI)	(0.202 0.408)	(0.083 0.294)	(0.057 0.204)	(0.295 0.511)	(0 0)
$\pi_{j,5,k}$	0	0	0.651	0	0.305
(CI)	(0 0)	(0 0)	(0.223 0.996)	(0 0)	(0 0.753)
$n_{j,k}$	3304	792	608	92	4

- Codling, E. A., Plank, M. J., and Benhamou, S. (2008). “Random walk models in biology.” *Journal of The Royal Society Interface*, 5(25): 813–834.
- Dunn, J. E. and Gipson, P. S. (1977). “Analysis of radiotelemetry data in studies of home range.” *Biometrics*, 33(1).
- Escobar, M. D. and West, M. (1995). “Bayesian density estimation and inference using mixtures.” *Journal of the American Statistical Association*, 90(430): 577–588.
- Fortin, D., Morales, J. M., and Boyce, M. S. (2005). “Elk winter foraging at fine scale in Yellowstone National Park.” *Oecologia*, 145(2): 334–342.
- Fox, E. B., Sudderth, E. B., Jordan, M. I., and Willsky, A. S. (2011). “A sticky HDP-HMM with application to speaker diarization.” *The Annals of Applied Statistics*, 5(2A): 1020–1056.
- Frühwirth-Schnatter, S. and Malsiner-Walli, G. (2019). “From here to infinity: sparse finite versus Dirichlet process mixtures in model-based clustering.” *Advances in Data Analysis and Classification*, 13(1): 33–64.
- Gates, A. J. and Ahn, Y.-Y. (2017). “The Impact of Random Models on Clustering Similarity.” *Journal of Machine Learning Research*, 18(87): 1–28.

Table 6: M1 - Rosie: posterior means and CIs of the model parameters (j=4).

	k=1	k=2	k=3
$\mu_{j,k,1}$	0.123	-0.07	0.103
(CI)	(-1.216 1.095)	(-0.314 0.771)	(-0.981 1.122)
$\mu_{j,k,2}$	0.117	0.145	0.136
(CI)	(-0.381 1.747)	(-0.381 0.383)	(-0.381 1.678)
$\eta_{j,k,1}$	-0.001	-0.012	0.671
(CI)	(-0.001 -0.001)	(-0.018 -0.007)	(-0.016 14.411)
$\eta_{j,k,2}$	0	0.001	0.088
(CI)	(0 0)	(-0.001 0.004)	(-0.001 1.771)
$\tau_{j,k}$	0.159	0.189	0.219
(CI)	(0 0.992)	(0.049 0.499)	(0 0.993)
$\rho_{j,k}$	0.984	0.965	0.737
(CI)	(0.948 1)	(0.941 0.986)	(0.005 1)
$\Sigma_{j,k,1,1}$	0	0.022	0.211
(CI)	(0 0)	(0.02 0.025)	(0.179 0.31)
$\Sigma_{j,k,1,2}$	0	0.001	-0.04
(CI)	(0 0)	(0 0.001)	(-0.083 -0.024)
$\Sigma_{j,k,2,2}$	0	0.016	0.302
(CI)	(0 0)	(0.014 0.018)	(0.253 0.457)
$\pi_{j,1,k}$	0.835	0.165	0.001
(CI)	(0.821 0.847)	(0.152 0.178)	(0 0.002)
$\pi_{j,2,k}$	0.411	0.582	0.007
(CI)	(0.384 0.439)	(0.553 0.61)	(0.002 0.016)
$\pi_{j,3,k}$	0.05	0.455	0.482
(CI)	(0 0.281)	(0.162 0.755)	(0.221 0.727)
$n_{j,k}$	3421	1362	17

- Gehring, T. M., VerCauteren, K. C., and Cellar, A. C. (2017). “Good Fences Make Good Neighbors: Implementation of Electric Fencing for Establishing Effective Livestock-Protection Dogs.” *Human-Wildlife Interactions*, 5(1): 106–111.
- Gelman, A., Carlin, J. B., Stern, H. S., and Rubin, D. B. (2013). *Bayesian Data Analysis*. Chapman and Hall/CRC, third edition edition.
- Gnedin, A., Gnedin, E., and Kerov, S. (2001). “A Characterization of GEM Distributions.” *Combin. Probab. Comp*, 10: 213–217.
- Hastie, D. I. and Green, P. J. (2012). “Model choice using reversible jump Markov chain Monte Carlo.” *Statistica Neerlandica*, 66(3): 309–338.
- Hebblewhite, M. and Merrill, E. (2008). “Modelling wildlife and uman relationships for social species with mixed-effects resource selection models.” *Journal of Applied Ecology*, 45(3): 834–844.
- Hooten, M., Johnson, D., McClintock, B., and Morales, J. (2017). *Animal Movement: Statistical Models for Telemetry Data*. CRC Press.
- Hooten, M. B., Scharf, H. R., Hefley, T. J., Pearse, A. T., and Weegman, M. D. (2018). “Animal movement models for migratory individuals and groups.” *Methods in Ecology and Evolution*, 9(7): 1692–1705.
- Ishwaran, H. and Zarepour, M. (2002). “Exact and approximate sum representations for the Dirichlet process.” *Canadian Journal of Statistics*, 30(2): 269–283.

Table 7: M1 - Bear: posterior means and CIs of the model parameters (j=5).

	k=1	k=2	k=3
$\mu_{j,k,1}$	0.108	-0.049	-0.147
(CI)	(-1.009 1.091)	(-0.287 0.726)	(-0.283 -0.006)
$\mu_{j,k,2}$	0.095	0.114	0.148
(CI)	(-0.381 1.709)	(-0.381 0.344)	(-0.013 0.332)
$\eta_{j,k,1}$	-0.001	-0.008	14.031
(CI)	(-0.001 -0.001)	(-0.016 -0.001)	(10.04 18.192)
$\eta_{j,k,2}$	0	0.001	1.529
(CI)	(0 0)	(0 0.004)	(-1.812 4.744)
$\tau_{j,k}$	0.151	0.236	0.128
(CI)	(0 0.992)	(0 0.549)	(0.101 0.161)
$\rho_{j,k}$	0.979	0.969	0.007
(CI)	(0.947 1)	(0.941 1)	(0.005 0.01)
$\Sigma_{j,k,1,1}$	0	0.022	0.199
(CI)	(0 0)	(0.02 0.025)	(0.162 0.228)
$\Sigma_{j,k,1,2}$	0	0.001	-0.037
(CI)	(0 0)	(0 0.001)	(-0.054 -0.024)
$\Sigma_{j,k,2,2}$	0	0.016	0.287
(CI)	(0 0)	(0.014 0.018)	(0.244 0.333)
$\pi_{j,1,k}$	0.773	0.21	0.017
(CI)	(0.756 0.789)	(0.194 0.227)	(0.009 0.026)
$\pi_{j,2,k}$	0.386	0.528	0.085
(CI)	(0.359 0.415)	(0.492 0.565)	(0.065 0.107)
$\pi_{j,3,k}$	0.069	0.426	0.504
(CI)	(0.035 0.109)	(0.331 0.53)	(0.408 0.591)
$n_{j,k}$	2852	1624	324

- Jammalamadaka, S. R. and Kozubowski, T. J. (2004). “New Families of Wrapped Distributions for Modeling Skew Circular Data.” *Communications in Statistics - Theory and Methods*, 33(9): 2059–2074.
- Jonsen, I. (2016). “Joint estimation over multiple individuals improves behavioural state inference from animal movement data.” *Scientific Reports*, 6(1): 20625.
- Jonsen, I. D., Flemming, J. M., and Myers, R. A. (2005). “Robust state-space modeling of animal movement data.” *Ecology*, 86(11): 2874–2880.
- Langrock, R., King, R., Matthiopoulos, J., Thomas, L., Fortin, D., and Morales, J. M. (2012). “Flexible and practical modeling of animal telemetry data: hidden Markov models and extensions.” *Ecology*, 93(11): 2336–2342.
- Leos-Barajas, V., Gangloff, E. J., Adam, T., Langrock, R., van Beest, F. M., Nabe-Nielsen, J., and Morales, J. M. (2017). “Multi-scale Modeling of Animal Movement and General Behavior Data Using Hidden Markov Models with Hierarchical Structures.” *Journal of Agricultural, Biological and Environmental Statistics*, 22(3): 232–248.
- Maruotti, A., Punzo, A., Mastrantonio, G., and Lagona., F. (2016). “A time-dependent extension of the projected normal regression model for longitudinal circular data based on a hidden Markov heterogeneity structure.” *Stochastic Environmental Research and Risk Assessment*, 30: 1725–1740.
- Mastrantonio, G. (2018). “The joint projected normal and skew-normal: A distribution for polycylindrical data.” *Journal of Multivariate Analysis*, 165: 14 – 26.

Table 8: M1 - Lucy: posterior means and CIs of the model parameters (j=6).

	k=1	k=2	k=3
$\mu_{j,k,1}$	0.134	-0.092	-0.147
(CI)	(-1.006 1.107)	(-0.284 0.576)	(-0.282 -0.006)
$\mu_{j,k,2}$	0.088	0.118	0.148
(CI)	(-0.381 1.747)	(-0.381 0.33)	(-0.013 0.33)
$\eta_{j,k,1}$	-0.001	-0.01	13.918
(CI)	(-0.001 -0.001)	(-0.017 -0.001)	(9.441 18.192)
$\eta_{j,k,2}$	0	0.001	1.522
(CI)	(0 0)	(-0.001 0.004)	(-1.773 4.744)
$\tau_{j,k}$	0.152	0.259	0.128
(CI)	(0 0.991)	(0.107 0.548)	(0.101 0.159)
$\rho_{j,k}$	0.984	0.965	0.007
(CI)	(0.948 1)	(0.941 0.984)	(0.005 0.01)
$\Sigma_{j,k,1,1}$	0	0.022	0.201
(CI)	(0 0)	(0.02 0.025)	(0.177 0.229)
$\Sigma_{j,k,1,2}$	0	0.001	-0.037
(CI)	(0 0)	(0 0.001)	(-0.053 -0.024)
$\Sigma_{j,k,2,2}$	0	0.016	0.289
(CI)	(0 0)	(0.014 0.018)	(0.248 0.333)
$\pi_{j,1,k}$	0.729	0.24	0.031
(CI)	(0.71 0.747)	(0.221 0.259)	(0.02 0.043)
$\pi_{j,2,k}$	0.34	0.552	0.108
(CI)	(0.315 0.366)	(0.516 0.59)	(0.085 0.133)
$\pi_{j,3,k}$	0.157	0.375	0.467
(CI)	(0.12 0.195)	(0.301 0.46)	(0.381 0.542)
$n_{j,k}$	2537	1825	438

— (2020). “Modeling animal movement with directional persistence and attractive points.” *arXiv*. 2012.03248.

Mastrantonio, G., Jona Lasinio, G., Pollice, A., Teodonio, L., and Capotorti, G. (2021). “A Dirichlet process model for change-point detection with multivariate bioclimatic data.” *Environmetrics*.

McClintock, B. T., King, R., Thomas, L., Matthiopoulos, J., McConnell, B. J., and Morales, J. M. (2012). “A general discrete-time modeling framework for animal movement using multistate random walks.” *Ecological Monographs*, 82(3): 335–349.

McClintock, B. T., Russell, D. J. F., Matthiopoulos, J., and King, R. (2013). “Combining individual animal movement and ancillary biotelemetry data to investigate population-level activity budgets.” *Ecology*, 94(4): 838–849.

McGrew, J. C. and Blakesley, C. S. (1982). “How Komondor dogs reduce sheep losses to coyotes.” *Journal of Range Management*, 6(35): 693–696.

Merrill, S. B. and David Mech, L. (2000). “Details of Extensive Movements by Minnesota Wolves (*Canis lupus*).” *The American Midland Naturalist*, 144(2): 428–433.

Michelot, T., Langrock, R., Bestley, S., Jonsen, I. D., Photopoulou, T., and Patterson, T. A. (2017). “Estimation and simulation of foraging trips in land-based marine predators.” *Ecology*, 98(7): 1932–1944.

Table 9: M2 - Woody: posterior means and CIs of the model parameters (j=1).

	k=1	k=2	k=3
$\mu_{j,k,1}$	-0.236	-0.287	-0.164
(CI)	(-8.941 8.273)	(-0.831 0.221)	(-0.334 0.002)
$\mu_{j,k,2}$	-0.161	0.02	0.222
(CI)	(-8.892 8.281)	(-0.497 0.507)	(0.009 0.436)
$\eta_{j,k,1}$	-0.002	-0.008	17.502
(CI)	(-0.002 -0.001)	(-0.012 -0.004)	(12.141 23.362)
$\eta_{j,k,2}$	0	0.004	1.508
(CI)	(0 0)	(0.001 0.007)	(-2.707 5.842)
$\tau_{j,k}$	0.503	0.543	0.144
(CI)	(0.021 0.973)	(0.192 0.957)	(0.118 0.175)
$\rho_{j,k}$	1	0.985	0.006
(CI)	(1 1)	(0.968 0.993)	(0.004 0.008)
$\Sigma_{j,k,1,1}$	0	0.023	0.197
(CI)	(0 0)	(0.02 0.026)	(0.172 0.227)
$\Sigma_{j,k,1,2}$	0	0	-0.037
(CI)	(0 0)	(0 0.001)	(-0.054 -0.022)
$\Sigma_{j,k,2,2}$	0	0.017	0.291
(CI)	(0 0)	(0.014 0.019)	(0.253 0.34)
$\pi_{j,1,k}$	0.77	0.2	0.03
(CI)	(0.754 0.787)	(0.183 0.218)	(0.02 0.041)
$\pi_{j,2,k}$	0.354	0.493	0.153
(CI)	(0.326 0.383)	(0.444 0.542)	(0.119 0.189)
$\pi_{j,3,k}$	0.15	0.388	0.462
(CI)	(0.115 0.187)	(0.32 0.467)	(0.384 0.529)
$n_{j,k}$	2742	1565	493

- Michelot, T., Langrock, R., and Patterson, T. A. (2016). “moveHMM: an R package for the statistical modelling of animal movement data using hidden Markov models.” *Methods in Ecology and Evolution*, 7(11): 1308–1315.
- Milner, J. E., Blackwell, P. G., and Niu, M. (2021). “Modelling and inference for the movement of interacting animals.” *Methods in Ecology and Evolution*, 12(1): 54–69.
- Niu, M., Frost, F., Milner, J. E., Skarin, A., and Blackwell, P. G. (2020). “Modelling group movement with behaviour switching in continuous time.” *Biometrics*, <https://doi.org/10.1111/biom.13412>: 1–14.
- Patterson, T., Thomas, L., Wilcox, C., Ovaskainen, O., and Matthiopoulos, J. (2008). “State-space models of individual animal movement.” *Trends in Ecology & Evolution*, 23(2): 87–94.
- Pohle, J., Langrock, R., van Beest, F. M., and Schmidt, N. M. (2017). “Selecting the Number of States in Hidden Markov Models: Pragmatic Solutions Illustrated Using Animal Movement.” *Journal of Agricultural, Biological and Environmental Statistics*, 22(3): 270–293.
- Scharf, H. R. and Buderman, F. E. (2020). “Animal movement models for multiple individuals.” *WIREs Computational Statistics*.
- Sethuraman, J. (1994). “A constructive definition of Dirichlet priors.” *Statistica Sinica*, 4: 639–650.
- Teh, Y. W., Jordan, M. I., Beal, M. J., and Blei, D. M. (2006). “Hierarchical Dirichlet processes.” *Journal of the American Statistical Association*, 101(476): 1566–1581.

Table 10: M2 - Sherlock: posterior means and CIs of the model parameters (j=2).

	k=1	k=2	k=3	k=4	k=5
$\mu_{j,k,1}$	-0.236	-0.287	-0.164	0.165	0.593
(CI)	(-8.941 8.273)	(-0.831 0.221)	(-0.334 0.002)	(-8.559 8.967)	(0.587 0.6)
$\mu_{j,k,2}$	-0.161	0.02	0.222	-0.189	-0.369
(CI)	(-8.892 8.281)	(-0.497 0.507)	(0.009 0.436)	(-8.188 8.476)	(-0.374 -0.364)
$\eta_{j,k,1}$	-0.002	-0.008	17.502	-0.051	-0.08
(CI)	(-0.002 -0.001)	(-0.012 -0.004)	(12.141 23.362)	(-8.867 8.43)	(-8.868 8.416)
$\eta_{j,k,2}$	0	0.004	1.508	0.055	0.013
(CI)	(0 0)	(0.001 0.007)	(-2.707 5.842)	(-8.746 8.624)	(-8.35 8.601)
$\tau_{j,k}$	0.503	0.543	0.144	0.487	0.953
(CI)	(0.021 0.973)	(0.192 0.957)	(0.118 0.175)	(0.017 0.975)	(0.93 0.975)
$\rho_{j,k}$	1	0.985	0.006	0.418	0
(CI)	(1 1)	(0.968 0.993)	(0.004 0.008)	(0 1)	(0 0)
$\Sigma_{j,k,1,1}$	0	0.023	0.197	4.858	0.005
(CI)	(0 0)	(0.02 0.026)	(0.172 0.227)	(0.146 18.378)	(0.004 0.007)
$\Sigma_{j,k,1,2}$	0	0	-0.037	-1.274	0.001
(CI)	(0 0)	(0 0.001)	(-0.054 -0.022)	(-5.08 4.609)	(0 0.001)
$\Sigma_{j,k,2,2}$	0	0.017	0.291	3.102	0.003
(CI)	(0 0)	(0.014 0.019)	(0.253 0.34)	(0.14 13.914)	(0.003 0.004)
$\pi_{j,1,k}$	0.781	0.179	0.04	0	0
(CI)	(0.765 0.797)	(0.162 0.197)	(0.027 0.052)	(0 0.001)	(0 0)
$\pi_{j,2,k}$	0.375	0.521	0.103	0	0
(CI)	(0.346 0.403)	(0.489 0.555)	(0.081 0.126)	(0 0.003)	(0 0.001)
$\pi_{j,3,k}$	0.213	0.383	0.403	0	0
(CI)	(0.168 0.261)	(0.295 0.491)	(0.301 0.486)	(0 0)	(0 0.005)
$\pi_{j,4,k}$	0.287	0.197	0.029	0.453	0.012
(CI)	(0 0.791)	(0 0.725)	(0 0.245)	(0 0.978)	(0 0.15)
$\pi_{j,5,k}$	0.342	0.183	0.027	0.001	0.428
(CI)	(0 0.852)	(0 0.641)	(0 0.231)	(0 0)	(0 0.978)
$n_{j,k}$	2925	1475	398	1	1

van Bommel, L. and Invasive Animals Cooperative Research Centre (2010). *Guardian Dogs: Best Practice Manual for the Use of Livestock Guardian Dogs*. Invasive Animals Cooperative Research Centre.

van Bommel, L. and Johnson, C. (2014a). “Data from: Where do livestock guardian dogs go? Movement patterns of free-ranging Maremma sheepdogs, doi:10.5441/001/1.pv048q7v.”

van Bommel, L. and Johnson, C. N. (2012). “Good dog! Using livestock guardian dogs to protect livestock from predators in Australia’s extensive grazing systems.” *Wildlife Research*, 39(3): 220–229.

— (2014b). “Where Do Livestock Guardian Dogs Go? Movement Patterns of Free-Ranging Maremma Sheepdogs.” *PLOS ONE*, 9(10): 1–12.

— (2016). “Livestock guardian dogs as surrogate top predators? How Maremma sheepdogs affect a wildlife community.” *Ecology and Evolution*, 6(18): 6702–6711.

Van Gael, J., Saatci, Y., Teh, Y. W., and Ghahramani, Z. (2008). “Beam sampling for the infinite hidden Markov model.” In *Proceedings of the 25th International Conference on Machine Learning, ICML ’08*, 1088–1095. New York, NY, USA: ACM.

Table 11: M2 - Alvin: posterior means and CIs of the model parameters (j=3).

	k=1	k=2	k=3	k=4	k=5
$\mu_{j,k,1}$	-0.236	0.593	-0.287	0.797	-1.992
(CI)	(-8.941 8.273)	(0.587 0.6)	(-0.831 0.221)	(0.59 1.043)	(-5.598 -0.642)
$\mu_{j,k,2}$	-0.161	-0.369	0.02	-0.189	3.423
(CI)	(-8.892 8.281)	(-0.374 -0.364)	(-0.497 0.507)	(-0.459 0.057)	(1.675 8.501)
$\eta_{j,k,1}$	-0.002	-0.08	-0.008	0.02	-0.034
(CI)	(-0.002 -0.001)	(-8.868 8.416)	(-0.012 -0.004)	(-8.51 8.206)	(-8.861 8.627)
$\eta_{j,k,2}$	0	0.013	0.004	-0.09	-0.004
(CI)	(0 0)	(-8.35 8.601)	(0.001 0.007)	(-8.92 8.665)	(-8.818 9.066)
$\tau_{j,k}$	0.503	0.953	0.543	0.399	0.64
(CI)	(0.021 0.973)	(0.93 0.975)	(0.192 0.957)	(0.287 0.513)	(0.232 0.978)
$\rho_{j,k}$	1	0	0.985	0.001	0.002
(CI)	(1 1)	(0 0)	(0.968 0.993)	(0 0.004)	(0 0.026)
$\Sigma_{j,k,1,1}$	0	0.005	0.023	0.171	0.236
(CI)	(0 0)	(0.004 0.007)	(0.02 0.026)	(0.124 0.238)	(0.074 0.692)
$\Sigma_{j,k,1,2}$	0	0.001	0	0.028	-0.077
(CI)	(0 0)	(0 0.001)	(0 0.001)	(-0.013 0.076)	(-0.408 0.085)
$\Sigma_{j,k,2,2}$	0	0.003	0.017	0.257	0.252
(CI)	(0 0)	(0.003 0.004)	(0.014 0.019)	(0.178 0.37)	(0.083 0.802)
$\pi_{j,1,k}$	0.861	0.081	0.047	0.01	0.001
(CI)	(0.849 0.874)	(0.068 0.096)	(0.032 0.06)	(0.006 0.016)	(0 0.002)
$\pi_{j,2,k}$	0.509	0.418	0.057	0.015	0
(CI)	(0.46 0.557)	(0.369 0.468)	(0.03 0.086)	(0 0.036)	(0 0.004)
$\pi_{j,3,k}$	0.159	0.341	0.415	0.076	0.008
(CI)	(0.113 0.212)	(0.274 0.409)	(0.343 0.484)	(0.034 0.128)	(0 0.02)
$\pi_{j,4,k}$	0.11	0.386	0.15	0.352	0
(CI)	(0.046 0.186)	(0.282 0.491)	(0.059 0.258)	(0.254 0.46)	(0 0.003)
$\pi_{j,5,k}$	0.381	0.003	0.173	0.173	0.249
(CI)	(0.114 0.706)	(0 0.038)	(0.005 0.483)	(0.023 0.45)	(0 0.628)
$n_{j,k}$	3537	818	342	96	7

Wade, S. and Ghahramani, Z. (2018). “Bayesian Cluster Analysis: Point Estimation and Credible Balls (with Discussion).” *Bayesian Analysis*, 13(2): 559 – 626.

Walton, Z., Samelius, G., Odden, M., and Willebrand, T. (2017). “Variation in home range size of red foxes *Vulpes vulpes* along a gradient of productivity and human landscape alteration.” *PLOS ONE*, 12(4): 1–14.

Westley, P. A. H., Berdahl, A. M., Torney, C. J., and Biro, D. (2018). “Collective movement in ecology: from emerging technologies to conservation and management.” *Philosophical Transactions of the Royal Society B: Biological Sciences*, 373(1746): 20170004.

Table 12: M2 - Rosie: posterior means and CIs of the model parameters (j=4).

	k=1	k=2	k=3
$\mu_{j,k,1}$	-0.236	-0.287	-0.164
(CI)	(-8.941 8.273)	(-0.831 0.221)	(-0.334 0.002)
$\mu_{j,k,2}$	-0.161	0.02	0.222
(CI)	(-8.892 8.281)	(-0.497 0.507)	(0.009 0.436)
$\eta_{j,k,1}$	-0.002	-0.008	17.502
(CI)	(-0.002 -0.001)	(-0.012 -0.004)	(12.141 23.362)
$\eta_{j,k,2}$	0	0.004	1.508
(CI)	(0 0)	(0.001 0.007)	(-2.707 5.842)
$\tau_{j,k}$	0.503	0.543	0.144
(CI)	(0.021 0.973)	(0.192 0.957)	(0.118 0.175)
$\rho_{j,k}$	1	0.985	0.006
(CI)	(1 1)	(0.968 0.993)	(0.004 0.008)
$\Sigma_{j,k,1,1}$	0	0.023	0.197
(CI)	(0 0)	(0.02 0.026)	(0.172 0.227)
$\Sigma_{j,k,1,2}$	0	0	-0.037
(CI)	(0 0)	(0 0.001)	(-0.054 -0.022)
$\Sigma_{j,k,2,2}$	0	0.017	0.291
(CI)	(0 0)	(0.014 0.019)	(0.253 0.34)
$\pi_{j,1,k}$	0.834	0.165	0.001
(CI)	(0.82 0.848)	(0.152 0.179)	(0 0.003)
$\pi_{j,2,k}$	0.411	0.583	0.006
(CI)	(0.383 0.439)	(0.554 0.61)	(0.002 0.014)
$\pi_{j,3,k}$	0.17	0.313	0.506
(CI)	(0.018 0.374)	(0.111 0.563)	(0.254 0.734)
$n_{j,k}$	3419	1363	18

Table 13: M2 - Bear: posterior means and CIs of the model parameters (j=5).

	k=1	k=2	k=3
$\mu_{j,k,1}$	-0.236	-0.287	-0.164
(CI)	(-8.941 8.273)	(-0.831 0.221)	(-0.334 0.002)
$\mu_{j,k,2}$	-0.161	0.02	0.222
(CI)	(-8.892 8.281)	(-0.497 0.507)	(0.009 0.436)
$\eta_{j,k,1}$	-0.002	-0.008	17.502
(CI)	(-0.002 -0.001)	(-0.012 -0.004)	(12.141 23.362)
$\eta_{j,k,2}$	0	0.004	1.508
(CI)	(0 0)	(0.001 0.007)	(-2.707 5.842)
$\tau_{j,k}$	0.503	0.543	0.144
(CI)	(0.021 0.973)	(0.192 0.957)	(0.118 0.175)
$\rho_{j,k}$	1	0.985	0.006
(CI)	(1 1)	(0.968 0.993)	(0.004 0.008)
$\Sigma_{j,k,1,1}$	0	0.023	0.197
(CI)	(0 0)	(0.02 0.026)	(0.172 0.227)
$\Sigma_{j,k,1,2}$	0	0	-0.037
(CI)	(0 0)	(0 0.001)	(-0.054 -0.022)
$\Sigma_{j,k,2,2}$	0	0.017	0.291
(CI)	(0 0)	(0.014 0.019)	(0.253 0.34)
$\pi_{j,1,k}$	0.773	0.211	0.016
(CI)	(0.756 0.789)	(0.195 0.228)	(0.008 0.025)
$\pi_{j,2,k}$	0.384	0.532	0.084
(CI)	(0.354 0.414)	(0.494 0.568)	(0.065 0.105)
$\pi_{j,3,k}$	0.071	0.429	0.499
(CI)	(0.038 0.11)	(0.336 0.533)	(0.398 0.585)
$n_{j,k}$	2850	1639	311

Table 14: Lucy: posterior means and CIs of the model parameters (j=6).

	k=1	k=2	k=3	k=4
$\mu_{j,k,1}$	-0.236	-0.287	-0.05	-1.992
(CI)	(-8.941 8.273)	(-0.831 0.221)	(-0.414 0.318)	(-5.598 -0.642)
$\mu_{j,k,2}$	-0.161	0.02	0.244	3.423
(CI)	(-8.892 8.281)	(-0.497 0.507)	(-0.147 0.679)	(1.675 8.501)
$\eta_{j,k,1}$	-0.002	-0.008	6.462	-0.034
(CI)	(-0.002 -0.001)	(-0.012 -0.004)	(-5.942 15.635)	(-8.861 8.627)
$\eta_{j,k,2}$	0	0.004	1.203	-0.004
(CI)	(0 0)	(0.001 0.007)	(-5.868 7.427)	(-8.818 9.066)
$\tau_{j,k}$	0.503	0.543	0.114	0.64
(CI)	(0.021 0.973)	(0.192 0.957)	(0.077 0.162)	(0.232 0.978)
$\rho_{j,k}$	1	0.985	0.011	0.002
(CI)	(1 1)	(0.968 0.993)	(0 0.067)	(0 0.026)
$\Sigma_{j,k,1,1}$	0	0.023	0.196	0.236
(CI)	(0 0)	(0.02 0.026)	(0.16 0.25)	(0.074 0.692)
$\Sigma_{j,k,1,2}$	0	0	-0.031	-0.077
(CI)	(0 0)	(0 0.001)	(-0.059 -0.008)	(-0.408 0.085)
$\Sigma_{j,k,2,2}$	0	0.017	0.263	0.252
(CI)	(0 0)	(0.014 0.019)	(0.209 0.34)	(0.083 0.802)
$\pi_{j,1,k}$	0.729	0.24	0.031	0
(CI)	(0.711 0.747)	(0.22 0.26)	(0.019 0.044)	(0 0)
$\pi_{j,2,k}$	0.34	0.552	0.108	0
(CI)	(0.314 0.368)	(0.511 0.592)	(0.083 0.134)	(0 0)
$\pi_{j,3,k}$	0.158	0.371	0.471	0
(CI)	(0.122 0.198)	(0.29 0.461)	(0.381 0.551)	(0 0.001)
$\pi_{j,4,k}$	0.232	0.262	0.005	0.452
(CI)	(0 0.728)	(0 0.776)	(0 0.058)	(0 0.978)
$n_{j,k}$	2535	1834	430	1

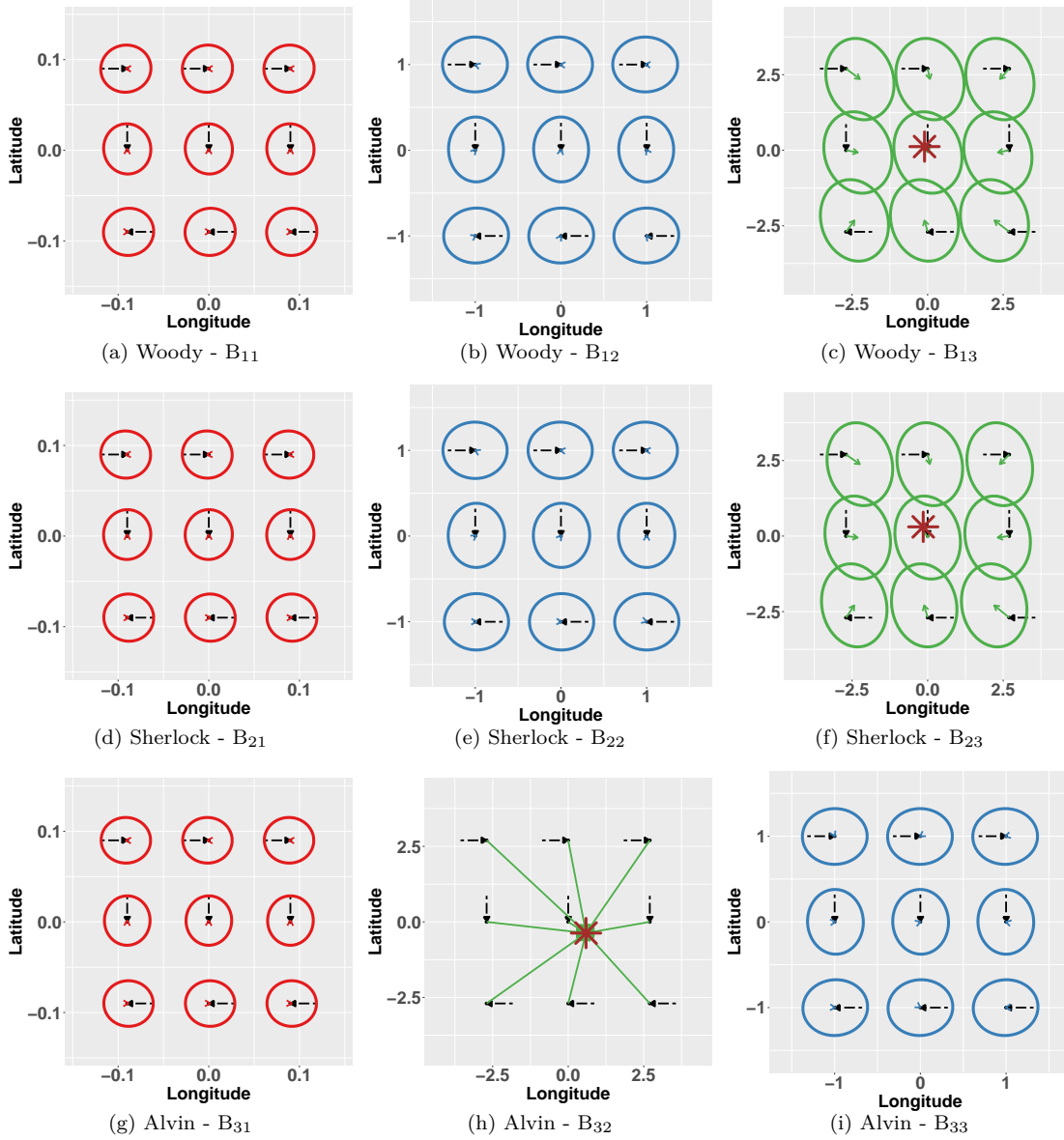


Figure 6: M2 - Graphical representation of the conditional distribution of $\mathbf{s}_{j,t_j,i+1}$ for the first three dogs, for different possible values of $\mathbf{s}_{j,t_j,i}$ and previous directions. The images have been obtained by using the posterior values that maximize the data likelihood of each animal, given the representative clusterization $\hat{z}_{j,t_j,i}$. The dashed arrow represents the movement between $\mathbf{s}_{j,t_j,i-1}$ and $\mathbf{s}_{j,t_j,i}$. The solid arrow is $\bar{\mathbf{F}}_{j,t_j,i}$, while the ellipse is an area containing 95% of the probability mass of the conditional distribution of $\mathbf{s}_{j,t_j,i+1}$. The asterisk represents the attractor, and it is only shown for behaviors that have posterior values of $\rho_{j,k} < 0.9$ and $\tau_{j,k} > 0.1$.

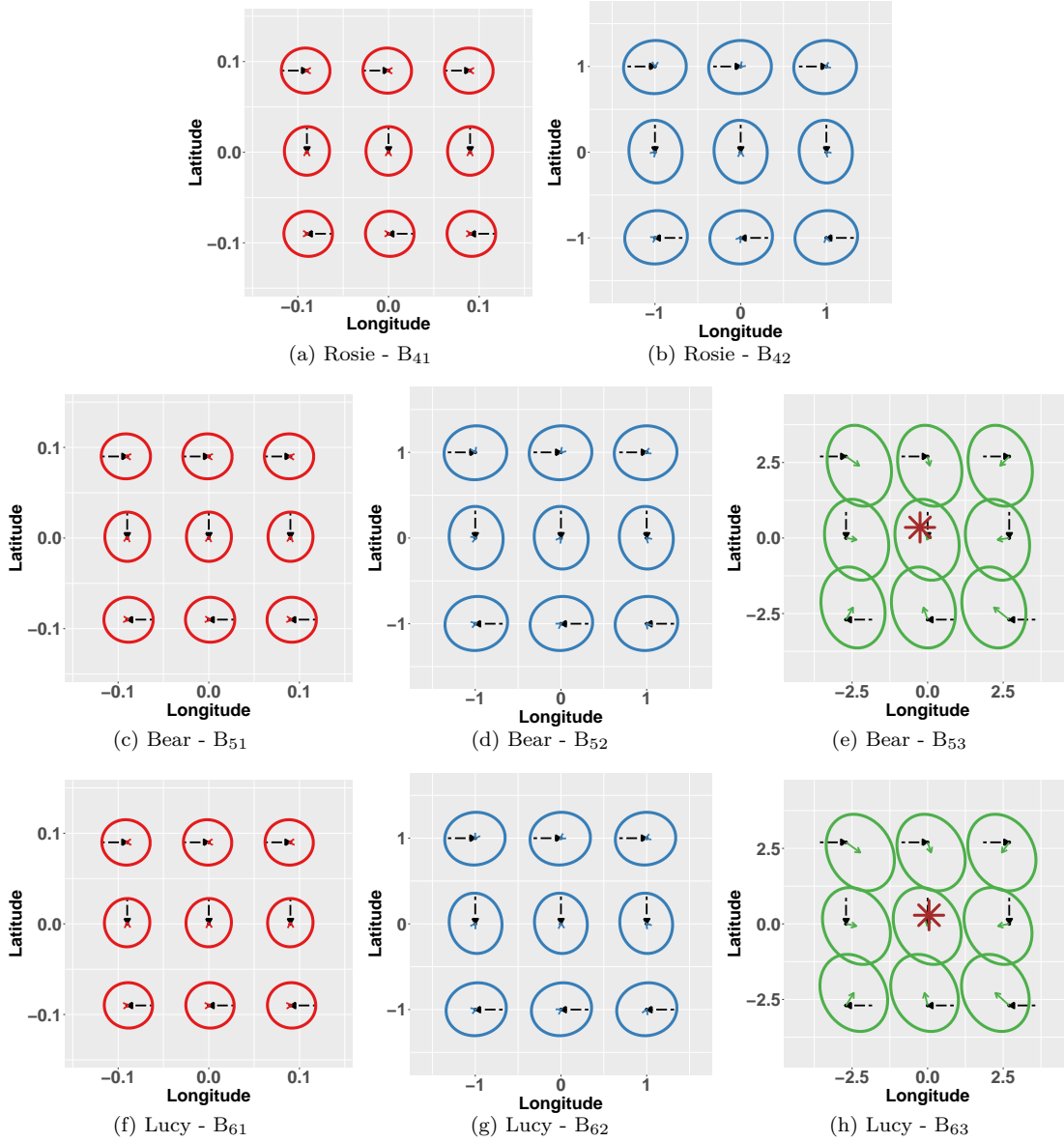


Figure 7: M2 - Graphical representation of the conditional distribution of $\mathbf{s}_{j,t_{j,i+1}}$ for the last three dogs, for different possible values of $\mathbf{s}_{j,t_{j,i}}$ and previous directions. The images have been obtained by using the posterior values that maximize the data likelihood of each animal, given the representative clusterization $\hat{z}_{j,t_{j,i}}$. The dashed arrow represents the movement between $\mathbf{s}_{j,t_{j,i-1}}$ and $\mathbf{s}_{j,t_{j,i}}$. The solid arrow is $\vec{\mathbf{F}}_{j,t_{j,i}}$, while the ellipse is an area containing 95% of the probability mass of the conditional distribution of $\mathbf{s}_{j,t_{j,i+1}}$. The asterisk represents the attractor, and it is only shown for behaviors that have posterior values of $\rho_{j,k} < 0.9$ and $\tau_{j,k} > 0.1$.

Table 15: M3 - Woody: posterior means and CIs of the model parameters ($j=1$).

	k=1	k=2	k=3
$\mu_{j,k,1}$	2.827	-0.157	-0.301
(CI)	(-4.211 9.069)	(-0.529 0.214)	(-2.109 1.54)
$\mu_{j,k,2}$	0.103	0.131	0.459
(CI)	(-6.173 6.606)	(-0.231 0.506)	(-2.069 2.062)
$\eta_{j,k,1}$	-0.085	0.035	0.055
(CI)	(-8.901 8.846)	(0.017 0.054)	(-8.647 8.947)
$\eta_{j,k,2}$	-0.027	0.002	0.13
(CI)	(-8.622 8.429)	(-0.013 0.018)	(-8.406 8.445)
$\tau_{j,k}$	0	0.726	0.631
(CI)	(0 0.001)	(0.356 0.984)	(0.074 0.981)
$\rho_{j,k}$	0	0.937	0.001
(CI)	(0 0)	(0.877 0.96)	(0 0.013)
$\Sigma_{j,k,1,1}$	0.001	0.108	0.875
(CI)	(0.001 0.001)	(0.096 0.118)	(0.327 2.289)
$\Sigma_{j,k,1,2}$	0	-0.004	-0.867
(CI)	(0 0)	(-0.009 0.001)	(-2.264 -0.277)
$\Sigma_{j,k,2,2}$	0.001	0.085	1.455
(CI)	(0.001 0.001)	(0.077 0.094)	(0.607 3.361)
$\pi_{j,1,k}$	0.814	0.186	0
(CI)	(0.799 0.828)	(0.172 0.201)	(0 0)
$\pi_{j,2,k}$	0.362	0.628	0.009
(CI)	(0.337 0.388)	(0.602 0.654)	(0.003 0.023)
$\pi_{j,3,k}$	0.001	0.94	0.05
(CI)	(0 0.001)	(0.653 1)	(0 0.322)
$n_{j,k}$	3203	1587	10

Table 16: M3 - Sherlock: posterior means and CIs of the model parameters (j=2).

	k=1	k=2	k=3	k=4	k=5
$\mu_{j,k,1}$	-0.042	0.012	0.089	-2.476	2.245
(CI)	(-8.78 8.892)	(-0.325 0.352)	(-0.181 0.348)	(-5.019 -1.158)	(-7.673 10.247)
$\mu_{j,k,2}$	-0.128	-0.14	-0.927	3.947	0.257
(CI)	(-8.41 8.689)	(-0.548 0.281)	(-1.272 -0.596)	(1.81 7.873)	(-7.609 7.576)
$\eta_{j,k,1}$	-0.003	0.538	-0.097	0.087	-0.028
(CI)	(-0.004 -0.002)	(-5.408 5.995)	(-8.929 8.571)	(-8.56 8.862)	(-8.682 9.341)
$\eta_{j,k,2}$	0	0.371	-0.082	0.235	-0.017
(CI)	(-0.001 0.001)	(-5.128 5.73)	(-8.536 8.629)	(-8.33 8.733)	(-8.791 8.584)
$\tau_{j,k}$	0.5	0.048	0.813	0.359	0.46
(CI)	(0.027 0.975)	(0.034 0.063)	(0.674 0.949)	(0.159 0.629)	(0.043 0.965)
$\rho_{j,k}$	1	0.07	0.004	0.004	0.292
(CI)	(1 1)	(0 0.175)	(0 0.046)	(0 0.062)	(0 1)
$\Sigma_{j,k,1,1}$	0.001	0.067	0.183	0.16	2.052
(CI)	(0.001 0.001)	(0.06 0.074)	(0.094 0.365)	(0.074 0.352)	(0.133 9.781)
$\Sigma_{j,k,1,2}$	0	0.01	0.061	-0.021	0.28
(CI)	(0 0)	(0.005 0.016)	(-0.022 0.185)	(-0.161 0.107)	(-3.659 3.496)
$\Sigma_{j,k,2,2}$	0.001	0.097	0.207	0.25	2.274
(CI)	(0.001 0.001)	(0.085 0.11)	(0.106 0.407)	(0.109 0.552)	(0.117 10.195)
$\pi_{j,1,k}$	0.842	0.157	0	0	0
(CI)	(0.829 0.855)	(0.144 0.17)	(0 0)	(0 0.001)	(0 0.002)
$\pi_{j,2,k}$	0.408	0.569	0.013	0.01	0
(CI)	(0.375 0.44)	(0.538 0.6)	(0.005 0.029)	(0.004 0.017)	(0 0)
$\pi_{j,3,k}$	0.368	0.45	0.171	0	0
(CI)	(0.141 0.638)	(0.151 0.768)	(0 0.423)	(0 0)	(0 0)
$\pi_{j,4,k}$	0.001	0.724	0	0.26	0
(CI)	(0 0.002)	(0.475 0.929)	(0 0.001)	(0.056 0.505)	(0 0)
$\pi_{j,5,k}$	0.007	0.012	0.35	0.008	0.397
(CI)	(0 0.022)	(0 0.08)	(0 0.998)	(0 0.019)	(0 1)
$n_{j,k}$	3466	1301	16	14	3

Table 17: M3 - Alvin: posterior means and CIs of the model parameters (j=3).

	k=1	k=2	k=3	k=4
$\mu_{j,k,1}$	0.048	0.602	0.863	-1.208
(CI)	(-8.603 8.615)	(0.591 0.621)	(0.665 1.149)	(-5.366 4.64)
$\mu_{j,k,2}$	-0.202	-0.362	-0.211	2.213
(CI)	(-9.292 8.204)	(-0.371 -0.35)	(-0.423 0.024)	(-4.438 5.592)
$\eta_{j,k,1}$	-0.004	0.069	0.412	0.017
(CI)	(-0.005 -0.003)	(-8.273 8.831)	(-8.391 8.73)	(-8.527 8.38)
$\eta_{j,k,2}$	0	-0.022	-0.241	-0.077
(CI)	(-0.001 0.001)	(-8.691 8.888)	(-8.45 8.582)	(-8.723 8.379)
$\tau_{j,k}$	0.496	0.916	0.238	0.683
(CI)	(0.024 0.969)	(0.827 0.96)	(0.14 0.318)	(0.126 0.915)
$\rho_{j,k}$	1	0	0.004	0.095
(CI)	(1 1)	(0 0)	(0 0.05)	(0 1)
$\Sigma_{j,k,1,1}$	0.001	0.011	0.104	0.883
(CI)	(0.001 0.001)	(0.008 0.019)	(0.079 0.158)	(0.065 3.261)
$\Sigma_{j,k,1,2}$	0	0.002	0.005	0.098
(CI)	(0 0)	(0 0.006)	(-0.013 0.022)	(-0.82 0.765)
$\Sigma_{j,k,2,2}$	0	0.008	0.141	0.639
(CI)	(0 0)	(0.005 0.015)	(0.106 0.216)	(0.068 3.051)
$\pi_{j,1,k}$	0.899	0.069	0.032	0.001
(CI)	(0.887 0.909)	(0.058 0.084)	(0.015 0.043)	(0 0.002)
$\pi_{j,2,k}$	0.527	0.41	0.058	0.004
(CI)	(0.458 0.589)	(0.346 0.493)	(0.031 0.086)	(0 0.011)
$\pi_{j,3,k}$	0.152	0.436	0.41	0
(CI)	(0.095 0.209)	(0.366 0.515)	(0.335 0.485)	(0 0.003)
$\pi_{j,4,k}$	0.282	0.003	0.146	0.493
(CI)	(0 0.651)	(0 0.014)	(0 0.469)	(0.002 0.999)
$n_{j,k}$	3907	627	253	13

Table 18: M3 - Rosie: posterior means and CIs of the model parameters (j=4).

	k=1	k=2	k=3
$\mu_{j,k,1}$	0	-0.222	-0.005
(CI)	(-8.879 8.897)	(-2.847 2.427)	(-8.67 8.758)
$\mu_{j,k,2}$	-0.008	0.987	0.034
(CI)	(-9.01 8.879)	(-1.65 4.187)	(-8.876 8.487)
$\eta_{j,k,1}$	-0.002	-0.284	0.167
(CI)	(-0.002 -0.001)	(-8.681 8.557)	(-8.144 8.953)
$\eta_{j,k,2}$	0	0.116	0.25
(CI)	(-0.001 0.001)	(-8.305 8.793)	(-8.742 9.179)
$\tau_{j,k}$	0.502	0.007	0.501
(CI)	(0.028 0.974)	(0.001 0.015)	(0.026 0.973)
$\rho_{j,k}$	1	0.002	0.487
(CI)	(1 1)	(0 0.019)	(0 1)
$\Sigma_{j,k,1,1}$	0.001	0.031	8.024
(CI)	(0 0.001)	(0.028 0.034)	(0.14 14.776)
$\Sigma_{j,k,1,2}$	0	0	-3.989
(CI)	(0 0)	(-0.002 0.002)	(-5.117 5.942)
$\Sigma_{j,k,2,2}$	0	0.033	6.494
(CI)	(0 0)	(0.03 0.037)	(0.133 17.609)
$\pi_{j,1,k}$	0.884	0.116	0
(CI)	(0.872 0.895)	(0.105 0.128)	(0 0)
$\pi_{j,2,k}$	0.449	0.549	0
(CI)	(0.41 0.49)	(0.508 0.589)	(0 0)
$\pi_{j,3,k}$	0.031	0.014	0.595
(CI)	(0 0.567)	(0 0.069)	(0 1)
$n_{j,k}$	3841	957	2

Table 19: M3 - Bear: posterior means and CIs of the model parameters (j=5).

	k=1	k=2	k=3
$\mu_{j,k,1}$	-0.09	-0.245	-0.762
(CI)	(-8.953 9.085)	(-0.636 0.153)	(-4.482 3.091)
$\mu_{j,k,2}$	0	0.252	0.97
(CI)	(-8.605 8.655)	(-0.21 0.722)	(-3.735 4.985)
$\eta_{j,k,1}$	-0.001	0.209	0.517
(CI)	(-0.002 0)	(-8.325 8.759)	(-8.878 9.856)
$\eta_{j,k,2}$	0	-0.069	-0.105
(CI)	(-0.001 0.001)	(-8.79 8.872)	(-8.846 8.431)
$\tau_{j,k}$	0.517	0.033	0.313
(CI)	(0.028 0.977)	(0.023 0.044)	(0.007 0.879)
$\rho_{j,k}$	1	0	0.013
(CI)	(1 1)	(0 0)	(0 0.103)
$\Sigma_{j,k,1,1}$	0.001	0.055	0.567
(CI)	(0.001 0.001)	(0.049 0.061)	(0.271 1.203)
$\Sigma_{j,k,1,2}$	0	-0.005	-0.361
(CI)	(0 0)	(-0.01 -0.001)	(-1.013 0.021)
$\Sigma_{j,k,2,2}$	0.001	0.079	1.131
(CI)	(0.001 0.001)	(0.067 0.089)	(0.506 2.469)
$\pi_{j,1,k}$	0.831	0.169	0
(CI)	(0.817 0.844)	(0.156 0.183)	(0 0)
$\pi_{j,2,k}$	0.383	0.607	0.01
(CI)	(0.356 0.411)	(0.576 0.635)	(0.003 0.024)
$\pi_{j,3,k}$	0.001	0.571	0.42
(CI)	(0 0.006)	(0.331 0.817)	(0.171 0.655)
$n_{j,k}$	3337	1447	16

Table 20: M3 - Lucy: posterior means and CIs of the model parameters (j=6).

	k=1	k=2	k=3
$\mu_{j,k,1}$	1.986	-0.105	-0.409
(CI)	(-4.873 8.395)	(-0.438 0.259)	(-6.908 7)
$\mu_{j,k,2}$	1.196	0.005	0.72
(CI)	(-5.206 7.673)	(-0.413 0.404)	(-6.704 7.169)
$\eta_{j,k,1}$	-2.121	-0.042	0.629
(CI)	(-10.102 7.19)	(-8.624 8.723)	(-9.071 11.768)
$\eta_{j,k,2}$	0.466	0.012	0.006
(CI)	(-7.098 7.046)	(-8.756 8.734)	(-8.964 8.851)
$\tau_{j,k}$	0	0.038	0.523
(CI)	(0 0.001)	(0.028 0.047)	(0.032 0.957)
$\rho_{j,k}$	0.001	0	0.235
(CI)	(0 0.007)	(0 0)	(0 1)
$\Sigma_{j,k,1,1}$	0.001	0.068	2.064
(CI)	(0.001 0.001)	(0.06 0.075)	(0.17 8.422)
$\Sigma_{j,k,1,2}$	0	0	-0.084
(CI)	(0 0)	(-0.006 0.005)	(-2.633 2.692)
$\Sigma_{j,k,2,2}$	0.001	0.086	2.821
(CI)	(0.001 0.001)	(0.076 0.097)	(0.179 9.906)
$\pi_{j,1,k}$	0.795	0.205	0
(CI)	(0.779 0.812)	(0.188 0.221)	(0 0)
$\pi_{j,2,k}$	0.365	0.626	0.005
(CI)	(0.34 0.39)	(0.6 0.652)	(0 0.017)
$\pi_{j,3,k}$	0.008	0.397	0.408
(CI)	(0 0.05)	(0 0.998)	(0 1)
$n_{j,k}$	3082	1704	14

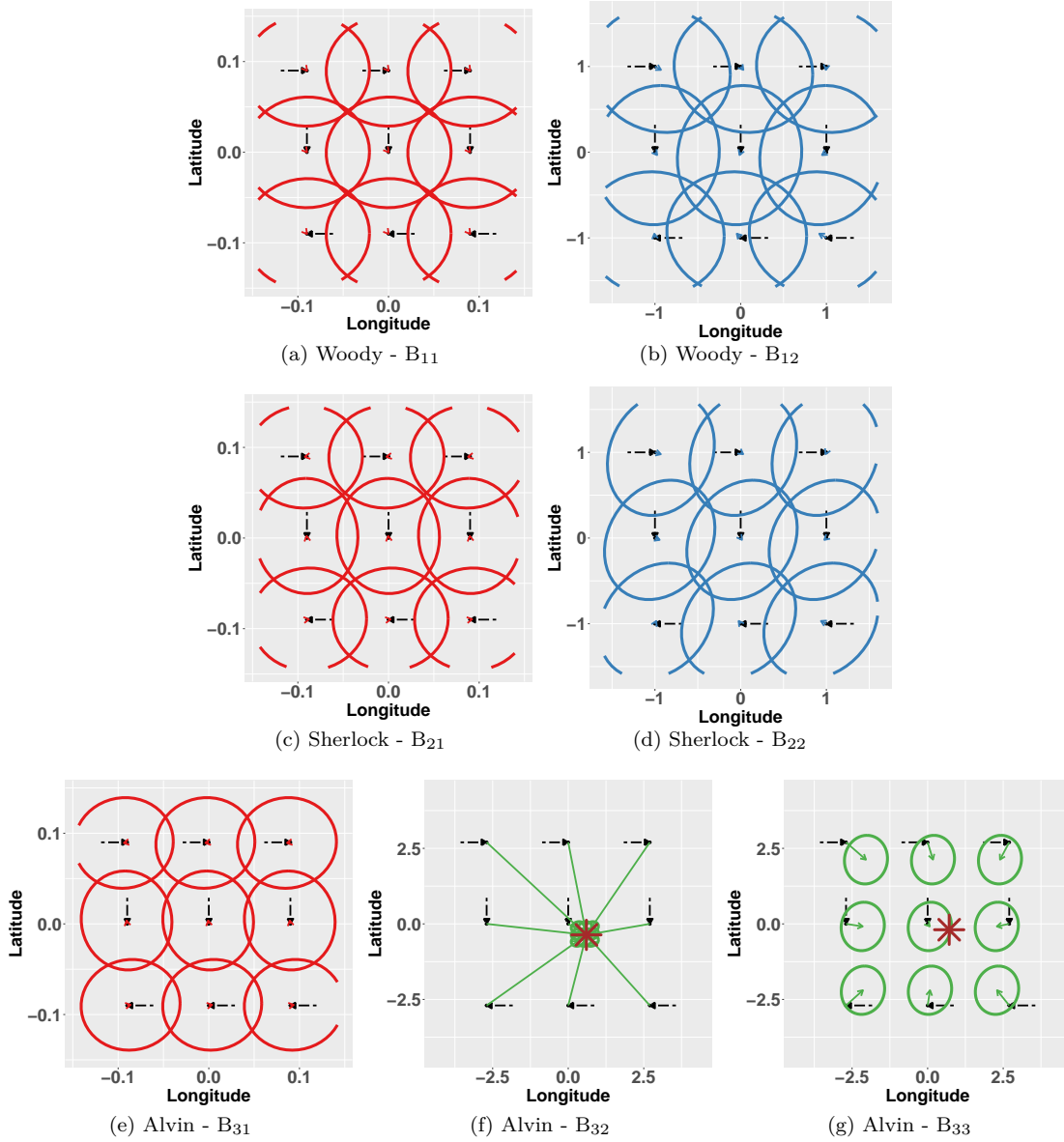


Figure 8: M3 - Graphical representation of the conditional distribution of $\mathbf{s}_{j,t_j,i+1}$ for the first three dogs, for different possible values of $\mathbf{s}_{j,t_j,i}$ and previous directions. The images have been obtained by using the posterior values that maximize the data likelihood of each animal, given the representative clusterization $\hat{z}_{j,t_j,i}$. The dashed arrow represents the movement between $\mathbf{s}_{j,t_j,i-1}$ and $\mathbf{s}_{j,t_j,i}$. The solid arrow is $\vec{\mathbf{F}}_{j,t_j,i}$, while the ellipse is an area containing 95% of the probability mass of the conditional distribution of $\mathbf{s}_{j,t_j,i+1}$. The asterisk represents the attractor, and it is only shown for behaviors that have posterior values of $\rho_{j,k} < 0.9$ and $\tau_{j,k} > 0.1$.

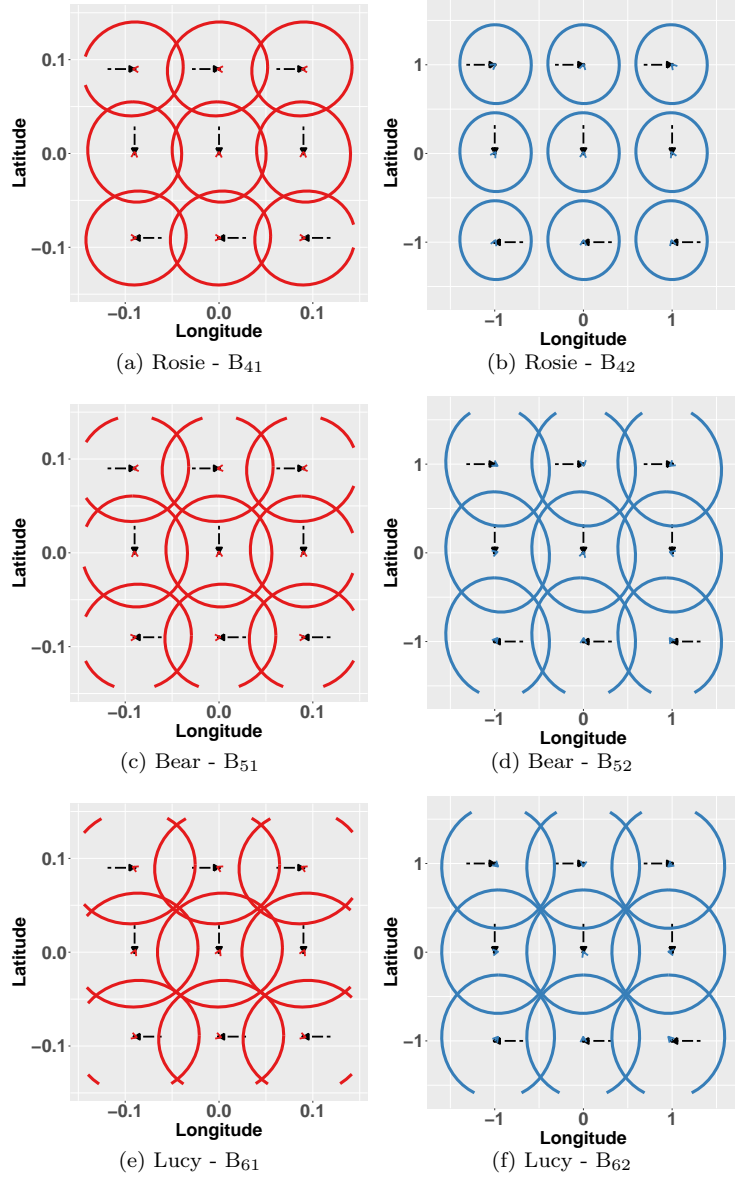


Figure 9: M3 - Graphical representation of the conditional distribution of $\mathbf{s}_{j,t_{j,i+1}}$ for the last three dogs, for different possible values of $\mathbf{s}_{j,t_{j,i}}$ and previous directions. The images has been obtained by using the posterior values that maximize the data likelihood of each animal, given the representative clusterization $\hat{z}_{j,t_{j,i}}$. The dashed arrow represents the movement between $\mathbf{s}_{j,t_{j,i-1}}$ and $\mathbf{s}_{j,t_{j,i}}$. The solid arrow is $\vec{\mathbf{F}}_{j,t_{j,i}}$, while the ellipse is an area containing 95% of the probability mass of the conditional distribution of $\mathbf{s}_{j,t_{j,i+1}}$.